UC Santa Cruz

UC Santa Cruz Electronic Theses and Dissertations

Title

Physical-Biological Drivers of Population Replenishment for an Ecologically Important Fish Species of the California Current

Permalink

Author

Morales, Mark Matthew

Publication Date

2023

UNIVERSITY OF CALIFORNIA
SANTA CRUZ

**PHYSICAL-BIOLOGICAL DRIVERS OF POPULATION
REPLENISHMENT FOR AN ECOLOGICALLY IMPORTANT FISH
SPECIES OF THE CALIFORNIA CURRENT**

A dissertation submitted in partial satisfaction of
the requirements for the degree of

DOCTOR OF PHILOSOPHY

in

ECOLOGY AND EVOLUTIONARY BIOLOGY

by

Mark M. Morales

December 2023

The Dissertation of Mark M. Morales
is approved:

_____

Professor Mark H. Carr, chair

_____

Elliott L. Hazen, Ph.D.

_____

Professor Peter T. Raimondi

_____

Professor Jerome Fiechter

_____
Peter Biehl
Vice Provost and Dean of Graduate Studies

Table of Contents

List of Tables

List of Figures

Abstract

Physical-Biological Drivers of Population Replenishment for an Ecologically Important Fish Species of the California Current

Mark M. Morales

Marine fish population fluctuations are pervasive. A primary driver of marine fish population fluctuation is annual recruitment variability. For over a century, fisheries oceanographers have tried to attribute cause to observed recruitment variability with varying degrees of success. While several hypotheses of recruitment variability can be found in the literature, most can be grouped into either food web- or transport-dependent mechanisms. The mechanistic basis of food web-dependent drivers is that larval survival, and eventual recruitment, is determined by starvation or predation mortality. Transport-dependent drivers are related to advective processes that disperse larvae into or out of habitat favorable for recruitment. In this dissertation I address these two mechanisms of recruitment variability for Shortbelly Rockfish, a highly abundant and ecologically important fish species of the California Current System. In Chapter 1, I develop and apply a bioenergetics growth model to understand how spatial variation in ocean conditions determines growth potential. I find that spatial patterns of early life stage-specific growth potential correspond with important early life history events. In Chapter 2, I introduce interannual variability in ocean conditions to the growth model and find that hotspots of spatial growth potential explain 78.6% of Shortbelly recruitment variability. This result supports the

hypothesis that food web-dependent processes are important for recruitment strength. In Chapter 3, I introduce transport-dependent processes to the model framework and find that the relative importance of food limitation and transport on recruitment are dependent on interannual climate cycles (El Niño Southern Oscillation). The preponderance of recruitment drivers being context dependent amongst a backdrop of differing climate conditions may explain why understanding recruitment mechanisms has been so challenging.

Acknowledgements

It took a village to get me to this point and there are far too many to thank to be able to thank everyone in this short acknowledgement letter. Thank you to my advisors, Mark Carr and Elliott Hazen, who have both provided me with their gracious professional and personal support throughout my time in graduate school. Mark, your caring and light hearted nature has made it a joy to come into the lab every day and I will miss our frequent morning rants. Your careful and thoughtful criticism has taught me how to think more succinctly about ecological interactions.

Elliott, if it were not for you, I would not be in graduate school at UCSC. From your initial response to my "cold-call" email, to our first phone conversation to chat about the effects of climate on marine ecosystem dynamics, I knew that you were the advisor I was looking for – one that would provide me with the freedom to follow my passion and develop a thesis on my own accord. With this privilege, and your continual support of my ideas, you have always provided me with momentum to keep chugging along the dissertation path.

Pete, as the "R" to the RC Lab, you've been an incredible surrogate advisor to me. From holding the EEB Chair position when I first joined the lab, to Interim Director of the Institute of Marine Sciences, to being the unofficial statistics tutor for students (and faculty) of EEB, your leadership as a teacher, ecologist, and administrator will always be a source of inspiration for me.

Jerome, your breadth of research will forever inspire me to think outside the box and to aspire to work across disciplines within the marine sciences with a level of elegance. You have so kindly and selflessly shared your knowledge of ecosystem modeling (and ROMS-NEMUCSC output) with me and your ecosystem oceanography expertise has made me a much more well-rounded marine scientist.

Collectively, I thank all my committee members from the bottom of my heart, and I look forward to remaining lifetime colleagues and friends.

To my fellow grad student colleagues in the RC Lab, both past and present, thank you all for being such amazing lab mates and for putting up with me all these years. Your academic and emotional support is what has made graduate school one of the most rewarding experiences of my life. We are a big lab and you guys have always made it feel like a family to me.

To my other lab, the Climate and Ecosystem Group at the NOAA NMFS SWFSC Lab in Monterey. Never have I ever met such a driven and productive group of people in my life. While I may not have visited as much as I would have liked, seeing your faces at so many conferences, workshops, and summer schools (both national and international) has given me a sense of comfortability within and among the broader marine scientific community.

To all the members of the Fisheries and Ecosystem Oceanography Team and Habitat and Groundfish Ecology Team at the NOAA-NMFS SWFSC Santa Cruz Lab, you are all rockstars in my eyes. A special shoutout to Keith Sakuma and Rebecca

Chapter 1 is reproduced from the following manuscript:

Morales, M.M., Fiechter, J., Field, J.C., Kashef, N.S, Hazen, E.L., and Carr, M.H. (2024). Development and application of a bionenergetics model for multiple early life stages of an ecologically important marine fish. *Ecological Modeling*. Vol. 488.

Chapter 2 is a version of the following manuscript in prep:

Morales, M.M., Fiechter, J., Field, J.C., Kashef, N.S, Hazen, E.L., and Carr, M.H. (*in prep*). Spatial patterns of growth potential from a Eulerian individual-based model explains interannual recruitment variability of Shortbelly Rockfish (*Sebastes jordani*).

Chapter 3 is a version of the following manuscript in prep:

Morales, M.M., *et al*. Context matters: mechanisms of recruitment dynamics associated with contrasting ENSO events in the California Current.

Introduction

Background

For many marine fish populations, the early life stages (ELS) are the most vulnerable period of the life cycle with ~99.9% mortality within the first year of life (Houde 2008). Most fish species have high fecundity, producing in some cases millions of eggs per female per reproductive batch (Nelson 2016). Given these characteristics, small changes in survivability during the first year of life can lead to orders of magnitude changes in recruitment (the number of larval fish that survive to become adults). Differential survival during the first year of life can be attributed to environmental processes that directly affect physiological rates, disease outbreaks, and larval dispersal, and indirectly through food availability and predation pressure (Sheperd et al., 1984). For relatively short-lived species, year-to-year fluctuations of recruitment yield to natural variation in adult abundance (Checkley et al., 2009). In contrast, long-lived species suffer fewer negative effects from fluctuations in recruitment through the storage effect (Warner and Chesson 1985; Secor 2007). For such fish species, however, a single large year class can change population structure, the magnitude of density-dependence, population biomass, and predator-prey relationships, and for exploitable fish populations, change fisheries selectivity (Bjørnstad et al., 2004). Understanding and predicting recruitment therefore has major implications for understanding ecosystem structure and for the sustainable management of exploitable marine fish populations.

1

Fisheries oceanography is a discipline that straddles the interface between marine ecology and oceanography by relating the distribution and abundance of fish populations to environmental variability, either natural or anthropogenic in source, to understand processes that drive recruitment fluctuations (Cury et al., 2008; Bograd et al., 2014). For over a century, fisheries oceanographers have strived to understand the environmental drivers of recruitment. Johan Hjort's hypotheses (Hjort 1914; 1926) were the first to scientifically link natural changes in the physical and biological environment to recruitment and the productivity of fish populations (Browman 2014). Hjort hypothesized that year-class strength was largely driven by changes in available food for first feeding larvae ("the critical period hypothesis") through food web-dependent processes. He also posited that ocean currents could disperse larvae into habitat favorable or unfavorable to life cycle closure ("the aberrant drift hypothesis"), thereby affecting recruitment strength through transport-dependent processes. From this viewpoint, if the biophysical factors driving recruitment variability can be identified, and the indicators of forcing factors reliably measured, then accurate predictions of year-class strength could be attainable.

Study System

The California Current System (CCS) is one of four major eastern boundary upwelling systems. The CCS is characterized by the California Current (CC), a nearshore coastal jet, a subsurface undercurrent, the Davidson Current, and the Southern California Eddy (Checkley and Barth, 2009). The CC is fed from the

north by the North Pacific Current, an eastward flowing current on the northern margin of

the North Pacific Gyre. The CC is in geostrophic balance with the North Pacific Gyre, resides within 1,000 km from the west coast of North America and flows southward from the U.S. – Canadian border to Baja California (Checkley and Barth, 2009). The coastal jet is a narrower southward flowing current shoreward of the CC, most dominate during the spring and summer months (Huyer et al., 1991). The Davidson Current is a seasonal northward flowing current which dominates during winter months (King et al., 2011). At Point Conception, the CC bifurcates eastward and forms the southern California Eddy, a nearly year-round cyclonic eddy in the Santa Barbara Basin, although it is most pronounced in the late spring, early summer when the coastal jet is at its maximum velocity (Washburn and McPhee-Shaw, 2013).

The CCS is typified by strong seasonal upwelling, a process in which northwest winds in the spring and summer drive the Ekman layer (i.e. surface waters) offshore via friction (i.e. wind stress) and the rotation of the earth (i.e. the Coriolis force). The offshore flowing surface waters generate a cross-shelf pressure gradient which is geostrophically balanced by the southward flowing coastal jet. During the process of upwelling, deep, nutrient-rich, high salinity seawater is advected to the sunlit surface waters and fuels a highly productive food web. Furthermore, there is a latitudinal gradient in the strength and timing of seasonal upwelling (Checkley and

3

Barth, 2009). In the south (i.e. Point Conception, CA to Punta Eugenia, Baja Sur),

coastal upwelling is active nearly year-round, however, peaks occur during the

summer months. In the central CCS (Cape Mendocino to Point Conception),

upwelling is relatively more seasonal with the spring transition occurring in March

and persisting until fall but peaking in July. In the northern CCS (i.e. Cape

Mendocino to Juan de Fuca Straight), upwelling is strongly seasonal, beginning in

late spring and persisting to early fall (Bograd et al., 2009). These seasonal dynamics

drive local and regional productivity in the CCS.

Equally important are the wintertime wind reversals that occur in the northern

CCS, and to a lesser extent in the central CCS. These wind reversals power a

phenomenon known as downwelling which severely depresses the southward flowing

jet, drives the dynamics of the Davidson Current, and transports surface waters

(Ekman layer) towards the coast.

Complicating the seasonal dynamics of the CCS physics are the dramatic

natural variations occurring at interannual, decadal and secular scales. At the

interannual scale, the El Niño Southern Oscillation (ENSO; Trenberth 1997) can have

severe impacts on physical and biological processes in the CCS with a periodicity of

3-7 years (McGowan et al., 1998; Chavez et al., 2002a,b; Jacox et al., 2016). ENSO

can display three states; El Niño, La Niña and ENSO neutral. El Niño is indicative of

high sea surface temperature anomalies (SSTa), a deepening of the thermocline and

nutricline, delayed and weakened seasonal upwelling, and lower primary productivity.

La Niña is characterized by lower SSTa, strong seasonal upwelling, and high

4

productivity. ENSO neutral lies in between these two states. At the decadal scale are the Pacific Decadal Oscillation (PDO; Manuta and Hare, 2002) and the North Pacific Gyre Oscillation (NPGO, Di Lorenzo et al., 2008) characterized as the first mode of sea surface temperature (SST) variability and the second mode of sea surface height anomalies in the North Pacific, respectively. A negative PDO can be thought of a longer term La Niña like state whereas a positive state of the PDO is similar to EL Niño, with fluctuations between the two occurring with a periodicity of ~40-70 years. The NPGO is correlated with sea surface salinity anomalies, nutrient availability and primary productivity (Di Lorenzo et al., 2008). At the secular scale is anthropogenic climate change caused by the burning of fossil fuels and positive feedbacks within the Earth system. Climate change will have many synergistic effects on the physical environment such as increased water temperatures, increased stratification, shoaling oxygen minimum zones, ocean acidification, and rising sea levels which will directly impact marine organisms through physiological responses and redistributions, and indirectly through changes in species interactions and population connectivity (Doney et al., 2012). It is currently unclear at this time how climate change will specifically affect the biology of the CCS, though modeling efforts, laboratory studies and retrospective empirical biophysical studies (e.g. space-for-time substitutions; Ohman et al., 2013) are beginning to shed light on the matter, particularly when mechanistic drivers are explored in an ecosystem oceanography context (Curry et al., 2008). Perhaps most relevant to understanding recruitment is identifying mechanistic

5

linkages between physical processes in the ocean and the biological response, as well as the ability to tease out natural variation on multiple spatiotemporal scales from anthropogenic stressors.

Rockfish Biology

The interplay between upwelling/downwelling dynamics, natural climate variability and anthropogenic climate change in the CCS have significant implications for the growth, survival and recruitment of marine organisms that are of economic and ecological importance, such as the rockfish complex (i.e. Sebastes spp.). Rockfish are a highly speciose group of fishes with large year-to-year fluctuations in recruitment (Ralston et al., 2013). As adults they occupy a variety of niches ranging from the land-sea interface (i.e. rocky intertidal pools), to near shore kelp forests, out to the continental shelf, and beyond to the shelf slope (Love et al., 2002). Rockfish are different from many fishes in that they exhibit viviparity by which embryos are internally fertilized and larvae are born alive and ready to feed. With a few exceptions, rockfish that inhabit the shelf and shelf-slope give birth in the winter months, and most nearshore species give birth in late-spring/early summer (Love et al., 2002). In general, most of the economically important rockfish give birth during the winter downwelling season, metamorphose to juveniles by April-May during the upwelling season and settle to the benthose during the late spring and summer months.

A wealth of evidence suggests that rockfish recruitment strength is set during the pelagic duration of their life history when density-independent processes

dominate (Woodbury and Ralston, 1991; Ainley et al., 1993; Ralston and Howard, 1995; Laidig, 2010; Laidig et al., 2007; Caselle et al., 2010; Field et al., 2010; Ralston et al., 2013; Schroeder et al., 2014; 2019; Friedman et al., 2018). Furthermore, recent studies suggests that growth rate variability results in differential survival (Fennie et al., 2020; 2023a; 2023b), which raises the question how coastal oceanographic processes interact to affect lower trophic level production, and how spatiotemporal changes in food availability and temperature affects growth rate. Additionally, some rockfish species spend up to six months in the pelagic environment before recruiting to adult benthic habitat and recognizing that the youngest larvae are relatively slow swimmers compared to the velocity of ocean current features (e.g., the coastal upwelling jet; Kashef et al., 2-14), a greater understanding of the influence of transport processes on recruitment success is needed.

Shortbelly Rockfish (*Sebastes jordani*) are an unexploited species generally assumed to be the most abundant rockfish species in the California Current System (CCS; Love et al., 2002). Relative to other Sebastes spp, Shortbelly have a life history more closely matching that of forage fishes (e.g. sardine and anchovy) as they exhibit fast growth, early age at maturity, and have relatively high natural mortality rates. Their parturition period is relatively broad, beginning in late December, peaking in February, and ending as late as May (Wyllie-Echeverria, 1987). After 3-4 months as pelagic larvae, Shortbelly metamorphose to pelagic juveniles before settling to their semi-benthic adult habitats at roughly 150-days old, or ~70 mm SL (Laidig et al., 1991). As pelagic juveniles, Shortbelly, and other members of the pelagic juvenile

7

rockfish assemblage, are important constituents of the forage community as their relatively small size and semi-pelagic schooling behavior make then particularly susceptible to predation from seabirds, marine mammals, and piscivorous fishes (Thayer et al., 2014; Warzybok et al., 2018; Lowry et al., 2022). Since Shortbelly recruitment covaries with other rockfish species (Ralston et al., 2013), understanding the mechanisms of their historical recruitment fluctuations would provide insights into the drivers of recruitment variability for many other commercially important and actively managed species, and as such would contribute greatly towards an ecosystem-based management approach in the CCS (Wells and Santora, 2023).

Overview of Dissertation

The overarching goal of this dissertation is to better understand how physical and biological mechanisms determine rockfish recruitment. To elucidate biophysical drivers of recruitment variability I develop and apply a mechanistic ecosystem modeling framework that successively builds in complexity throughout each chapter.

In Chapter 1 I develop and apply an ontogenetic bioenergetics growth model for multiple pre-recruitment life stages of Shortbelly rockfish: the preflexion, flexion, and postflexion larval stages and the pelagic juvenile stage. The model is first parameterized through a literature review, and where sufficient parameters could not be found, they are estimated through a model fitting process by confronting predictions with empirical data. The behavior of the model is then assessed through a sensitivity analysis and through scenario testing of the forcing factors (i.e., temperature and prey availability). Next, I expand the baseline ontogenetic

bioenergetics to include spatial variability and compare simulated growth potential with spatial patterns of reproduction, and the distribution and abundance patterns of pelagic juvenile shortbelly derived from a fisheries-independent survey.

In Chapter 2 I expand the bioenergetics model developed in Chapter 1 to include temporal patterns of spatial growth potential and evaluate ability of the intensity and size of growth potential hotspots (i.e., spatial regions of elevated growth) to explain recruitment patterns of Shortbelly rockfish. I use the model to test the hypothesis that spatial patterns of growth potential across multiple ELS's differentially contribute to explaining observed recruitment variability and that the directionality of the associations between growth and recruitment are life stage dependent.

In Chapter 3 I add a Lagrangian particle tracking algorithm to the overall modeling framework to simulate larval dispersal of Shortbelly rockfish using ocean currents calculated from a regional ocean circulation model. The bioenergetics model is coupled to the particle tracking model and estimates growth along dispersal trajectories. The coupled biophysical individual-based model estimates starvation mortality and retention near the coast to assess the relative influence of food web- and transport-dependent processes, respectively, on modeled and observed recruitment. The importance of the two mechanisms of recruitment variability are compared across cohorts within a year, and then compared across contrasting environmental conditions to test the hypothesis that mechanisms of recruitment variability are context dependent.

Chapter 1

Development and application of a bioenergetics growth model for multiple early life stages of an ecologically important marine fish

Abstract

Spatial and temporal variability in temperature and food availability are key drivers of growth of marine fishes. Growth during the early life stages (ELS's) is tightly coupled to survival, and in turn, can set year-class strength (i.e. annual recruitment) and overall stock productivity of populations and fished stocks. Ontogenetic changes in physiology, dietary preferences, and growth across ELS's can be accounted for within bioenergetics models, but existing models lack resolution within larval and early juvenile stages. We leveraged daily output from a coupled physical-biogeochemical model to force a highly resolved ontogenetic bioenergetics model parametrized for an ecologically important rockfish in the California Current System. Size-at-age predictions closely track empirical growth trajectories of the ELS's. Scenario testing revealed that growth performance is disproportionately driven by changes in temperature compared to food availability. We then expanded the model to incorporate spatial climatological differences in temperature and prey concentration and found that preflexion growth potential is maximized in areas of historical spawning, suggesting the timing and location of reproduction is an adaptive strategy that places larvae in habitat favorable for survival. Growth potential for late-stage larvae (postflexion) is greatest over a broad areal extent, implying that if a particle tracking algorithm was coupled to the bioenergetics model, a wide range of larval

dispersal pathways would place postflexion larvae in habitat suitable for rapid growth. Finally, growth potential of pelagic juveniles is maximized over the continental shelf and shelf-break, aligning with high juvenile catch rates from a fisheries-independent survey. In summary, this study (i) serves as a proof of concept that a bioenergetics model with high ontogenetic resolution can reproduce life stage-specific growth trajectories even though the underlying physiology data for model parameterization is imperfect and (ii) can aid future studies aimed at understanding how ecosystem processes interact with ontogenetic growth and changes in year class strength of early life stages of marine fishes.

1. Introduction

Temperature and food availability are key drivers of the rate of somatic growth of marine ectotherms (Winberg, 1956). Since body size is intimately linked with survival (Pepin, 1991; Sogard, 1997) and fecundity (Hixon et al., 2014; Dick et al., 2017), processes directly affecting the growth and condition of an individual contribute to their susceptibility to starvation and predation risk (Bailey and Houde, 1989; Houde, 1987), and influence reproductive output. Hence, characterizing growth rate variability is important for understanding the dynamics of fish populations alongside the communities and ecosystems that depend on them. For marine ectotherms, such as bony fishes, metabolic rates are dependent on body size (Brown et al., 2004), ambient (seawater) temperature (Fry 1971), oxygen concentration (Yang et al., 1992), and seawater pH (Hamilton et al., 2017). Marine fishes are adapted to a thermal range at which physiological function is optimized (Pörtner and Farrel 2008).

When water temperature exceeds the optima, growth rates can increase if increased prey availability can offset elevated metabolic rates (Munday et al., 2009). If adequate food is not available to offset increased maintenance costs, individuals will suffer greater mortality and populations can decline (Pörtner and Knust, 2007).

For the early life stages (ELS) of fishes, energy reserves are limited due to their small size and higher mass-specific metabolic rates (Peck and Moyano, 2016), ultimately putting them at higher risk of starvation relative to adult conspecifics. In the face of expected global change, increasing water temperatures are predicted to decrease developmental time and shorten pelagic larval durations (O'Connor et al., 2007), affecting population connectivity, genetic diversity, trophic interactions and population dynamics. Furthermore, since year-class strength (recruitment) is believed to be set primarily during early developmental stages (Hjort, 1914; Houde, 2016), there is a need to perform mechanistic studies of growth rate variability through use of energetic models in relation to natural climate variability, anthropogenic environmental change, and population productivity (Hollowed et al., 2011).

Energy budget modeling is a method used to assess the amalgamation of consumption, metabolism, somatic growth, excretion, and reproduction and how temperature and food availability interact with these rates (Chipps and Wahl, 2008). Bioenergetic models are grounded by the first law of thermodynamics where energy consumed is balanced by energy used for metabolism, excretion of waste products, and somatic and gonadal growth (Winberg 1956). Three modeling frameworks are commonly used in fish bioenergetics: (i) the metabolic theory of ecology (Brown et

al., 2004), (ii) dynamic energy budget (DEB; Kooijman, 2010), and (iii) the "Wisconsin model" (Kitchell et al, 1977; Sibly et al., 2013; Jørgensen et al., 2016). The Wisconsin model is a frequently used framework, primarily because of the development of accessible and computationally efficient software (Hewett and Johnson 1987, 1992; Hanson et al. 1997; Deslauriers et al., 2017).

Historically, bioenergetics models were forced by point source measurements of temperature to quantify the proportion of maximum consumption required to achieve observed growth rates (Kitchell et al., 1977). However, Rose et al., (1999a and 1999b) developed a consumption term based on a multispecies Holling's Type II functional response that allowed for the estimation of consumption rates given dietary preferences and variable prey densities. Until recently, measurements of food availability used to force the feeding module relied on sparse and infrequently sampled in situ prey concentrations, which suffer from insufficiencies due to high levels of variability within and among sampling sites (Young et al., 2009). Coupled physical-biogeochemical models allow bioenergetics modelers to circumvent the use of 'snapshot' empirical prey availabilities with fine-scale spatiotemporal temperature and prey fields (Ito et al., 2004; Megrey et al., 2007). Furthermore, ontogenetic changes in consumption, or growth, within larval development stages are not typically accounted for in bioenergetics models, despite the recognition that somatic growth varies across ELS's (Laidig et al., 1991) and the directionality of growth-dependent mortality can vary depending on developmental stage (Bailey and Houde, 1989; Houde, 1997). The lack of highly resolved ontogenetic bionenergetics models

for ELS fishes is primarily due to a paucity of life stage-specific estimates of allometric respiration and consumption measurements, which are difficult to accurately measure in controlled laboratory settings (Peck and Moyano, 2016). However, accounting for ontogenetic differences in growth within a bioenergetics framework could possibly be achieved if life stage-specific dietary preferences based off larval and juvenile feeding habit studies are available. In addition, stage-specific feeding rate parameters within the realized consumption term (Rose et al., 1999a; 1999b) could be calibrated by minimizing the deviance between predicted growth and empirical growth curves that account for ontogenetic growth differences in the ELS. Development of a model that accounts for fine-scale ontogenetic changes of ELS growth could help identify the conditions and early life history stage that is most important for setting year-class strength under the growth-dependent mortality paradigm (Anderson 1988; Miller et al.,1988). For example, there is evidence that juvenile quillback rockfish (*Sebastes maliger*) experience size-selective predation mortality, with smaller, slower growing individuals occurring more frequently in juvenile coho salmon stomachs (*Onorhynchus kisutch*), suggesting growth could be an important driver of survival for rockfish (Fennie et al., 2020).

Rockfishes (*Sebastes spp*.) are a highly speciose family of fishes in the California Current System (CCS) with ecological and economic importance. Rockfishes are viviparous, giving birth to live, ready-to-feed larvae (~5 mm standard length; SL) primarily during the winter and spring months (Love et al., 2002). Of the nearly 70 species of rockfish in the CCS, shortbelly rockfish (Sebastes jordani) are

among the most abundant, comprising ~50% of juvenile rockfish catch in midwater

trawls (Field et al., 2021), with the top ten species of rockfish caught in central

California covarying in abundance (Ralston et al., 2013). The ELS of rockfishes

display large interannual variation in survivorship as revealed through larval

abundance (Thompson et al. 2016,2017), pelagic juvenile abundance (Ralston et al.,

2013; Santora et al., 2017; Schroeder et al., 2014; 2019) and recruitment estimates

from stock assessments (PFMC https://www.pcouncil.org/). There is now a

substantial body of evidence suggesting a linkage between environmental conditions

during ELS and the strength of recruitment of rockfishes (Woodbury and Ralston,

1991; Ainley et al., 1993; Ralston and Howard, 1995; Laidig et al., 2007; Laidig,

2010; Caselle et al., 2010; Ralston et al., 2013; Schroeder et al., 2014; 2019;

Friedman et al., 2018). Dietary studies reveal that larval and juvenile rockfishes

preferentially feed on copepods and krill, respectively (Sumida and Moser, 1984;

Reilly et al., 1992; Shaffer et al., 1995; Miller and Broduer, 2007; Miller et al., 2010;

Bosley et al., 2014), whose abundances are forced by interannual changes in climatic

conditions (Rebstock, 2002; Bi et al., 2011; Santora et al., 2014). Variability in

growth and survival of larval and juvenile rockfishes in relation to temperature

variability and food availability has not been conducted beyond correlational studies

(e.g. Peterson et al., 2014). Mechanistic models grounded in first principles (i.e.

physiology) are the next step in understanding the relationship between temperature,

prey abundance and growth of ELS rockfishes.

Here we develop a novel ELS bioenergetics model that accounts for changes in growth rate (i.e., stanzas) across three larval stages (preflexion, flexion, and postflexion) and the pelagic juvenile stage for an ecologically important marine fish, the shortbelly rockfish (*Sebastes jordani*). Life stage transitions in the model (governed by changes in consumption parameters) are assumed to be deterministic and based off length alone, rather than morphological development which is not accounted for in bioenergetics models. Specifically, we parameterize the bioenergetic model and compare predictions to an empirical growth curve with high ontogenetic resolution, assess the behavior of the model through sensitivity analysis, and explore the relative influence of temperature and prey availability on growth through scenario testing. Then we apply the model to a 2-D Eulerian application to investigate ELS-specific spatial patterns of growth potential in relation to spawning locations and settlement sites by forcing it with temperature and prey concentration from an existing high resolution coupled physical-biogeochemical historical simulation for the central California Current region. This work acts as a proof concept that within-ELS growth stanzas can be modeled accurately using imperfect physiological parameterizations given sufficient ecological data. Further, the model can be extended for use in Lagrangian individual-based models to better understand the influence of biophysical interactions on within-ELS growth differences and to evaluate mechanisms of recruitment, the 'holy grail' of fisheries oceanography.

2. Methods

2.1 Coupled Physical-Biogeochemical Historical Simulation

Temperature and food availability are required inputs to bioenergetically model temporal changes in somatic growth of marine fishes. Since empirical observations of subsurface temperatures and prey fields in general are sparse and inconsistent, we rely here on output from an existing coupled physical-biogeochemical historical simulation for 1988-2010 (Fiechter et al., 2018; Fiechter et al., 2020). Briefly, the physical-biogeochemical model is a nested implementation of the Regional Ocean Modeling System (ROMS) (Shchepetkin et al., 2005; Haidvogel et al., 2008) at 3 km horizontal resolution, coupled to a customized biogeochemical model (NEMUCSC) adapted from the North Pacific Ecosystem Model for Understanding Regional Oceanography (NEMURO) of Kishi et al. (2007) and including two phytoplankton functional groups (nanophytoplankton and diatoms) and three zooplankton size classes (small, large, and predatory). The nested ROMS-NEMUCSC historical simulation for the central CCS has been used to examine variability in alongshore coastal upwelling intensity and primary production (Fiechter et al., 2018), phenology and drivers of krill aggregations (Fiechter et al., 2020), and spatiotemporal patterns of coastal ocean acidification and hypoxia (Cheresh and Fiechter, 2020; 2023). The historical simulation has also been evaluated for its capability to reproduce temperature, salinity and density variability adequately in the central CCS (Schroeder et al. 2014; 2019).

Daily mean values of temperature, small zooplankton (ZS), large zooplankton (ZL) and predatory zooplankton (ZP) from ROMS-NEMUCSC were calculated over the period 1988-2010 to produce a climatology of temperature and three prey

17

concentrations. For spatially invariant simulations (0-D) of the bioenergetics model,

these variables were spatially averaged over coastal central California (36°- 39°N;

124°-121.5°W; Figure 1) to calibrate simulated growth trajectories of ELS rockfish

with empirical growth from the same area (see 2.4 Simulations). We selected

temperature, ZS, ZL, and ZP at 30m depth as this is where the ELS of shelf and shelf-

slope rockfishes are most abundant (Moser and Boehlert, 1991; Ross and Larson,

2003) and is the target depth of midwater pelagic trawl data used for model

evaluation (Sakuma et al., 2016; Field et al. 2021).

2.2 Bioenergetics Model

Somatic growth of an individual is calculated daily as the difference between

consumption and the sum of respiration, specific dynamic action, egestion and

excretion. The formulation and terminology for the bioenergetics model follow that of

the Wisconsin Bioenergetics model (Kitchell et al., 1977; Hewett and Johnson, 1987;

1992; Hanson et al., 1997; Deslauriers et al., 2017), with adaptations to account for

variable food availability (Rose et al., 1999a; 1999b). The somatic growth rate of an

individual is given by:

$$\frac{dW}{dt} = [C - (R + SDA + EG + EX)] \cdot W \cdot \frac{ED_{zoopl}}{ED_{fish}} \qquad (1)$$

where W is the wet weight (g fish) of an individual at time t (d) . C is consumption,

R is respiration or losses through metabolism, SDA is the specific dynamic action or

costs to digestion, EG is egestion, EX is excretion, ED_{fish} is the energy density of

ELS rockfish (Joules · g fish^{-1}), and ED_{zoopl} is the energy density of zooplankton

(Joules · g prey^{-1}). The units of consumption, respiration, specific dynamic action,

egestion and excretion are in g prey · g fish^{-1} · d^{-1}, which are converted to g fish · g

fish^{-1} · d^{-1} through the ratio of the energy density of zooplankton (ED_zoopl) relative

to the energy density of fish (ED_fish), which we assume are constant following

Megrey et al. (2007) for simplicity. Parameter values and their sources are provided

in Table 1.

2.2.1 Consumption

Daily consumption rate (g prey · g fish^{-1} · d^{-1}) is calculated as the percentage

of maximum consumption, offset by a temperature-dependent scaling factor:

$$C_{max} = a_C \cdot W^{b_C} \cdot F_C(T) \qquad (2)$$

where C_{max} is maximum consumption rate (g prey · g fish^{-1} · d^{-1}), a_C is the intercept

for the allometric mass function, W is the wet weight (g) of ELS rockfish, b_C is the

allometric slope, T is temperature, and $F_C(T)$ is the temperature-dependence function.

Previous bioenergetics models of rockfishes were largely focused on settled juvenile

or adult life history stages (Harvey et al., 2011; Rooper et al., 2012), and did not

estimate growth given allometric consumption. Therefore, we derived a_C and b_C from

Boehlert and Yoklavich (1983) (Table 1), who evaluated the effects of temperature,

ration, and fish size upon growth for rockfish in the pelagic juvenile life history stage.

19

A dome-shaped temperature-dependence function is preferred over other functions when modeling effects of temperature on consumption for temperate fish species (Thornton and Lessem, 1978). Here we model the influence of temperature on maximum consumption as the product of two sigmoidal curves with one curve describing an increase in consumption with increasing temperature (gcta) and the other a decrease in consumption with increasing temperature (gctb; Ito et al., 2004).

$$F_C(T) = gcta \cdot gctb, \tag{3}$$

where T is seawater temperature (°C) and gcta is calculated as

$$gcta = \frac{xk1 \cdot t4}{(1 + xk1) \cdot (t4 - 1)}, \tag{4}$$

$$t4 = e^{t5 \cdot (T - te1)}, \tag{5}$$

$$t5 = tt5 * ln\left(\frac{xk2 \cdot (1 - xk1)}{xk1 \cdot (1 - xk2)}\right), \tag{6}$$

$$tt5 = \frac{1}{te2 - te1}, \tag{7}$$

and gctb is calculated as

$$gctb = \frac{xk4 \cdot t6}{(1 + xk4) \cdot (t6 - 1)}, \tag{8}$$

$$t6 = e^{t7 \cdot (te4 - T)}, \tag{10}$$

$$t7 = tt7 \cdot ln\left(\frac{xk3 \cdot (1 - xk1)}{xk4 \cdot (1 - xk3)}\right), \tag{11}$$

$$tt7 = \frac{1}{te4 - te3}. \tag{12}$$

To offset maximum consumption relative to the amount of prey available, we employed a variation of the Holling's type II functional response that accounts for multiple prey types (Rose et al., 1999a; 1999b) to calculate the realized daily consumption rate (Crel) for each life stage i (C_i; g prey $\cdot$ g fish^{-1} $\cdot$ d^{-1}) by summing consumption across each prey type j:

$$C_{rel_i} = \sum_{j=1}^{3} C_{rel_{ij}}, \tag{13}$$

$$C_{rel_{ij}} = \frac{C_{max} \cdot \dfrac{PD_{ij}v_{ij}}{K_{ij}}}{1 + \sum_{k=1}^{3} \dfrac{PD_{ik}v_{ik}}{K_{ik}}}, \tag{14}$$

where C_{max} is the maximum consumption rate (g prey · g fish-1 · d^{-1}) of an individual of stage i, PD_{ij} is the density of prey type j (g prey · m^{-3}) for life stage i, v_{ij} is the vulnerability of prey type j (dimensionless) for life stage i, and K_{ij} is the half saturation constant (g prey · m^{-3}) for life stage i of prey type j. Given ontogenetic dietary preferences of ELS shortbelly (Sumida and Moser, 1984; Reilly et al., 1992), we use three prey types produced by NEMUCSC for prey density; small zooplankton (ZS; micrograzers; j=1), large zooplankton (ZL; copepods; j = 2), and predatory zooplankton (ZP; Euphausiids or krill; j = 3). Prey composition of preflexion larvae (standard length (SL) < 8 mm) is comprised mainly of calanoid copepod nauplii (~ 75%) and copepodites (~2-12%), with the relative contribution of copepodites being largest at flexion (~25%) after which adult copepods dominate (>40%) throughout the postflexion stage (SL < 30mm; Sumida and Moser, 1984; Reilly et al., 1992). Various stages of Euphausiids comprise ~50% of pelagic juvenile diet, with considerable contribution of copepods (Reilly et al., 1992). Vulnerability values (v_{ik}) were assigned using these dietary preferences (Table 1). NEMUCSC treats the three zooplankton groups as functional groups based on prey size with ZL and ZP representing copepods and Euphausiids, respectively. The units of prey densities in NEMUCSC are tracked in mol N l^{-1} and were converted to g · prey · m^{-3} by:

$$\frac{14 \ g \ N}{mol \ N} \cdot \frac{1 \ g \ dry \ weight}{0.07 \ g \ N \ dry \ weight} \cdot \frac{1 \ g \ wet \ weight}{0.2 \ g \ dry \ weight} \cdot \frac{10^3 l}{m^3} =$$

$$10^{-6} g \ prey \ wet \ weight \ m^3. \tag{15}$$

Half-saturation coefficients, Kij, are used as a factor to scale satiation and represent the PDij at which half of maximum consumption is reached. Since very few

experiments have been conducted on multicellular organisms to determine half-saturation coefficients directly, irrespective of whether the taxa in question is a plant or animal (Mulder and Hendriks, 2014), we calibrate Kij by minimizing the deviation between length-at-age from model output relative to an empirical length-at-age curve that accounts for different growth stanzas separated out by life stage (preflexion, flexion, postflexion, and pelagic juveniles; Laidig et al., 1991). Tuning was achieved in a stepwise fashion by first calibrating the half saturation coefficient for life stage i before moving to life stage i+1 so that life stage transitions were achieved at the same age and size reported by Laidig et al (1991). Further, we assumed that life stage transitions were deterministically driven by length thresholds, rather than stage-based transition probabilities typical of structured matrix population models (Caswell, 2001) or through morphological developmental changes (Downie et al., 2020). We leveraged an empirical length-to-weight curve over the same life stages (Norton et al., 2001) to convert the state variable of the bioenergetics model (weight in grams) to standard length (SL) of fish (mm). In this way, while the parameterization of the consumption parameters, and the rest of the bioenergetics parameters for that matter, are meant to loosely represent a general rockfish, the calibrated consumption equation most closely matches that of shortbelly rockfish during four early life history stages, and as such likely provides appropriate estimates for many of the other co-occuring winter spawning rockfish, for which pelagic juvenile stages typically have comparable growth rates (Woodbury et al. 1991, Field, unpublished data).

2.2.2 Respiration

Respiration (R), or the rate of oxygen consumption during metabolic processes, is formulated in relation to body weight, seawater temperature, and activity due to swimming. The allometric function is given by:

$$R = a_R \cdot W^{b_R} \cdot F_R(T) \cdot ACT \cdot 5.258 \tag{16}$$

where a_R and b_R are the intercept and slope of the allometric relationship between resting respiration (g O2 $\cdot$ g fish^{-1} $\cdot$ d^{-1}) and W (g fish), $F_R(T)$ is the temperature dependence function for respiration, T is the temperature of seawater, ACT (dimensionless) is the metabolic cost due to swimming (applied as a scalar factor to respiration), and 5.258 is the standard conversion factor used in bioenergetics models to convert from g O2 $\cdot$ g fish^{-1} $\cdot$ d^{-1} to g fish $\cdot$ g fish^{-1} $\cdot$ d^{-1} (Kitchell et al., 1977; Hewett and Johnson, 1987; 1992; Hanson et al., 1997; Deslauriers et al., 2017).We employ a hump shaped function to relate temperature to respiration:

$$F_R(T) = V^X \cdot e^{X \cdot (1-V)}, \tag{17}$$

where:

$$V = \frac{RTM - T}{RTM - RTO}, \tag{18}$$

$$X = \frac{Z^2 \cdot \left(1 + \left(1 + \left(\frac{40}{Y}\right)^{0.5}\right)^2\right)}{400}, \tag{19}$$

$$Z = \ln RQ \cdot (RTM - RTO), \tag{20}$$

$$Z = \ln RQ \cdot (RTM - RTO). \tag{21}$$

Here T is the seawater temperature. RTO and RTM are the optimal and maximum temperature for routine metabolism, respectively. RQ approximates the standard Q10 (i.e., rates double for each 10C temperature increase). Since fish in the preflexion stage do not have much swimming capability (Kashef et al., 2014), we assume that their activity is minimal and assign ACT a value of 1. However, for flexion, postflexion, and pelagic juvenile stages, we assign values of 1.8, 1.7, and 1.6, which are similar to those used by Rose et al., (2015) for northern anchovy (Engraulis mordax), and assumes that the energetic costs to mobility decrease with ontogeny (Leis, 2007).

2.2.3 Specific Dynamic Action

Specific dynamic action (SDA) is the energy cost associated with the digestion of food. The percentage of total energy consumed that is used to digest food is believed to be relatively conserved, but the exact amount of energy lost to digestion is contingent on the amount of food consumed after accounting for egestion:

$$SDA = sda \cdot (C_{rel} - EG). \tag{22}$$

where sda is the specific dynamic action coefficient (dimensionless), C_{rel} is the realized consumption (g prey $\cdot$ g fish^{-1} $\cdot$ d^{-1}) and EG is egestion (g prey $\cdot$ g fish^{-1} $\cdot$ d^{-1}).

2.2.4 Egestion and Excretion

Egestion (fecal waste; EG) is the constant proportion (a_F) of food consumed that is indigestible and is formulated as such:

$$EG = a_F \cdot C_{rel}. \tag{23}$$

Excretion (nitrogenous waste; EX) is formulated as a constant proportion (aE) of consumption minus egestion (i.e. assimilation):

$$EX = a_E \cdot (C_{rel} - EG). \tag{24}$$

2.3 Empirical Data

Most California rockfish are winter or early spring spawners (Wyllie-Echeverria 1987, Love et al. 2002), and while the period of parturition is generally thought to be fairly constant by species, there is considerable variability in the timing of successful recruitment, as illustrated by variability in the birthdate distributions of surviving pelagic juveniles (Woodbury and Ralston, 1991; Lenarz et al., 1995). To initialize the bioenergetics model at the median date of parturition of surviving juveniles, we analyzed daily growth rings of sagittal otoliths (earbones) to determine birthdate frequency distributions from shortbelly specimens who survived early larval stages and were caught in the Rockfish Recruitment and Ecosystem Assessment

Survey (RREAS) midwater trawls as pelagic juveniles. The decision to initialize the bioenergetics model at the observed median date of parturition of survivors, rather than during the peak period of parturition (February; Wyllie-Echeverria 1987, Love et al. 2002), is so that we can align the environmental conditions in the model that would promote survival of shortbelly and hence so we can compare growth trajectories with the observed length-at-age curve of Laidig et al. (1991). RREAS has conducted annual midwater trawls in central California (36.5°N-38.2°N) from 1983-present and samples the micronekton assemblage from May-mid June (Sakuma et al., 2016; Field et al. 2021).

Daily ages are obtained from a subset of the collected fish through otolith microstructure analyses. Early years (1988-1992) are analyzed by Woodbury and Ralston (1991) and Lenarz et al. (1995) and we update birthdates to 2010 here. Briefly, sagittal otoliths are extracted, cleaned, and mounted on microscope slides using CrystalBond adhesive. Aluminum oxide films are utilized to hand polish otoliths down to a flat plane for better visualization. A compound microscope (25 – 100x magnification) and Image-Pro Premier imaging software (Media Cybernetics) are used to visualize otolith microstructure. As otolith formation and growth band-pair deposition begins during embryogenesis, the dark growth band denoting birthdate, the extrusion check (a distinctly darker band that forms the day the larvae are extruded from the mother), is identified to begin age determination. The concentric dark growth bands post-extrusion check through to the terminal edge of

the otolith are counted to determine fish age using standard procedures (Stevenson and Campana, 1992).

Subtracting the age of a fish from the date of capture gives an individual's birthdate. To back-calculate birthdates for all individuals (aged and unaged), we developed a length-at-age relationship using SL for all individual specimens that were aged. To account for interannual differences in growth, we fit linear regression models to each year with sufficient data. We used the overall length-at-age relationship (all years) for years that did not have age data but had length frequency data (1999, 2000 and 2002). The overall median birthdate of pelagic juveniles that survived from parturition to being caught in the survey, after accounting for interannual changes in growth, were used to initialize the start date of model simulations.

We compared spatial patterns of juvenile growth potential from the 2D Eulerian version of the coupled ROMS-NEMUCSC and bioenergetics model (see 2.4 Simulations) with spatial patterns of juvenile shortbelly abundance from the RREAS. To estimate observed spatial effects, we fit a delta-generalized linear model (Δ-GLM) to raw catch data over 1988-2010 (Stefánson, 1996; Dick, 2004; Maunder and Punt, 2004). A Δ-GLM first fits a binomial presence/absence model and then the probability of a presence is multiplied by the estimated mean conditioned on a positive observation from a lognormal model with zero catches removed. We included year, station, and period (based on binned intervals of Julian day, to account for seasonality) as main effects following Ralston et al. (2013) and Schroeder et al.

28

(2019). Station effects were then mapped to characterize empirical spatial distribution and to compare with a 2D Eulerian spatial growth potential simulation.

2.4 Simulations

A 0-D version of the bioenergetics model was used to calibrate half-saturation coefficients in Equation 14 across four early life stages (preflexion, flexion and postflexion larvae, and pelagic juveniles). To calibrate the model, we minimized the deviation between length-at-age produced by the model with that of an empirical length-at-age relationship accounting for life stage-specific growth stanzas (Laidig et al., 1991) by calibrating life stage i before moving to life stage i+1 so that the lengths separating each life stage in the model deterministically matched the same length and age of observations. The 0-D simulation was initialized on the median birthdate derived from otolith microstructure analysis over the period 1988-2010 and ran for 150 days, which is roughly the age at which pelagic juveniles settle out from the water column and recruit to their adult habitat (Love et al., 2002). Wet weight was updated each day using daily climatological temperature and prey concentration (1988-2010) at 30 m depth over 36°N-39°N, 124°W-121.5°W. Since fish cannot shrink in length, but can lose weight, we held length constant if a fish lost weight. Length would resume increasing once their weight returned to their expected weight-at-age. Therefore, fish could get skinny and be in poor condition or be fat and in good condition. We saved the following variables to output files: realized consumption (ZS, ZL, ZP, and total), proportional consumption (ZS, ZL, ZP, and total), egestion,

excretion, specific dynamic action, respiration, mass-specific growth, growth, weight-at-age, and length-at-age.

A 2-D version of the model was implemented over the RREAS sampling area (36°N-39°N, 124°W-121°W) to examine spatial patterns of growth potential in response to the spatial climatology (1988-2010) of temperature and prey availability. Bioenergetics formulations were embedded into the center of each grid cell at 30m depth and growth trajectories tracked for 150 days in a Eulerian sense. Thus, we model the growth potential throughout the central California region to assess what growing conditions would have been had a fish occupied a particular grid cell (Brandt et al., 1992; Henderson et al., 2019). Composite growth maps were produced for qualitative comparisons with empirical data by taking the mean of daily growth (in weight) across each of the four life stages for each grid cell in the model domain.

2.5 Sensitivity Analysis and Scenario Tests

2.5.1 Individual Parameter Perturbation

We conducted a sensitivity analysis using individual parameter perturbation (IPP) on the 0-D climatology simulation to quantify uncertainty in the standard parameters of the bioenergetics model (Bartell et al., 1986). Each parameter was allowed to vary by +/- 5%, +/- 10% and +/- 20% of the control run values, which are standard sensitivity perturbations explored in other sensitivity analyses of bioenergetics models (Hartman and Kitchell, 2008). Length-at-age plots between the control run and each perturbation were plotted to visually compare growth

trajectories. Model bias was calculated over each 150-day simulation by subtracting the length-at-age of the IPP simulation from the control run and standardized by dividing by length-at-age of the control. Overall model bias for each perturbation experiment was calculated by summing up the square root of daily model bias (analogous to sum of squares). We refer to the overall model bias as the total sum of squares (TSS). To examine the directionality of model bias, we calculate the ratio of change (ROC) as the difference in standard length for the final day of the simulation for an IPP run minus the control, standardized by the standard length of the control run at the final day of the simulation.

2.5.2 Scenario Tests

We performed a scenario test on the bioenergetics forcing factors to explore how changes in temperature and prey concentration affect model predictions and to make inference about future climate conditions. First, we examined the effect of holding temperature (prey) constant at the mean value (i.e., took the mean of prey (temperature) over the 150-day time series used in the 0-D control run) and allowed prey (temperature) to vary daily (same forcing as control run) to understand the influence of daily and seasonal variability in forcing variables on growth performance, relative to fixed temperature or prey concentration. Next, four separate scenario tests were conducted on different combinations of constant temperature and prey availability to understand the influence of novel conditions on growth performance. Scenario 1 allowed temperature to vary about the mean (+/- 5%, +/- 10% and +/- 20%) while holding prey concentrations constant at the mean. Scenario 2

allowed prey concentrations to vary about their respective mean (same as Scenario 1) while holding temperature constant at the mean. Scenario 3 allowed temperature and prey concentrations to vary (magnitude of change same as Scenario 1 & 2), but in equal fashion; temperature and prey concentrations were both added to, or subtracted from, the mean simultaneously. Finally, Scenario 4 allowed temperature and prey concentrations to vary but in opposite directions (i.e., add 5% of temperature and subtract 5% of prey concentrations and vice versa). We report ROC for all combinations of each scenario test.

3. Results

3.1. Simulated historical temperature and prey concentrations

Temperature, microzooplankton (ZS), mesozooplankton (ZL) and predatory zooplankton (ZP) from the 23-year climatology of ROMS-NEMUCSC for the focal area of our study exhibits marked seasonal cycles (Figure 2-3). When spatially averaged over the study region to produce the 0-D climatology at 30m depth, temperature decreases from January 1st-May14th, increases until the end of September, before decreasing for the remainder of the year (Figure 2). The thermocline is shallowest from April to July during peak upwelling and stratification is strongest from July to mid-November (Figure 3). As expected, temperature decreases with latitude, with the coolest temperatures (~10-11°C) at the northernmost latitudinal range (38-39°N) from late March to July (Figure 3), and the warmest temperatures (~14-15.5°C) being found at the southernmost latitudes (36-37°N) during the Fall (Figure 4). The coolest temperatures occur closest to the coast during

the winter and spring months and increase with distance offshore (not shown). These temperature patterns reflect the seasonality of coastal wind-driven upwelling and in turn drive primary and secondary productivity.

Zooplankton concentrations produced by NEMUCSC exhibit seasonal patterns (Figure 2-3). All three zooplankton functional groups increase from a minimum beginning on January 1st but peak at different times (Figure 2); ZS concentration is greatest in mid-March (0.45 mol N m^{-3}); ZL is greatest in mid-May (0.39 mol N m-3); and ZP is greatest in late-June (0.35 mol N m^{-3}). Horizontally, peak zooplankton concentrations occur at ~37.5 °N and between 123-122.25 °W (Figure 3), which is located just south of the Gulf of Farallones, near Pioneer Canyon (Figure 1).

3.2. Birthdate Distribution and 0-Dimensional Bioenergetics Climatology

Otolith microstructure analysis of pelagic juvenile shortbelly rockfish caught in the RREAS midwater trawls over the period 1988-2010 estimated a median back-calculated birthdate of March 15th, with a standard deviation of 24 julian days (n = 8,645; Figure S2). The frequency of back-calculated birthdates had a bimodal distribution with a peak occurring in mid-February and a second peak in late-March/early-April. The median birthdate was used as the day of year to initialize the 0-D climatology bioenergetics model.

Ontogenetic changes in respiration, consumption and subsequent growth are partially driven by daily and seasonal changes in temperature and prey availability

(Figures 2, 3 and 4A-B). Temperature declined from the start to three quarters of the way through the postflexion larval stage, after which temperature increased and continued to increase throughout the pelagic juvenile stage (Figures 2, 3 & 4A). 100% of the preflexion larval diet comes from ZS, with ZS comprising 50%, 50%, and 20% of flexion, postflexion and pelagic juvenile diets, respectively (Table 1). ZS concentration was relatively high and stable throughout the simulation. The preflexion stage coincided with the highest ZS concentration (~0.45 mol N m^{-3}), flexion occurred when ZS concentration were slightly decreased (~0.43 mol N m^{-3}), while postflexion and pelagic juvenile stages took place when ZS were slightly further decreased (~ 0.38 mol N m^{-3}; Figure 2, 3 & 4B). ZL comprises 0%, 50%, 50% and 30% of preflexion, flexion, postflexion and pelagic juvenile diets, respectively (Table 1). The flexion stage coincided when ZL concentrations were relatively high and stable (~0.36 mol N m^{-3}), with the postflexion stage occurring when ZL were slightly increased (~0.38 mol N m^{-3}) and the pelagic juvenile stage was slightly decreased from the preceding life stage (~0.37 mol N m-3 (Figure 2, 3 & 4B). ZP comprises 0% of the diet of preflexion, flexion, and postflexion larval stages and 50% of pelagic juvenile diet (Table 1). During the pelagic juvenile stage ZP concentration was at a maxima but declined slightly during the last 20 days of the simulation (Figures 2, 3 & 4B).

The final calibration of the ELS bioenergetics model yielded a length-at-age curve that closely matched the observed length-at-age curve for shortbelly rockfish (Figure 4I). Importantly, the starting and ending standard lengths for each life stage

(preflexion larvae, Stage I; flexion larvae, Stage II; postflexion larvae, Stage III; and pelagic juvenile, Stage IV) from the simulation closely match that of the empirical length-at-age curve, implying that the model, on average, reproduces ontogenetic developmental stages at the same age (Stage I <14 days old; Stage II < 26 days old; Stage III < 73 days old; Stage IV > 74 days old). The model produces a mean growth rate of ~0.667 mg day-1 (0.432 mm SL day^{-1}; Figure 4F-G) and closely tracks the empirical growth trajectory across all ontogenetic stages (Figure 4H-I). Within ontogenetic stages, average modeled growth for preflexion larvae is ~0.21 mm SL day-1 (~0.25 mg day^{-1}), ~0.10 mm SL day-1 (~0.37 mg day^{-1}) for flexion larvae, 0.45 mm SL day^{-1} (~8.12 mg day^{-1}) for postflexion larvae, and ~0.51 mm SL day-1 (~57 mg day^{-1}) for pelagic juveniles. In comparison, the empirical growth measurements for preflexion larvae are ~ 0.21 mm SL day^{-1}, ~0.08 mm SL day^{-1} for flexion larvae; ~0.47 mm SL day^{-1} for postflexion larvae, and 0.52 mm SL day^{-1} for the pelagic juvenile stage. However, along a growth trajectory, the model slightly overestimates growth for postflexion larvae as the model produces a more linear change in SL while the empirical trajectory is convex.

Ontogenetic changes occur for total mass-specific respiration rate (g fish · g fish^{-1} · d^{-1}), with the largest relative rate of oxygen consumption (~35%) happening during the flexion stage and declining thereafter (Figure 4C). These stepped changes in total mass-specific respiration are due to ontogenetic changes in activity levels (ACT; Table 1). Mass-specific consumption rates (g prey · g fish^{-1} · d^{-1}) are greatest at the transition between flexion and post-flexion stages (Figure 4D). Ontogenetic

35

changes in mass-specific consumption are primarily due to changes in half-saturation

coefficients (K_{ij}; Table 1) but are also attributed to changes in dietary preferences (v_{ij},

Table 1) and to seasonal changes in temperature and prey concentrations (Figure 1).

Proportional consumption relative to maximum consumption is at a minimum for

newborn larvae (~20%; preflexion larvae) and increase throughout ontogeny (up to

~50% by the end of the pelagic juvenile stage), with a pronounced, and stepped,

increase at the transition from flexion to postflexion larval stages (Figure 4E).

3.3. Sensitivity Analysis: Individual Parameter Perturbation

Sensitivity of bioenergetics parameters by individual parameter perturbation

(IPP) are quantified as the ratio of change (ROC (Figure 5). IPP identifies the

allometric slope and intercept of maximum consumption (cb and ca, respectively) as

having the largest effect on growth. The relative influence of decreasing the values of

cb and ca are larger compared to an increase because growth is slowed under smaller

values, and thus, more time is spent in earlier larval stages where mass-specific

growth rates are slower. A similar pattern is found for the slope and intercept of

allometric respiration (rb and ra, respectively), and the optimal temperature for

respiration (RTO), which had the third, fourth and fifth largest effect, respectively

(Figure 5). The temperature-dependence on maximum consumption parameter

describing the peak of the ascending limb of the temperature-dependence function

(te2), maximum temperature for respiration (RTM) has the smallest effect on growth

(Figure 5). All other parameters tested in the sensitivity analysis have a modest effect

on the final size of fish (Figure 5).

3.4. Scenario Tests: Sensitivity of Forcing Factors.

When holding temperature constant and allowing prey concentrations of ZS, ZL and ZP to vary daily (i.e. same as in control runs), the final SL did not vary much from the control (ROC = 0.002), nor did the trajectory over the 150 day simulation period (TSS = 0.48). When holding prey constant and allowing temperature to vary daily, the final SL was slightly smaller than the control (ROC = -0.019), however, the growth trajectory over the simulation period was faster compared to the control (TSS = 5.031). When holding both temperature and prey concentrations constant about their mean, length-at-age was consistently higher (TSS = 5.95), however, the final length-at-age was slightly smaller (ROC = -0.027).

Increasing mean temperature causes the largest discrepancies compared to a decrease in temperature or changes to prey concentration (Figure 6). For example, in Scenario 1, increasing temperature by 20% causes fish to grow more slowly, resulting in fish that were ~40% smaller by the end of the simulation (ROC = -0.40; Figure 6). In contrast, when decreasing temperature by 20%, fish grow faster and are ~14% larger by the end of the simulation (ROC = 0.135). By comparison, decreasing prey concentration by 20% (Scenario 2) causes fish to grow more slowly with the final length of fish being 27% smaller than the control (Figure 6). Increasing prey concentration has marginal improvements to growth with a 20% increase in prey concentration resulting in fish that are 16% larger at the end of the simulation (Figure 6). These results suggest that temperature has a larger impact on growth performance compared to prey availability and the directionality of change matters more than the

magnitude of change; increasing (decreasing) temperature (prey concentration) has a disproportionate negative influence on growth compared to decreasing temperature or increasing prey concentration. This result is strengthened by the ROC scores for Scenario 3 and Scenario 4. Scenario 3, which allows both temperature and prey concentrations to vary in the same direction, leads to a dampening effect; increasing temperature and prey concentration by 20% leads to a 20% decrease in the final length of fish at the end of the simulation, while decreasing both temperature and prey concentration leads to a ~10% decrease in final length (Figure 6). However, in Scenario 4, when temperature increases by 20% and prey concentration decreases by 20%, fish are 89% smaller at the end of the simulation relative to the control (Figure 6). Decreasing temperature by 20% and increasing prey concentration by 20% leads to a ~34% increase in final length (Figure 6). Importantly, when a scenario led to a decrease in growth, deviations were amplified because length-based stage transitions caused fish to get 'stuck' in the slow growing flexion stage and were unable to transition to the faster growing postflexion stage. The ROC for this situation was always -0.89.

3.5. 2-D Eulerian Climatology and Pelagic Juvenile Spatial Distribution

The Eulerian climatology (1988-2010) of spatial patterns of growth potential for preflexion, flexion, and postflexion larvae, and pelagic juveniles reveals heterogeneity of growth potential with different spatial patterns associated with each life stage (Figure 7). The spatial pattern of growth potential is patchiest for preflexion larvae with maximum growth (~0.4-0.45 mg day^{-1} (0.3-0.4 mm day^{-1})) constrained to

a localized region of the mid and outer shelf to the south of the Gulf of Farallones

Islands, containing Pioneer Canyon and Ascension Canyon (Figure 7A). A similar

pattern occurs for flexion larvae, albeit over a slightly larger area, with maximum

growth rates of ~0.6 mg day^{-1} (0.2-0.25 mm day^{-1} (Figure 7B). Spatial patterns of

growth potential for postflexion larvae are most homogeneous with maximum growth

of 9-10 mg day^{-1} (0.5-0.6 mm day^{-1}) over the shelf break along the entire latitudinal

extent of the study region (Figure 7C). Pelagic juvenile growth potential is slightly

more constrained to the shelf break compared to postflexion larvae, with maximum

growth rates of 70 mg day^{-1} (0.5 mm day^{-1}) just offshore of the greater Farallones

region and monotonically declining to 25 mg day^{-1} (~0.3 mm day^{-1}) towards the

southwest extent of the model domain (Figure 7D). Collectively, while there is

considerable variability in growth performance across individual grid cells (Figure 7),

an average of all growth trajectories fits well within empirical growth estimates,

noting a slight overestimation of mean growth potential for postflexion larvae (Figure

8), further supporting the notion that the model is well calibrated to handle a range of

temperature and prey conditions. Station-effects from the Δ-GLM of pelagic

juveniles caught by midwater trawls in the RREAS reveals peak abundance of

shortbelly over the 200m isobath, just to the south of the Gulf of Farallones, at two

stations near Ascension Canyon, and in the outer Monterey Bay area (Figure 9),

which is consistent with the spatial patterns of growth potential for the pelagic

juvenile stage (Figure 7D).

4. Discussion

This study presents a highly resolved ontogenetic bioenergetics model for the ELS of an ecologically important fish in the central California Current System (CCS), the shortbelly rockfish. When accounting for ontogenetic dietary preferences and feeding rates through a realized consumption term (Rose et al., 1999a; 1999b), the baseline bioenergetics model presented here sufficiently reproduces empirical growth stanzas of preflexion, flexion, and postflexion larvae and pelagic juvenile shortbelly rockfish in the central CCS (Laidig et al., 1991) which would not have been recovered if stage-specific adaptations to the model were ignored. Growth during ELS's can contribute to differential survival from year-to-year and lead to orders of magnitude changes in recruitment (Houde, 2008). At what ELS stage a bottleneck to survivorship occurs from growth-dependent mortality can vary in both space and time depending on the timing of reproduction, successional changes in preferred prey types, and changes in environmental forcing that affects growth rates (Peck and Hufnagl, 2012). A model that accounts for highly resolved changes in ELS growth stanzas, such as the one presented here, can help to elucidate at what early life stage growth-dependent mortality is most pronounced under a given set of environmental conditions. Conversely, failure to account for ontogenetic variability within mechanistic growth models can obscure growth-dependent survival if the directionality of the relationship changes across life stages (e.g., slow growth, high survival during early larval stages v. fast growth, high survival during later ELS's; Robert et al., 2023).

Some interesting patterns emerge when comparing the seasonality of forcing factors with the timing of model initialization and developmental transitions. First, the optimal temperature for consumption (~12°C) occurs at the beginning of March, just prior to model initialization. While upwelling is somewhat persistent in central California (36-39°N), the spring transition dates for this region occur on average during February (Bograd et al., 2009), which preconditions the ecosystem with cool waters and plankton production that is advantageous to shortbelly rockfish prior to the median parturition date of March 15th (Schroeder et al., 2009; 2013; Black et al., 2010). First feeding preflexion larvae are obligate feeders on small zooplankton which peak in abundance near the start of the simulation. Similarly, as shortbelly progress through ontogeny, the proportion of large zooplankton and krill (ZP) becomes increasingly important to diet and the temporal aspect of this prey switching mirrors the phenology/succession in prey concentration predicted by the ROMS-NEMUCSC historical simulation. Taken together, this suggests, at least in a climatological sense, a temporal match between prey production, the timing of average reproduction leading to survival of pelagic juveniles (based off otolith microstructure analysis), and transitions between developmental stages. The match-mismatch hypothesis posits year class success is enhanced when there is a temporal overlap between fish larvae and zooplankton prey (Cushing 1969; 1982; 1990; Durant et al., 2005; 2007; 2013). However, the CCS is highly dynamic (Checkley and Barth, 2009) over multiple scales (Chavez and Messié, 2009) and exhibits pronounced interannual variability in plankton production (McGowan et al., 1998). If fish spawning times are fixed, or spatially invariable, a mismatch between predator and

prey can occur, causing recruitment failure. For example, atmospheric blocking of poleward winds in 2005 (Sydeman *et al*., 2006) delayed coastal upwelling in the central CCS (Schwing *et al*., 2006) which led to reduced plankton production in late winter and early spring (Thomas and Brickley, 2006; Jahncke *et al.*, 2008) when peak rockfish production occurs (Love et al., 2002). These series of events coincided with low biomass anomalies of pelagic juvenile shortbelly rockfish for our study region (Ralston and Stewart, 2013), possibly owing to a temporal mismatch between peak reproduction and prey availability. Over longer time scales, however, natural selection should favor the timing of life history events that align with the long-term seasonality of environmental conditions (Ji et al., 2010; Giménez, 2011; Durant et al., 2019). Using a temperature and zooplankton climatology from a coupled physical-biogeochemical simulation to force a bioenergetics model that accounts for ontogenetic changes in feeding parameters fortuitously demonstrates the temporal alignment between temperature, zooplankton succession, and the timing of developmental transitions, inline with the match-mismatch hypothesis.

Empirical growth rates for ELS rockfish in the CCS are known to vary interannually (Crane, 2014; Fennie et al., 2023a; 2023b; Johnson et al., 2001; Lenarz et al., 1995; Wheeler et al., 2017). For shortbelly rockfish specifically, empirical growth rates of surviving pelagic juveniles during the 1980s ranged between 0.524 mm/day to 0.638 mm/day (Woodbury and Ralston, 1991), which are within our predictions for the same life stage. However, ontogenetic changes in growth are known to occur for marine fishes (e.g. Hare and Cowen, 1995) and we found that

somatic growth of larvae is slower, especially for flexion larvae, than that of pelagic juveniles. Considerable developmental and physiological changes occur during larval metamorphosis, e.g. during flexion, the posterior end of the notochord turns upward and fins begin to differentiate, changing the rate of somatic growth (Blaxter, 1969; Ricker, 1979). The physiological response for flexion larvae, in the context of our model, is an abrupt increase in mass-specific respiration (driven by an increase ACT) which must be compensated for by an increase in consumption to meet energetic demands. This has implications for the effect of temperature changes due to natural climate variability and anthropogenic climate change, and associated changes in lower trophic level productivity on growth since respiration and consumption are temperature-dependent. Moreover, we note that our parameterization of allometric formulations (e.g. respiration and consumption) did not account for ontogenetic changes, but rather our model only considers changes in observed dietary preferences (vulnerability; v_{ij}) and feeding rate parameters that were estimated within the model (i.e. half saturation constants; K_{ij}) to account for life stage-specific growth rates. This suggests that even with a paucity of detailed species-specific experimental data on ontogenetic changes in physiology, the bioenergetics model can still generate realistic predictions of somatic growth across larval and pelagic juvenile ELS's given a highly resolved length-at-age curve with designated length-based stage transitions.

We subjected the 0-D climatological bioenergetic model to a sensitivity analysis by individually perturbing parameters at set percentages (Bartell et al., 1986). Our results indicate that the most sensitive parameters are associated with allometric

consumption and respiration, which is similar to the findings of other bioenergetics sensitivity analyses (Kitchell et al., 1977; Bartell et al., 1986; Megrey et al., 2007; Brodie et al., 2016). We adopted most of our parameter values from a generic adult rockfish bioenergetic model (Harvey, 2005; 2009) and consumption parameters from settled juveniles (Boehlert & Yoklavich, 1983), which, given ontogenetic changes in physiology and allometry (Peck and Moyano, 2016), likely caused larger deviations than would have occurred if we had access to ELS specific parameters of consumption and respiration. However, we used the best available data at the time of model development. The use of a realized consumption term that accounts for seasonal changes in prey concentration (from NEMUCSC) as well as ontogenetic differences in preferred prey from field data (Sumida and Moser, 1984; Reilly et al., 1992) may offset the bias between predicted and observed length-at-age when using energetics parameters for settled juveniles and adults. Our findings could be refined with consumption and respiration experiments on the ELS of commercially and ecologically important rockfishes (e.g. Boehlert, 1978; 1981; Boehlert and Yoklavich, 1983) to get more reliable estimates of allometric parameters to reduce model uncertainty. However, logistical constraints may complicate this call as culturing the appropriate prey items for rearing larval rockfishes in a laboratory setting is a time-intensive challenging endeavor. Furthermore, care must be taken when using controlled laboratory experiments that estimate temperature-dependence parameters of performance (i.e. respiration, consumption, and activity) because of Jensen's inequality (Jensen, 1906; Ruel and Ayres, 1999). Typically, temperature- and weight-specific parameters are calculated from controlled laboratory experiments where

temperatures are held constant within treatments. Performance of an individual under average temperature is different compared to the average performance in a thermally variable environment. Nonlinear averaging techniques can alleviate these biases (Bernhardt et al., 2018), but caution is still warranted because they do not account for time-dependent interactions between body temperature and physiological plasticity (Denny, 2019).

We assessed the relative influence of temperature and prey concentrations on growth through an orthogonal manipulation of respective forcing factors. Temperature had a larger effect on growth trajectories than prey concentration, but the deviance in growth rates depended on the directionality of temperature change with warmer temperatures disproportionately decreasing growth relative to cooler temperatures increasing growth. This is because increasing temperatures had a large effect on consumptive rates as the temperature moved outside of the optimum and decreased consumption; decreasing temperature, even by 20%, allowed consumption to stay within the optimum. As expected, decreasing food availability led to a decrease in growth and vice versa. Moreover, both a synergistic and antagonistic effect was found when temperature and food availability were allowed to covary. An antagonistic effect was found when forcing changed in the same direction since the relative effect of increasing (decreasing) temperature was partially offset by an increase (a decrease) in food availability. Conversely, a synergistic effect was found when temperature and prey concentration varied in opposite directions. This scenario is what is predicted for the CCS under anthropogenic climate change, specifically an

increase in temperature and a possible decrease in zooplankton concentrations (Pozo Buil et al., 2021; Fiechter et al., 2021; Koenigstein et al., 2022), which according to our model, could lead to a substantial decline in growth, and under the extreme case (20% increase in temperature, 20% decrease in prey concentration), fish were unable to grow out of the flexion stage which is probably not realistic. Nevertheless, recognizing that growth is linked to mortality (e.g., the stage duration hypothesis; Houde, 1989), this scenario would lead to severe mortality and a significant decline in recruitment unless fish can move to cooler habitat with increased food production. The coastal pelagic environment of the central CCS is a biodiversity hotspot for marine predators (Hazen et al., 2013) and many species are reliant upon shortbelly rockfish and co-occurring juvenile rockfishes as a prey source (Szoboszlai et al., 2015). For example, diets of the common murre (*Uria aalge*) switch from pelagic juvenile rockfish to northern anchovy under low rockfish regimes, which results in the incidental predation of juvenile salmon that frequently co-occur with northern anchovy in coastal waters (Wells et al., 2017). However, caution is warranted in our scenario approach because of Jensen's inequality. However, when we kept prey concentration the same as in the control run and held temperature constant at its nominal value (mean of temperature throughout the duration of the simulation), length-at-age over the duration of the simulation and the terminal length at the end of the simulation was nearly the same as the control run (TSS = 0.48; ROC = 0.002, respectively). Additional research on the impacts of Jensen's inequality to bioenergetic model predictions in relation to the scale of temporal variability of temperature is needed (e.g., Holsman and Danner, 2016).

The 2-D Eulerian climatology of spatial growth potential reveals spatial patterns strikingly similar to the known distribution of reproducing adults, the dispersal of larvae, as well as the distribution of pelagic juvenile shortbelly rockfish. Interestingly, the model produced patchy spatial patterns of growth for the earliest life stages and more homogenous patterns for later ELS's. For preflexion (<14 days old) and postflexion larvae (15-26 days old), growth is maximized along the shelf break just offshore of San Francisco, near the Farallones Islands and Pioneer Canyon, and to a lesser extent, Ascension Canyon. This region is federally protected under the United States Greater Farallones National Marine Sanctuary and overlays the main spawning grounds for shortbelly rockfish, as revealed by extensive spatial sampling of recently born larvae (age 0-2 days; Ralston et al., 2003; their Fig. 11). Furthermore, nutritional dynamics of embryos from gestating females in this region contain a higher prevalence of lipids and proteins that aid in starvation resistance relative to areas to the north (i.e. Cordell Bank), suggesting this region is favorable for both larval production, and in light of our study, larval survival (MacFarlane and Norton, 1999). Spawning site fidelity is, on average, an adaptive strategy that places larvae in habitat favorable for survival (Ellersten et al., 1989). Recognizing that faster early larval growth is tied with reduced mortality (Houde, 1989), adults who reproduce in areas of enhanced growth, on average, ensure a higher probability of early life survival and life cycle closure (Cushing, 1969; Sinclair, 1988). Furthermore, as larvae progress through ontogeny, and are vulnerable to dispersal by ocean currents, survival is contingent upon starvation resistance and predator avoidance (Peck and Hufnagle, 2012). Our spatial climatology of growth reveals favorable growing conditions for

postflexion larvae throughout the study area suggesting that, on average, late-stage larvae can find sufficient food to resist starvation as long as they are not advected too far offshore where zooplankton production is reduced and temperatures are warmer (Checkley and Barth, 2009). Finally, there is spatial coherence between the distribution of pelagic juveniles and the spatial pattern of maximum growth potential. The preponderance of pelagic juvenile rockfish having the ability to resist offshore advection (Larson et al., 1994; Kashef et al., 2014) along with our results, points to the possibility of pelagic juvenile rockfish behaviorally aggregating in areas that are favorable for growth, survival, and settlement. Taken together, our model generates spatial patterns of growth potential for each of the four early life stages of shortbelly rockfish that are in line with known attributes of their life history strategies which would not be quantifiable if life stage-specific parameterizations of feeding rates and dietary preferences were ignored.

To conclude, we demonstrate, to the first of our knowledge, that a bioenergetics model with high ontogenetic resolution of the early life stages for a marine fish can produce accurate predictions of somatic growth using imperfect physiological data (i.e. adult parameters). We relied on imprecise ontogenetic parameterizations of key physiological functions (e.g. allometric metabolism) which can be offset with accurate environmental forcing, knowledge of reproductive phenology and ontogenetic changes in dietary preferences. Bioenergetic growth models that account for within ELS growth stanzas can be nested within Lagrangian individual-based models to understand the mechanisms of recruitment variability, and

at what life stage(s) bottlenecks to survival occur. Mechanistic models, such as the

one we present here, can be applied under the backdrop of various climate change

scenarios, or be used to inform ecosystem-based fisheries management objectives.

Tables and Figures

Table 1. Summary of parameter values used in the shortbelly rockfish (*Sebastes jordani*) bioenergetics model.

Parameter	Description	Units	Value	Source
	Consumption			
a_C	Intercept for C_{max} at (te1+te3)/2	-	0.4613	Boehlert & Yoklavich, 1983
b_C	Coefficient for C_{max} vs. weight	-	-0.335	Boehlert & Yoklavich, 1983
te1	Temperature for xk1	°C	5	Derived
te2	Temperature for xk2	°C	8	Derived
te3	Temperature for xk3	°C	12	Derived
te4	Temperature for xk4	°C	20	Derived
xk1	Proportion of C_{max} at te1	-	0.1	Megrey et al., 2007
xk2	Proportion of C_{max} at te2	-	0.98	Megrey et al., 2007
xk3	Proportion of C_{max} at te3	-	0.98	Megrey et al., 2007
xk4	Proportion of C_{max} at te4	-	0.1	Megrey et al., 2007
	Multispecies functional response			
u_{11}	Vulnerability of ZS to	-	1	Sumida & Moser 1984

	preflexion larvae			
u_{12}	Vulnerability of ZS to flexion larvae	-	0.5	Sumida & Moser 1984
u_{13}	Vulnerability of ZS to postflexion larvae	-	0.5	Sumida & Moser 1984; Reilly et al., 1992
u_{14}	Vulnerability of ZS to pelagic juveniles	-	0.2	Reilly et al., 1992
u_{21}	Vulnerability of ZL to preflexion larvae	-	0	Sumida & Moser 1984
u_{22}	Vulnerability of ZL to flexion larvae	-	0.5	Sumida & Moser 1984
u_{23}	Vulnerability of ZL to postflexion larvae	-	0.5	Sumida & Moser 1984; Reilly et al., 1992
u_{24}	Vulnerability of ZL to pelagic juveniles	-	0.3	Reilly et al., 1992
u_{31}	Vulnerability of ZP to preflexion larvae	-	0	Sumida & Moser 1984
u_{32}	Vulnerability of ZP to flexion larvae	-	0	Sumida & Moser 1984
u_{33}	Vulnerability of ZP to	-	0	Sumida & Moser 1984;

	postflexion larvae			Reilly et al., 1992
u_{34}	Vulnerability of ZP to pelagic juveniles	-	0.5	Reilly et al., 1992
K_{11}	Half saturation constant for ZS to preflexion larvae	g fish wet weight m^{-3}	2	Calibrated
K_{12}	Half saturation constant for ZS to flexion larvae	g fish wet weight m^{-3}	1.5	Calibrated
K_{13}	Half saturation constant for ZS to postflexion larvae	g fish wet weight m^{-3}	0.5	Calibrated
K_{14}	Half saturation constant for ZS to pelagic juveniles	g fish wet weight m^{-3}	0.2	Calibrated
K_{21}	Half saturation constant for ZL to preflexion larvae	g fish wet weight m^{-3}	0	Calibrated
K_{22}	Half saturation constant for ZL to flexion larvae	g fish wet weight m^{-3}	1.4	Calibrated
K_{23}	Half saturation constant for ZL to postflexion larvae	g fish wet weight m^{-3}	0.5	Calibrated

K_{24}	Half saturation constant for ZL to pelagic juveniles	g fish wet weight m^{-3}	0.4	Calibrated
K_{31}	Half saturation constant for ZP to preflexion larvae	g fish wet weight m^{-3}	0	Calibrated
K_{32}	Half saturation constant for ZP to flexion larvae	g fish wet weight m^{-3}	0	Calibrated
K_{33}	Half saturation constant for ZP to postflexion larvae	g fish wet weight m^{-3}	0	Calibrated
K_{34}	Half saturation constant for ZP to pelagic juveniles	g fish wet weight m^{-3}	0.4	Calibrated
Respiration				
a_R	Intercept for R	-	0.0143	Harvey et al., 2011; Rooper et al., 2012
a_C	Coefficient for R vs. weight	-	-0.2385	Harvey et al., 2011; Rooper et al., 2012
RQ	Slope for temperture dependence of respiration (Q10)	-	2	Harvey et al., 2011; Rooper et al., 2012
RTO	Optimum temperature for respiration	°C	23	Harvey et al., 2011; Rooper et al., 2012

RTM	Maximum temperature for respiration	°C	28	Harvey et al., 2011; Rooper et al., 2012
ACT	Activity Multiplier	-	1[a]; 1.8[b]; 1.7[c]; 1.6[d]	Rose et al., 2015
Egestion and Excretion (Eg and U)				
a_F	Proportion of consumed food egested	-	0.104	Harvey et al., 2011; Rooper et al., 2012
a_E	Proportion of consumed food excreted	-	0.068	Harvey et al., 2011; Rooper et al., 2012
Specific Dynamic Action				
SDA	Specific Dynamic Action	-	0.163	Harvey et al., 2011; Rooper et al., 2012
Energy Density				
ED_{zoopl}	Energy density of zooplankton	J g prey^{-1}	2580	Megrey et al., 2007
ED_{fish}	Energy density of rockfish	J g fish^{-1}	4850	Spear, 1993; Warzybok et al., 2018
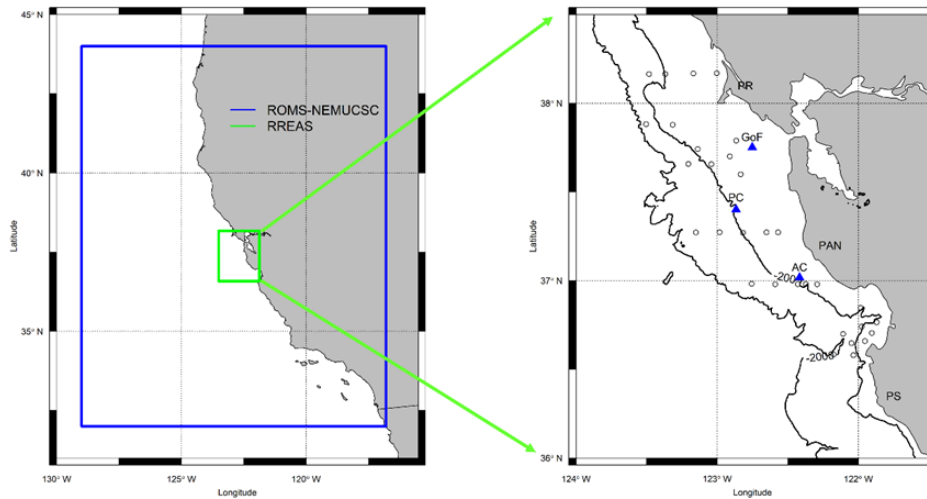
Figure 1. Map of the California Current System and focal study area (inset). Spatial extents for the 3km resolution ROMS-NEMUCSC (blue box) and the core Rockfish Recruitment and Ecosystem Assessment Survey (RREAS) survey area (green box and inset). Spatial extent used for generating the 0-D climatology temperature and zooplankton concentrations from ROMS-NEMUCSC with RREAS sampling stations (open circles) and 200m and 2,000m isobaths shown. (inset) Major promontories are labeled on land (PR = Point Reyes; PAN = Point Año Nuevo; PS = Point Sur) and the Gulf of Farallones (GoF) and two canyon systems (blue diamond: PC = Pioneer Canyon; AC = Ascension Canyon) important to shortbelly rockfish (*Sebastes jordani*) life history.
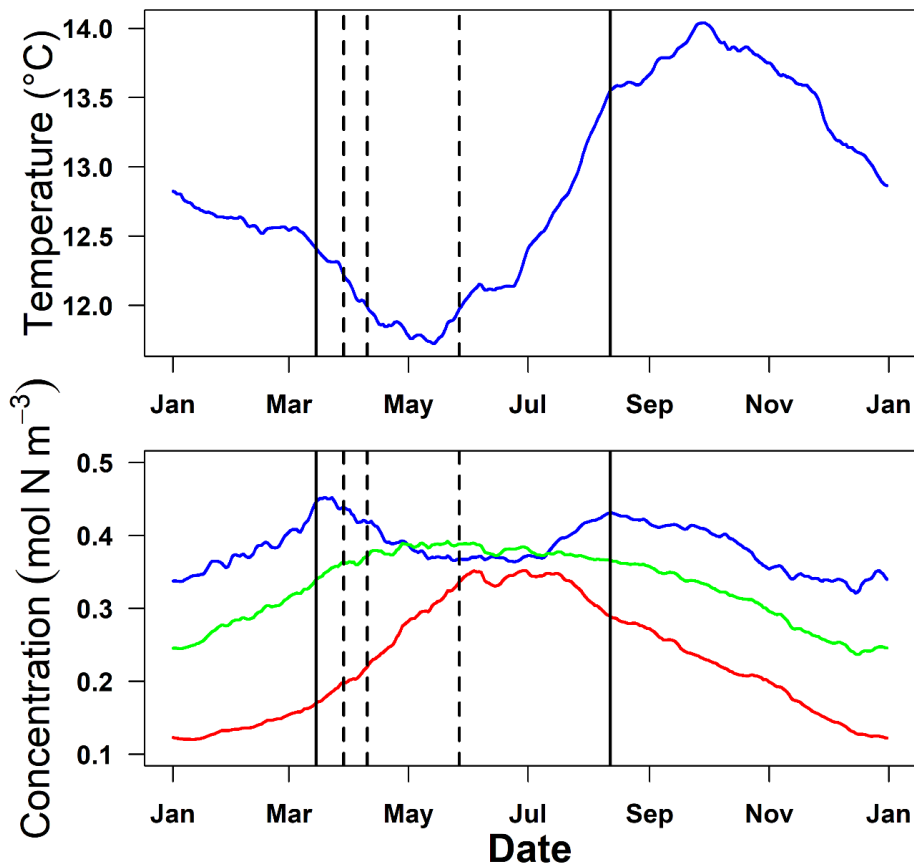
Figure 2. 30m depth 0-D climatological (1988-2010) time series of temperature and concentration (mol N m^{-3}) of microzooplankton (ZS; blue), mesozooplankton (ZL; green), and predatory zooplankton (ZP; red) used to force the bioenergetics model. Solid vertical lines denote the beginning and end dates of the bioenergetics simulation. Dashed vertical lines denote the transition from preflexion-to-flexion, flexion-to-postflexion, and postflexion-to-juvenile stages.
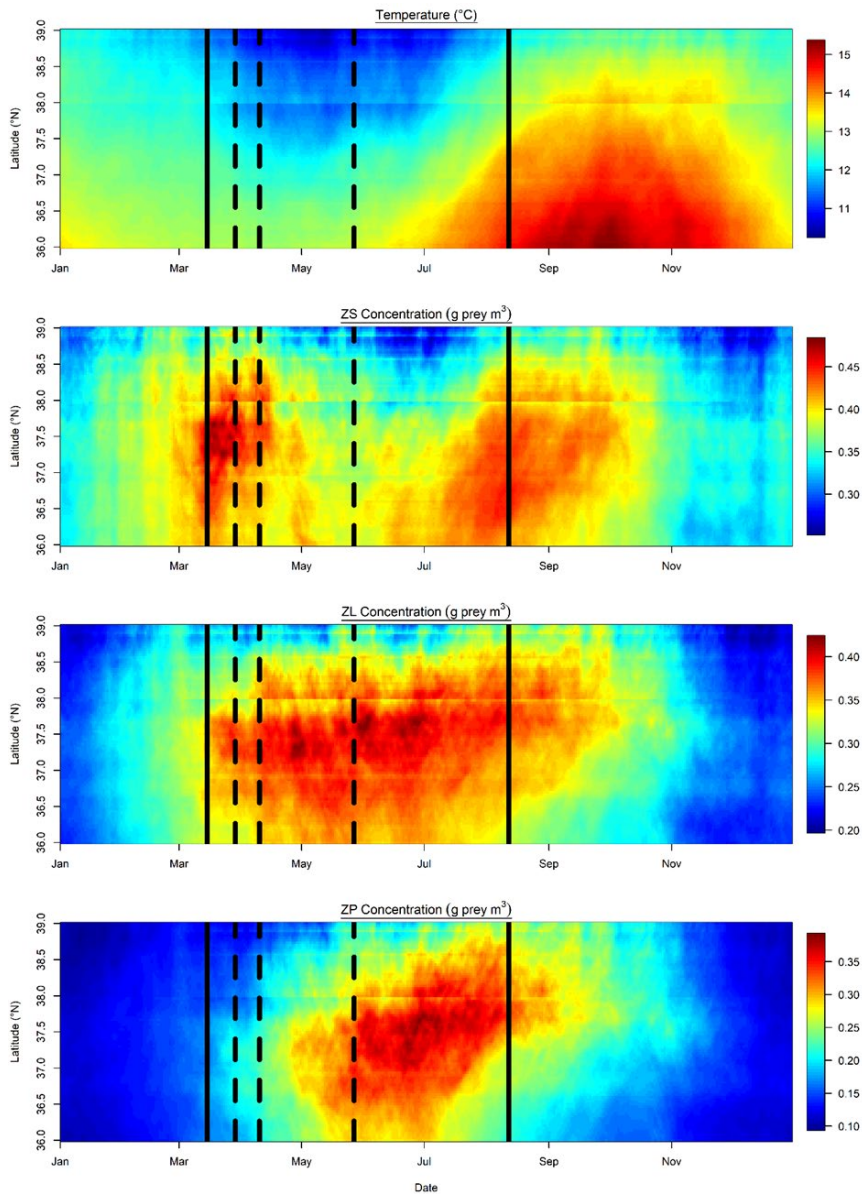
Figure 3. Latitudinal Hovmöller plots of climatological temperature, microzooplankton (ZS), mesozooplankton (ZL), and predatory zooplankton (ZP) from ROMS-NEMUCSC. Solid vertical lines denote the beginning and end dates of the bioenergetics simulation. Dashed vertical lines denote the transition from preflexion-to-flexion, flexion-to-postflexion, and postflexion-to-juvenile stages.
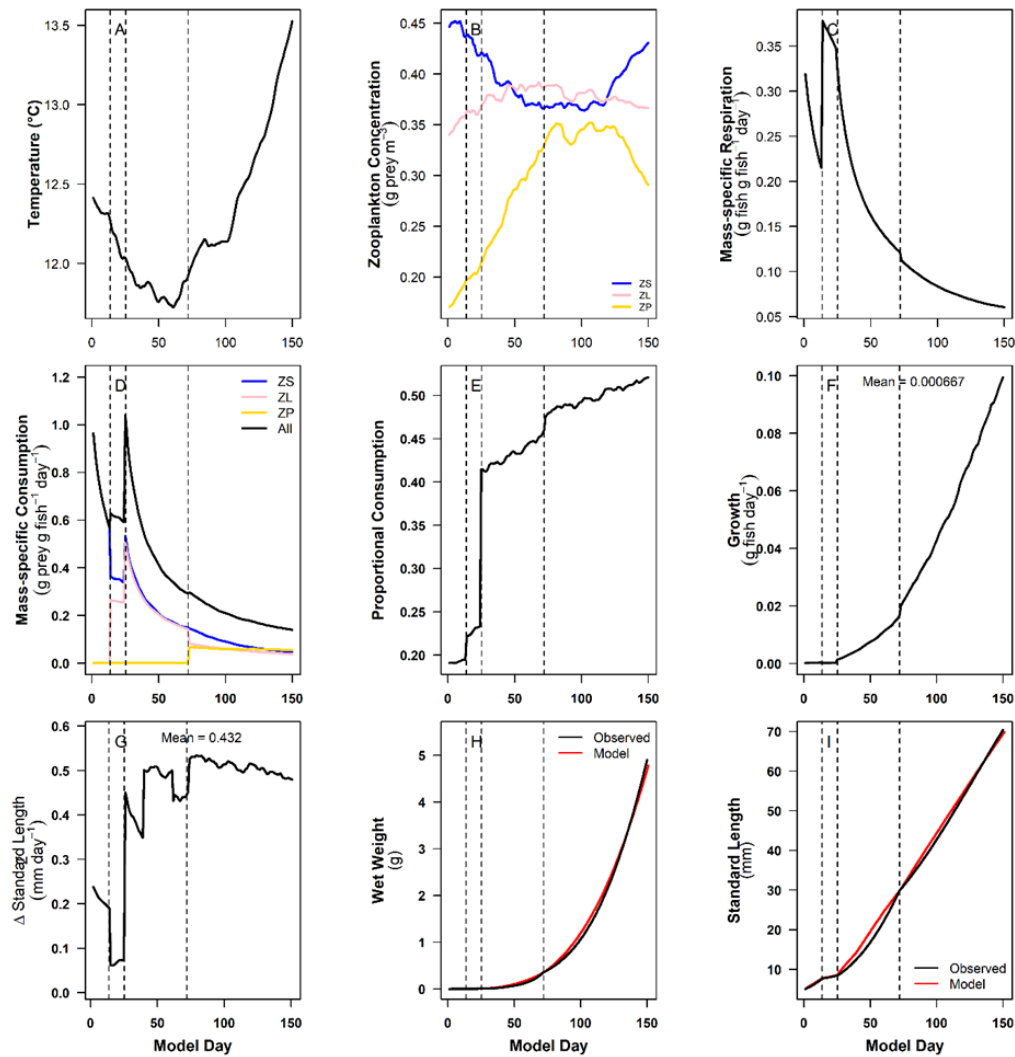
Figure 4. Bioenergetics processes of the 150-day 0-D climatology simulation. (A) Daily temperature at 30m depth used to force the bioenergetics model. (B) Daily concentrations (g prey m^{-3}) of small zooplankton (ZS; blue line), large zooplankton (ZL; pink line), and predatory zooplankton (ZP; gold line) used to force consumption in the bioenergetics model. (C) Total daily mass-specific respiration (g fish fish^{-1} day^{-1}) resulting from the bioenergetics simulation. (D) Daily mass-specific consumption (g prey g fish^{-1} day^{-1}) given temperature and prey concentrations. (E) Proportion of

maximum allometric consumption (dimensionless). (F) Daily growth in weight (g fish day^{-1}) and (G) daily growth in length (mm day^{-1}). (H) Weight-at-age (g) and (I) length-at-age from the bioenergetics simulation (red lines) relative to empirical size-at-age (black lines; Norton *et al.*, 2001; Laidig *et al.*, 1991).
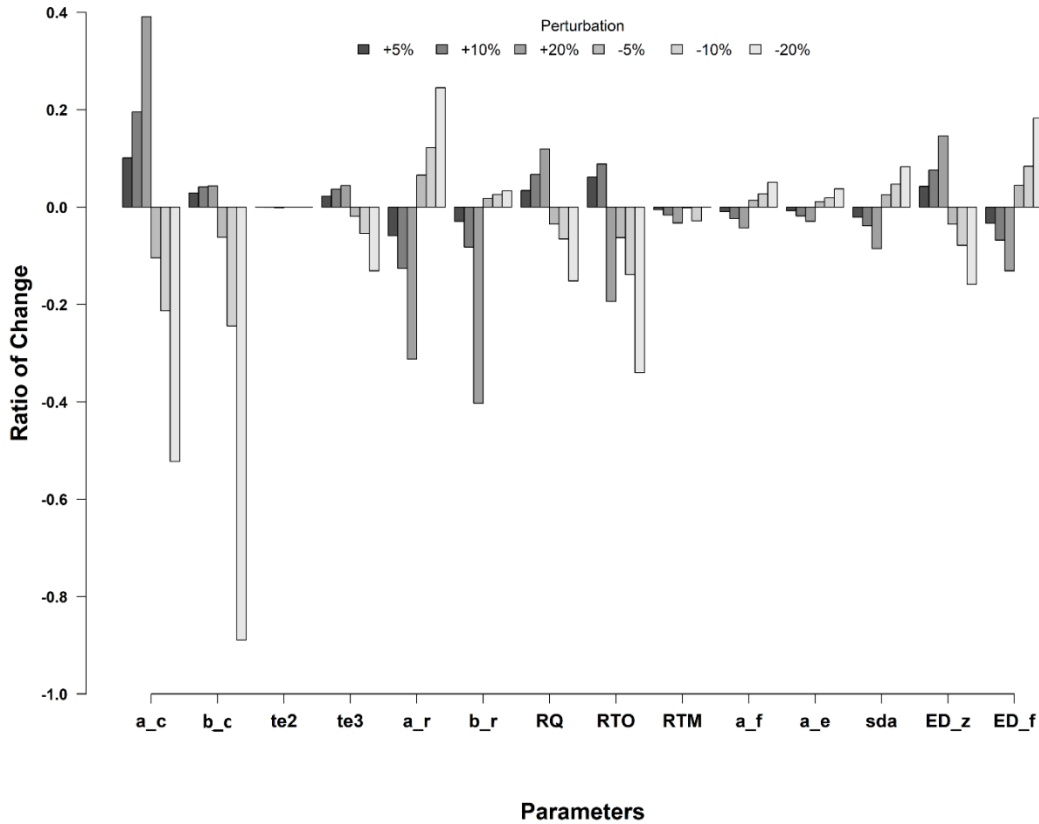
Figure 5. Ratio of Change (ROC), or the ending standard length (SLend) of the perturbed simulation minus SLend control, divided by SLend control, for the individual parameter perturbation (IPP). Refer to Table 1 for a description of each parameter and their nominal value.
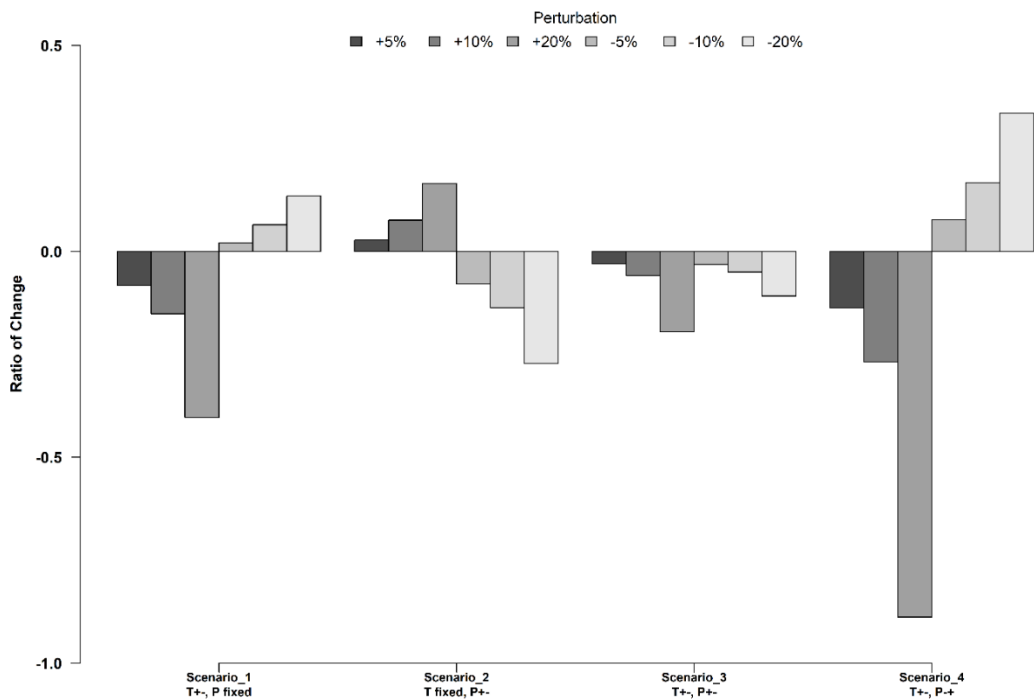
Figure 6. Ratio of Change (ROC) of the input scenario tests. In Scenario 1, temperature to vary about the mean (+/- 5%, +/- 10% and +/- 20%) while holding prey concentrations constant at the mean. In Scenario 2, prey concentrations to vary about the mean while holding temperature constant at the mean. In Scenario 3, temperature and prey concentrations to vary, but in equal fashion; temperature and prey concentrations were both added to, or subtracted from, the mean simultaneously. In Scenario 4, temperature and prey concentrations to vary but in opposite directions (i.e. add 5% of temperature and subtract 5% of prey concentrations and vice versa). Importantly, the three bars on the left of Scenario_4 are the ROC scores when

temperature additions were made and prey concentration reduced, and vice versa for

the three bars on the right.
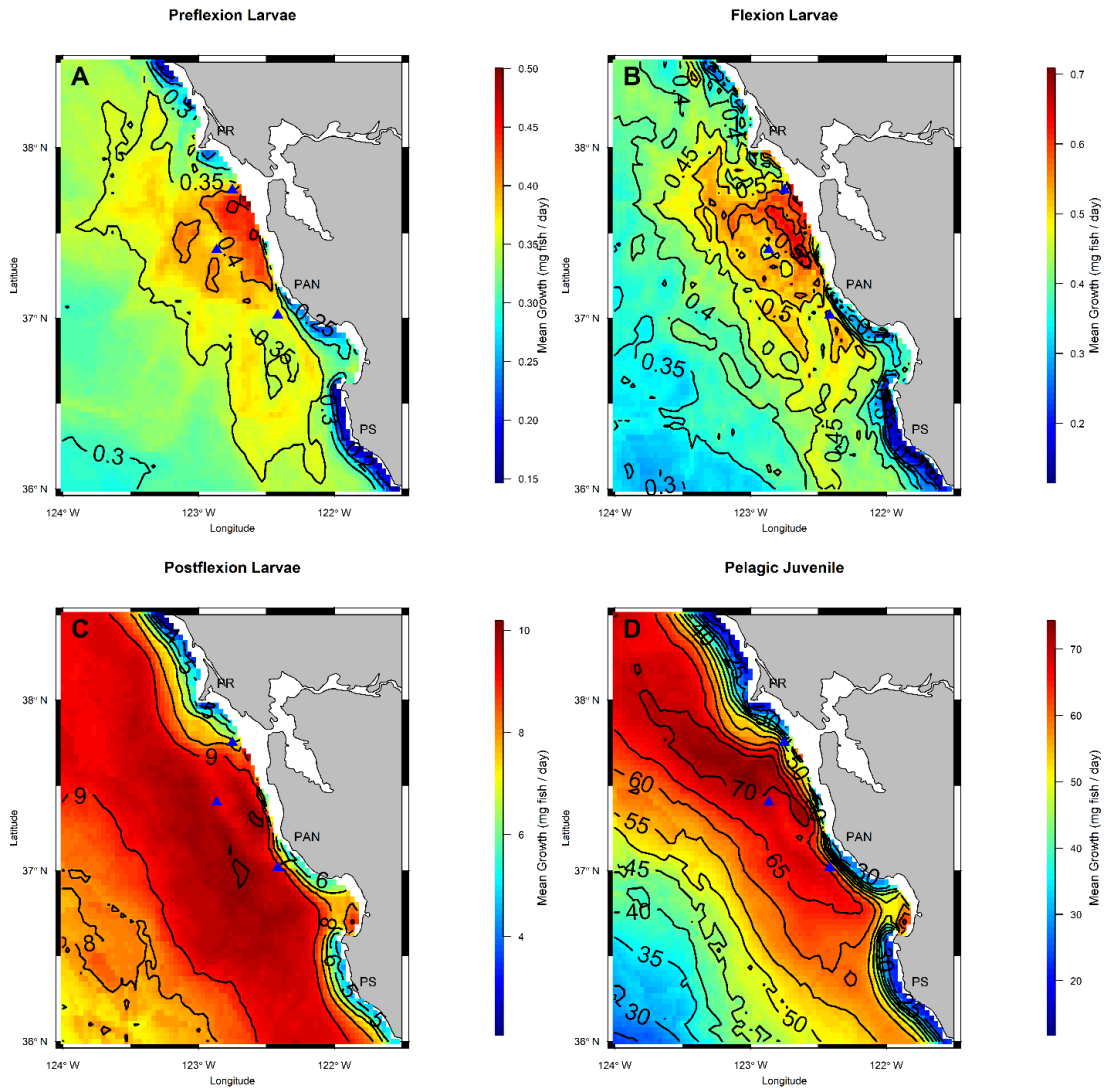
Figure 7. Mean stage-specific growth potential maps of the 2-D Eulerian climatology

for (A) preflexion, (B) flexion, (C) and postflexion larvae, and (D) the pelagic

juvenile stage..
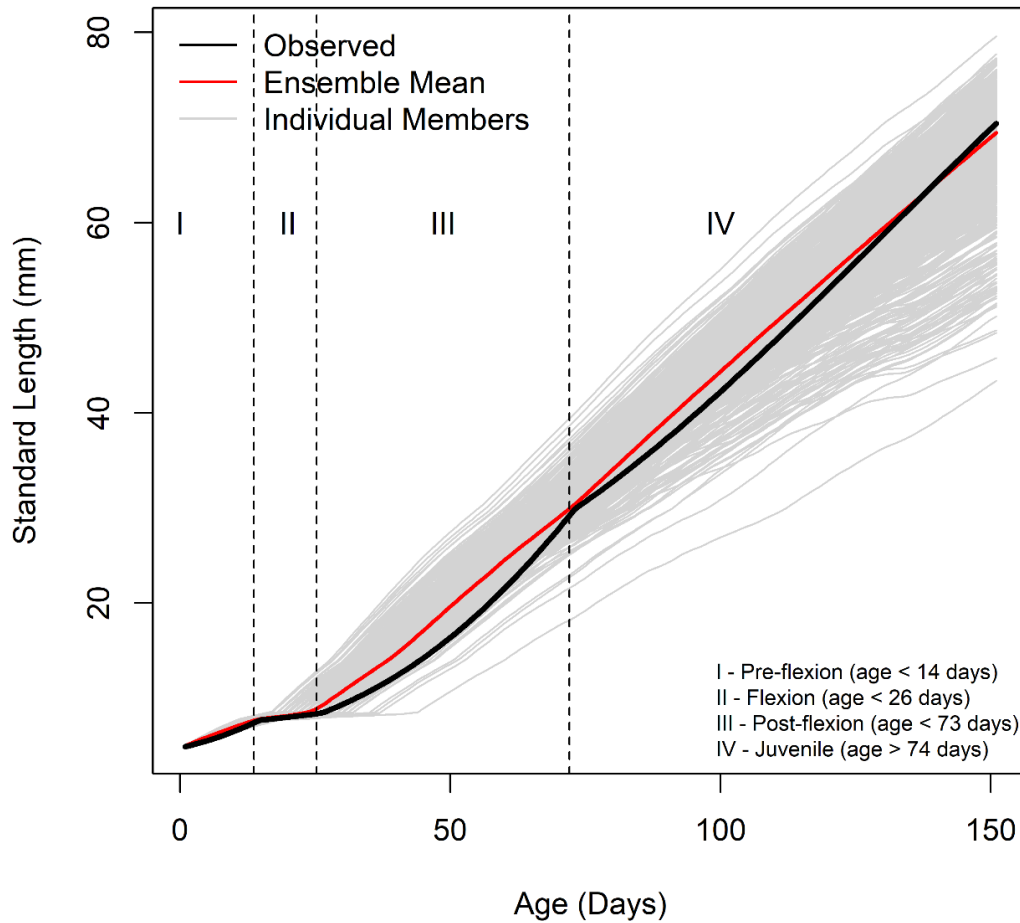
Figure 8 Standard length (SL) at age ensemble for all 3,750 individuals tracked in the 2D Eulerian climatology (grey lines). The mean of all individuals (red line) is plotted relative to the empirical length-at-age curve (black line) from Laidig et al., (1991). Vertical dashed lines denote transitions between life stages.
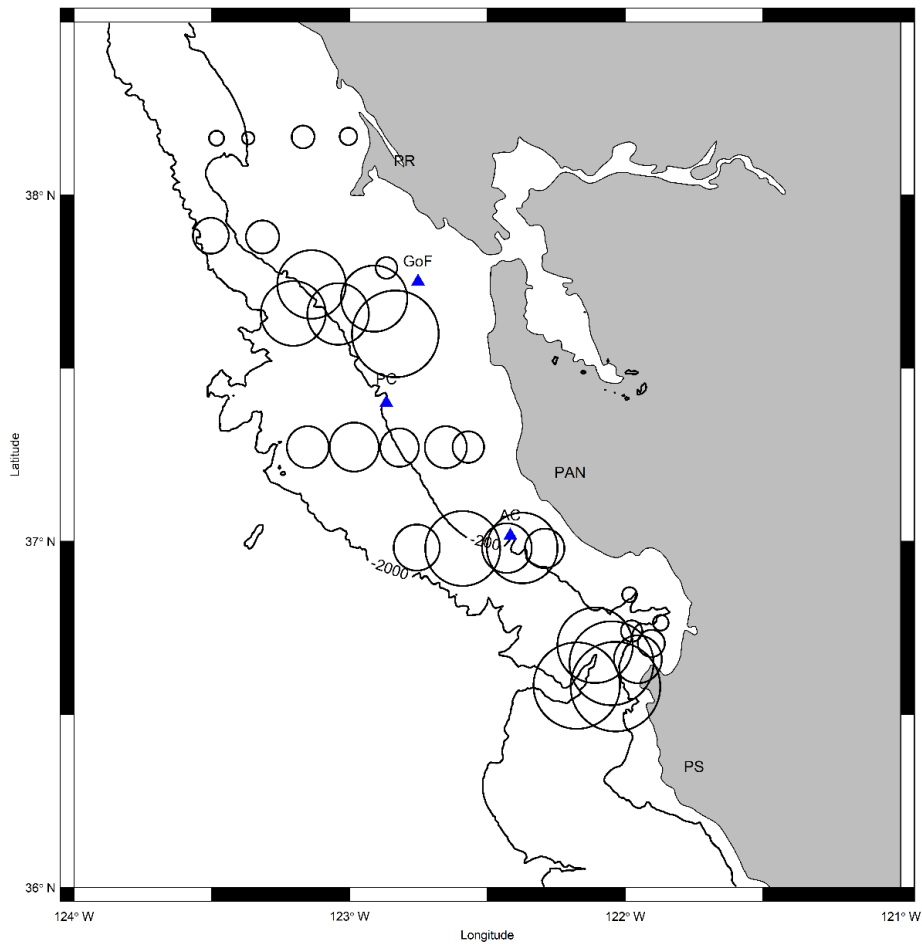
Figure 9. Pelagic juvenile shortbelly rockfish (*Sebastes jordani*) station-effects from

Δ-GLM of the core stations from the Rockfish Recruitment and Ecosystem

Assessment Survey over the period 1988-2010. The size of the circle indicates the

relative abundance at that station. Major promontories are labeled on land (PR = Point

Reyes; PAN = Point Año Nuevo; PS = Point Sur) and the Gulf of Farallones (GoF)

and two canyon systems (blue diamond: PC = Pioneer Canyon; AC = Ascension

Canyon) important to shortbelly life history.
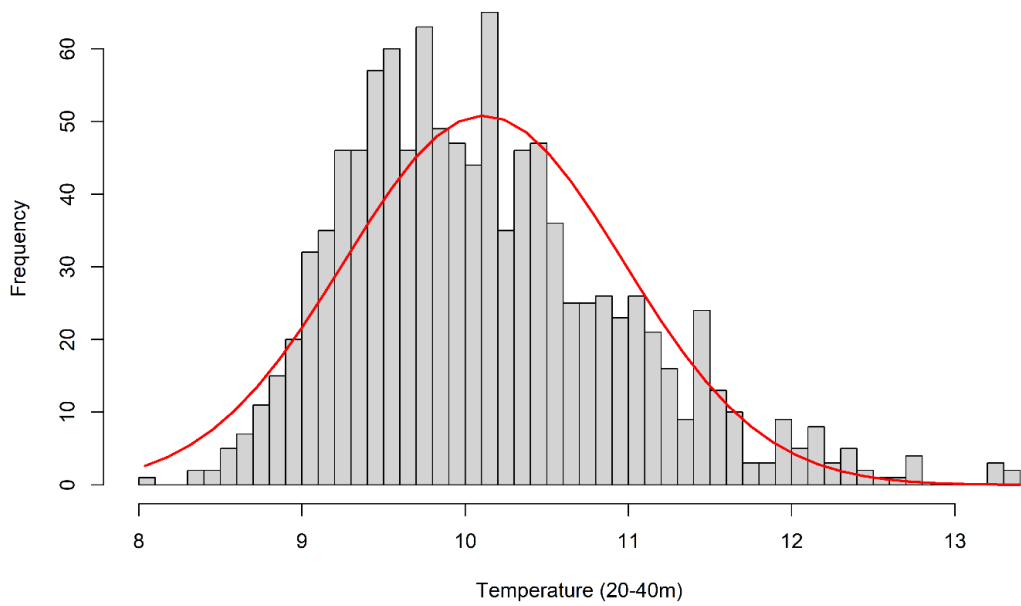
Figure S1. Frequency of subsurface temperature at 20-40m depth at sampling stations with positive shortbelly rockfish (*Sebastes jordani*) from the Rockfish Recruitment and Ecosystem Assessment Survey (RREAS). The red curve is the estimated normal distribution ($\mu = 10.7$ °C, $\sigma = 1.6$°C).
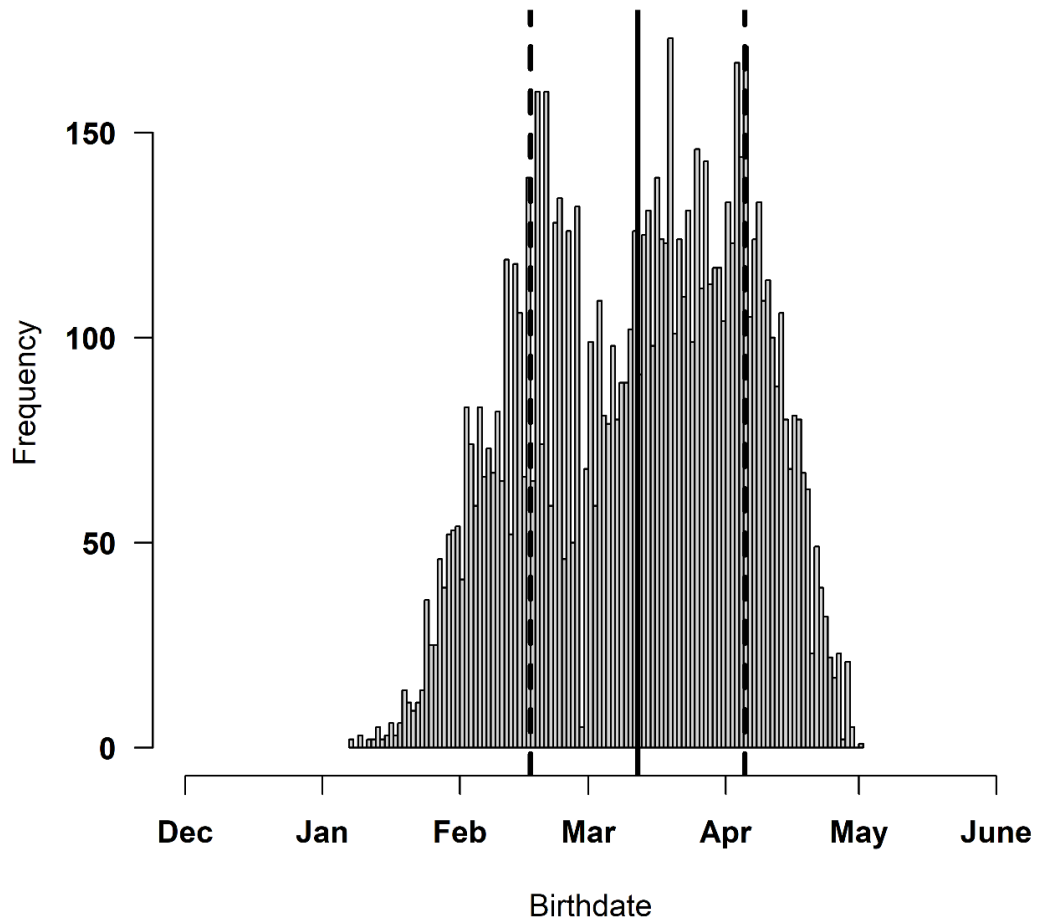
Figure S2. Back-calculated birthdate distribution of 8,645 pelagic juvenile shortbelly rockfish (*Sebastes jordani*) collected by the Rockfish Recruitment and Ecosystem Assessment Survey over the period 1990-2010. The solid vertical line denotes the median and the dashed vertical lines denote +/- 1 SD.

Spatial patterns of growth potential from a Eulerian individual-based model explains interannual recruitment variability of Shortbelly Rockfish (Sebastes jordani).

Abstract

Understanding mechanisms driving year-to-year changes in the survival of the early life stages (ELS) of marine fishes has challenged fisheries oceanographers for over a century. One promising approach, however, is to relate variability in somatic growth to early survival, and eventual recruitment. Temperature and zooplankton abundance from a high-resolution physical-biogeochemical model of the central California Current System (cCCS) were used to model early life growth potential of Shortbelly Rockfish (*Sebastes jordani*), a highly abundant and ecologically important marine fish species. Growth potential across four ELS's (preflexion larvae, flexion larvae, postflexion larvae, and pelagic juvenile stage) explained 78.6% of the variance of a recruitment index derived from a fisheries-independent survey. Functional response curves showed that growth potential of each of the four ontogenetic life stages differentially affects recruitment. These results highlight the relative importance of growth potential to explain recruitment, and that the influence of growth on recruitment is life stage-dependent, with growth during the preflexion, flexion and pelagic juvenile stages contributing the greatest to recruitment success. The relationships between growth and recruitment indicate that more rapid growth during the earliest life stages leads to reduced recruitment, but that fast growth during the

pelagic juvenile stage contributes to higher recruitment, which both supports and contradicts the fast growth-survival hypothesis (or at least suggests that it may be life stage dependent). The use of a mechanistic ecosystem model framework to understand relationships between growth, survival, and subsequent recruitment strength underscores the complexities of elucidating mechanisms of recruitment variability, the "holy grail of fisheries oceanography".

Introduction

Since the days of Hjort, elucidating biophysical mechanisms of recruitment variability has challenged fisheries scientists and resource managers alike (Browman, 2014; Kjesbu et al., 2016). Hjort (1914, 1926) posited that marine fish population fluctuations were the result of changes in year-class strength determined by cohort-level modifications of mortality rates during early life stages (ELS's). Hjort attributed these modifications to both food web-dependent ('critical period') and transport-dependent ('aberrant drift') processes. Extensions of Hjort's hypotheses were made throughout the late-20th century and include the 'migration triangle' (Harden Jones, 1968), 'match-mismatch' (Cushing, 1969; 1990), 'stable ocean' (Lasker, 1975; 1981), 'member/vagrant' (Sinclair, 1988; Sinclair and Iles, 1989), 'optimal environmental window' (Cury and Roy, 1989), 'ocean triad' (Bakun, 1996), and 'single process' (Cushing, 1975; Houde, 1987; Anderson, 1988). Despite each hypothesis being theoretically sound, support for any given one of these hypotheses has not been universal, likely because determinants of recruitment strength can differentially

operate across multiple life stages (Houde, 2008; Tolimieri et al., 2018; Haltuch et al., 2020; Vestfalls et al., 2023).

The 'single process' relates growth to mortality and how the two vital rates can determine recruitment strength under three separate, but related mechanisms (Cushing, 1975, Houde, 1987, Anderson, 1988). The 'stage duration' mechanism predicts fast growth will reduce time spent in highly vulnerable ELS's and lead to reductions in cumulative mortality (Houde, 1989). The 'bigger-is-better' mechanism posits larger size-at-age will confer lower mortality through faster swimming speeds and allow individuals to capture prey and evade predators more easily (Miller et al., 1988). The 'growth-survival' mechanism proposes that faster growing individuals will be in greater condition to resist starvation and more easily detect and escape predators (Takasuka et al., 2003). A recent meta-analysis found that 56% of field, mesocosm, laboratory, and numerical modeling studies support the faster growth-higher survival hypotheses while 16% of studies show that higher survival is related to slower growth rates (Robert et al., 2023). Less known is how ontogenetic stages could mediate the degree to which fast growth is more advantageous for survival. For example, if predation is the dominant agent of differential survival (Bailey and Houde, 1989), and predators are large relative to larval prey, then slow growth may cause disproportionate survival during the earliest larval stages (Litvak and Leggett, 1992; Robert et al., 2010). On the other hand, fast growth could be advantageous in later stages (e.g. postflexion larvae) once individuals have acquired all of their morphological features required for swimming and predator/prey detection. The

degree to which differential survival acts for or against fast growth across ontogenetic stages has not been fully tested, though Ishihara et al., (2019) concluded that for Pacific Bluefin tuna larvae, fast growth enhanced survival of postflexion larval stages but that the opposite was shown for preflexion and flexion stages.

Individual-based models (IBMs) grounded in first principles (e.g. physiology) have the potential to explicate mechanisms driving year class strength as population-level dynamics emerge from individual-based vital rate variability (Miller, 2007; Peck and Hufnagl, 2012). An element of marine fish IBMs are somatic growth submodels that respond to changes in temperature and prey availability from coupled physical-biogeochemical models (North et al., 2009). Lagrangian IBMs utilize ocean circulation models to track growth of individual larvae along their dispersal routes while Eulerian IBMs track growth at fixed locations, usually across grid cells of the coupled physical-biogeochemical model. The latter can be used to model growth rate potential across a spatiotemporal mosaic of environmental conditions to understand the relative importance of growth on survival. For example, simulated growth potential from an Eulerian IBM for juvenile Chinook Salmon (*Oncorhynchous tshawytscha*) in coastal central California explained a high proportion of early ocean survival, providing a greater understanding of the ocean conditions that determine growth and eventually drive productivity (Henderson et al., 2019). Recently, Morales et al. (in press) developed a bioenergetics model for Shortbelly Rockfish (*Sebastes jordani*) at high ontogenetic resolution that reproduced the observed growth trajectories of preflexion, flexion, and postflexion larvae as well as pelagic juveniles

69

under climatological ocean conditions (temperature and prey availability). Extension of the model to incorporate spatiotemporal variability in growth potential through an Eulerian IBM could illuminate the directionality of the growth-survival hypothesis across ontogenetic stages and identify the role that growth plays in recruitment.

Shortbelly Rockfish (*Sebastes jordani*) are an unexploited species generally assumed to be the most abundant rockfish species in the California Current System (CCS; Love et al., 2002). Relative to other *Sebastes spp*, Shortbelly Rockfish (hereafter "Shortbelly") have a life history more closely matching that of forage fishes (e.g. sardine and anchovy) as they exhibit fast growth, early age at maturity, and have relatively high natural mortality rates. In contrast to broadcast spawning forage fishes, Shortbelly like all rockfishes, are livebearers, and produce live, ready-to-feed larvae (~5mm standard length; SL) that are extruded at parturition (a.k.a. birth; Wyllie-Echeverria, 1987; Love et al., 2002). Their parturition period is relatively broad, beginning in late December, peaking in February, and ending as late as May (Wyllie-Echeverria, 1987; Woodbury and Ralston, 1991; Lenarz et al., 1995; Morales *et al*., in press). After 3-4 months as pelagic larvae, Shortbelly metamorphose to pelagic juveniles before settling to their semi-benthic adult habitats at roughly 150-days old, or ~70 mm SL (Laidig *et al*., 1991).

Shortbelly exhibit marked recruitment fluctuations (Field et al., 2007) that covary with other rockfishes in the central CCS (Ralston et al., 2013; Schroeder et al., 2019). Furthermore, Shortbelly experience ontogenetic changes in somatic growth during their early life stages (Laidig et al., 1991) but the degree to which

spatiotemporal variability in growth during the pelagic larval and juvenile stages contributes to recruitment strength has not been investigated. As pelagic juveniles, Shortbelly, and other members of the pelagic juvenile rockfish assemblage, are important constituents of the forage community as their relatively small size and semi-pelagic schooling behavior make then particularly susceptible to predation from seabirds, marine mammals, and piscivorous fishes (Thayer et al., 2014; Warzybok et al., 2018; Lowry et al., 2022). Although Shortbelly are not currently targeted by commercial fisheries, in recognition of their key role as forage to other higher trophic level predators, significant bycatch can occur at times in commercial rockfish and Pacific Hake trawl fisheries (PFMC 2022, Free et al., 2023). Moreover, understanding the mechanisms of their historical recruitment fluctuations would also provide insights into the drivers of recruitment variability for many other commercially important and actively managed species, and as such would contribute greatly towards an ecosystem-based management approach in the CCS (Wells and Santora, 2023).

Through application of a Eulerian IBM of Shortbelly in the central CCS, we test the hypothesis that recruitment strength is partially determined by spatiotemporal patterns of growth potential during their pelagic duration. We analyze simulated growth potential across the preflexion, flexion, and postflexion larval stages and the pelagic juvenile stage to determine if variability in life-stage specific growth contributes to year class strength. Furthermore, we seek to determine whether the direction of the association between Shortbelly recruitment and growth potential

71

changes across ontogenetic stages. It is generally accepted that year-class strength has been set via density-independent mechanisms by the end of the pelagic juvenile phase (Ralston and Howard, 1995; Field et al., 2010), so we test our hypotheses by relating spatiotemporal indices of growth potential to an index of pelagic juvenile Shortbelly abundance from a fisheries-independent survey.

Methods

Overview

In this study we expand the spatial bioenergetics model of Morales et al., (in press) to include interannual variability and to assess the influence of life stage-specific spatial growth patterns on Shortbelly recruitment. This effort utilizes temperature and secondary production from a historical physical-biogeochemical simulation to force the ontogenetic bioenergetics model. We calculated spatial statistics on simulated growth maps to identify hotspots of growth potential and develop annual life stage-specific indices of spatial growth potential using the mean intensity and areal extent of hotspots for a given year and life stage. Life stage-explicit indices of spatial growth patterns are then statistically related to a time series of Shortbelly recruitment to identify the relationships between growth during the preflexion, flexion, postflexion and pelagic juvenile stages on subsequent year-class strength through nonlinear, semiparametric models. Our analysis identifies the life stages that contribute most to year-class strength under the growth-survival hypothesis and the directionality of the relationship between growth rate and recruitment for each life stage.

<u>Fisheries-Independent Survey</u>

The Rockfish Recruitment and Ecosystem Assessment Survey (RREAS) has conducted annual midwater trawl surveys from 1983-present to provide recruitment indices for stock assessments and to otherwise inform fisheries and ecosystem oceanography studies (Sakuma et al., 2016; Field et al., 2021, Santora et al. 2021a). The survey has a fixed station sampling design that samples pelagic young-of-the-year rockfish (hereafter pelagic juvenile), as well as the micronekton community in central California from May-mid June, which, on average, is just prior to when the pelagic juveniles of winter-spawning rockfish species recruit to their benthic adult habitats (Love et al., 2002). Briefly, a modified-Cobb midwater trawl, with a 9.5mm cod-end liner and 26 m headrope is fished at ~30 m headrope depth for 15 minutes, except where stations are shallow (<60m depth) and the net is fished at 10 m depth to avoid bottom contact. Specimens caught are identified to the lowest taxonomic level and enumerated, and for all rockfishes (*Sebastes spp.*), the standard length (SL) of fish is measured. A subset of pelagic juvenile rockfishes are aged in most years using daily age analysis (Woodbury and Ralston, 1991).

We used a delta-generalized linear model (Δ-GLM; Stefánson, 1996; Dick et al., 2004) to standardize raw catch of Shortbelly from the RREAS over 1988-2010. This approach is consistent with the approach developed and used to provide indices of abundance for pelagic juvenile rockfish and other frequently encountered taxa (Ralston et al., 2013; Santora et al. 2021b). Indices of standardized pelagic juvenile rockfish abundance from the RREAS are significantly and positively correlated to

recruitment estimates from statistical catch-at-age stock assessments that use more robust demographic data from adult populations (Field et al., 2007; Ralston et al., 2013), and are used as indicators of recruitment within many rockfish stock assessments (Field et al. 2021). For this reason, we treat the standardized pelagic juvenile abundance as an index of recruitment for shortbelly rockfish, which are not routinely assessed using integrated analysis (stock assessment) models. Explanatory variables in the Δ-GLM were the same as those used by Ralston et al. (2013) (year, station, and period). Period is used to account for seasonal variability in the availability of Shortbelly to the survey and is calculated by taking the Julian day of a single haul, dividing by 10 and taking the integer (Ralston et al., 2013). Year effects were extracted from the Δ-GLM to obtain the Shortbelly recruitment index.

Previous efforts have back-calculated birthdates of pelagic juvenile Shortbelly caught in the RREAS from 1983-1992, based on age data from collected specimens (Woodbury and Ralston, 1991; Lenarz et al., 1995). We updated the yearly back-calculated birthdate distributions from 1993-2010 and reanalyzed data from 1990-1992 (Morales et al., *in press*). Importantly, these birthdates reflect the parturition dates that led to individuals surviving to the pelagic juvenile phase rather than reflect the total parturition window within a given year. Back-calculated birthdates were used to initialize model simulations at the median birthdate of surviving juveniles for a given year to assess what the growing conditions were like that led to the survival of a cohort in a way empirical approaches employ the 'characteristics of survivors' approach (Miller, 1997).

Eulerian IBM

The Eulerian IBM contains three coupled submodels; (i) an ocean circulation model that simulates the coastal oceanography of the central CCS, (ii) a bioegeochemical model that simulates lower trophic levels (phytoplankton and zooplankton), and (iii) a biogenetics model that simulates the somatic growth of Shortbelly larvae and pelagic juveniles. Details of each of the three submodels can be found in Fiechter et al. (2018; 2020) and Morales et al. (in press). Briefly, the ocean circulation model is a nested implementation of the Regional Ocean Model System (ROMS) (Shchepetkin & McWilliams, 2005; Haidvogel et al., 2008). The outer domain consists of a 1/10° horizontal resolution (~10 km) data assimilative historical reanalysis product (Neveu et al., 2016) and the inner domain has a 1/30° (~3 km) horizontal resolution (Fiechter et al., 2018). The biogeochemical model, NEMUCSC (Fiechter et al., 2018; 2020), is a customized version of the North Pacific Ecosystem Model for Understanding Regional Oceanography (NEMURO) (Kishi et al., 2007). NEMUCSC simulates three zooplankton size classes (small, large, and predatory), which become the prey for larval and pelagic juvenile Shortbelly in the bioenergetics model.

The bioenergetics model for Shortbelly is based off the Wisconsin bioenergetics model formulations (Kitchell et al., 1977; Hewett and Johnson, 1987; 1992; Hanson et al., 1997; Deslauriers et al., 2017) and was adapted from a generalized rockfish energetics model (Harvey, 2005). A full description of the model, along with details of model parameterization, a sensitivity analysis, scenario testing,

and a 2-D spatial climatology of simulated growth across preflexion, flexion, and postflexion larval stages, and pelagic juveniles, is documented in Morales et al., (in press). The temperature and small, large, and predatory (krill) zooplankton fields used to force the bioenergetics model are generated from daily output files of ROMS and NEMUCSC, respectively. Maximum consumption and respiration rates are allometric (body size-dependent) and temperature-dependent (Morales et al., in press). Specific dynamic action, egestion and excretion are modeled following the standard formulations from the Wisconsin bioenergetics model. Realized consumption is based on a multispecies Holling's type II functional response (Rose et al., 1999a; 1999b) that relates the rate of prey consumption to the amount of prey available in the environment and accounts for ontogenetic dietary preferences from studies of ELS Shortbelly food habits (Sumida and Moser, 1984; Reilly et al., 1992). Because fish cannot shrink in length, but can lose weight, we held length constant if a fish lost weight and only increased length afterwards once weight returned to the last maxima. A zero-dimensional (spatially invariant) climatological simulation of the fully parameterized bioenergetics model could reproduce life stage-specific growth stanzas that compare well with observed length-at-age curves (Morales et al., in press).

The Eulerian IBM simulated growth over the 'core' RREAS sampling area (36°N-39°N, 124°W-121°W) from 1988-2010 at 30m depth, the depth where both larval and juvenile shortbelly are found in highest abundance (Moser and Boehlert, 1991; Ross and Larson, 2003). This time frame was chosen because the ROMS-NEMUCSC hindcast only covered 1988-2010, despite the RREAS data existing post

2010. Bioenergetics formulations were solved in each grid cell from ROMS-NEMUCSC (n = 3,750 grid cells) and tracked in a Eulerian sense (i.e. spatially fixed). In this way, we simulated what the growing conditions would have been had a fish occupied a particular grid cell (Brandt et al., 1992; Henderson et al., 2019). The start date of each yearly simulation was the median birthdate of surviving pelagic juveniles found through otolith microstructure analysis. Each yearly simulation tracked 3,750 individuals from birth (informed by the median birthdate of surviving pelagic juveniles) to the end of their pelagic juvenile duration (150 days). Composite growth maps were calculated for each of the four life stages (preflexion, flexion, and postflexion larvae, and pelagic juveniles) by counting the number of days an individual spent in a given life stage and then calculating the mean daily growth (in weight and length) over the days spent in a given life stage. This was repeated for all 3,750 individuals within the model domain resulting in four layers of mean growth potential across 23 years, or 92 growth potential maps across 86,250 individuals.

Statistical Analysis

We subjected annual life stage-specific mean growth potential maps to a spatial hotspot analysis by applying the Geti-Ord Gi* statistic (Getis and Ord, 1992; Ord and Getis, 1995) to objectively characterize regions of elevated growth potential. The Gi* statistic (a Z-score) quantifies clusters of growth potential that are significantly faster (hotspots) relative to the background spatial mean and standard deviation. To account for spatial autocorrelation, and to assign a spatial neighborhood with which the Gi* algorithm searches over, we first treated each of the 92 growth

77

potential maps to a local Moran's I test to determine the distance lags at which

autocorrelation drops to zero. Using this distance for each year and stage-specific

map, the local Gi* statistic was calculated using the *spdep* package in the R Statistical

Programming language. Z-scores above 1.15 were considered statistically significant

at the $\alpha < 0.1$ level (Yurlowski et al., 2018). Next, we calculated the average intensity

(mean Z-score) of significant hotspots to quantify the degree of spatial clustering and

the areal extent (in km^2) of hotspots for each stage-by-year combination to get annual

indicators of growth across the four life stages. The average intensity and areal extent

(size) of hotspots were used as independent variables to assess the association of

elevated growth potential with annual recruitment of Shortbelly. The choice to

evaluate hotspots of growth potential was to focus on statistically significant regions

of elevated growth potential rather than simply taking the average growth rate over

the entire model domain as this would smear an annual growth datum with both high

and low values.

We used generalized additive models (GAMs) to quantify the functional forms

between indices of modeled growth potential (i.e. intensity and size of stage-specific

growth hotspots) and recruitment. GAMs are a semi-parametric, nonlinear partial

regression approach that does not require *a priori* assumptions of a particular

functional form (Wood, 2017). The *mgcv* package in the R statistical programming

software was used to calculate GAMs. The full candidate statistical model is given

by:

$$R_y = s(HI_{y,i}) + s(HS_{y,i}) + \varepsilon, \tag{1}$$

where R is the Shortbelly recruitment index, s is the smoothing function, HI is the mean intensity of a hotspot for year y and life stage i (i = 1-4), HS is the hotspot size (km^2) for y and life stage i, and ε is the error term under a normal distribution. We limited the number of knots in the smoothing splines to a maximum of three (k = 3) to restrict flexibility to avoid ecologically unrealistic functional forms during model fitting. Preliminary assessment of the Gi* hotspot analysis found that there was not a significant hotspot of growth potential for the preflexion larval stage in 2003. Furthermore, we found that postflexion larvae hotspot intensity and size were significantly correlated to each other above ρ = 0.7, which is beyond the threshold recommended to prevent collinearity in GAMs (Wood, 2017). Therefore, we fit a maximum of 7 independent predictors to 22 data points (excluding 2003) and used backwards stepwise selection and Akaike Information Criterion with corrections for small sample size (AICc) using the *bbmle* package (v1.0.25) in the R Programming Language (v4.2.0).

To evaluate the contribution of each predictor variable in the final model, we removed each term one at a time, refitted the model while conserving the original vector of smoothing parameters (except for the term that was removed), and took the difference in deviance between the full model and the reduced model (with term of interest removed), and standardized the difference by the deviance of an intercept only model (the null model). Because there was some collinearity of remaining explanatory variables, the total sum of all single contributions could be more than 100%.

Results

<u>Recruitment Index, Observed Juvenile Growth Rate, and Birthdate Frequency</u>
<u>Distribution</u>

Shortbelly exhibited pronounced interannual variability in recruitment from 1988-2010 as indicated by the standardized index of pelagic juvenile abundance from the RREAS (Figure 1). 1988 and 1989 stand out as the two highest years on record while 1998 and 2005 were the two lowest. The slopes of annual linear length-at-age regressions indicated interannual variability of the estimated *in situ* growth rates of pelagic juvenile Shortbelly that survived the larval phase and were caught in the RREAS as pelagic juveniles (Table 1). The mean of the estimated annual growth rates for pelagic juveniles over 1988-2010 was 0.556 mm day^{-1}. The slowest observed growth rate for pelagic juveniles was 0.4082 mm day^{-1} in 2005 and the fastest was 0.6454 mm day^{-1} in 2009.

Estimates of back-calculated birthdates of surviving pelagic juveniles captured in the RREAS were quite variable from year to year with the earliest and latest birthdates being in late December to early January and late April to early May, respectively (Fig. S1). Median birthdates ranged from late January in 1988 to mid-April in 1996 (Table 1).

<u>Simulated Growth</u>

Length-at-age curves from the Eulerian IBM growth model indicated considerable spatial variability in growth rates within a given year, with some

individuals growing far below the annual mean and others above (Fig. S2). Overall, IBM simulations mostly overestimated length-at-age when comparing the grand mean of simulated length-at-age (1988-2010; n = 86,250) to empirical growth estimates of Laidig et al., (1991) (Fig. 2A). Specifically, simulations overestimated the mean daily growth rate for preflexion, flexion, and postflexion larval stages while the daily growth rate of pelagic juveniles was underestimated (Fig. 2A and 2B). The overestimation of mean growth during larval stages and the underestimation of mean growth during the pelagic juvenile stage meant that for any given year, the mean length at the end of any given simulation was close to that of the observed length at 151 days old (Fig. 2A and S2). The overall mean growth rate of preflexion larvae was 0.27 mm day^{-1} from the model compared to the observed growth rate of 0.2 mm day^{-1} from Laidig et al. (1991). In the model, life stage transitions are size-based thresholds, with the mean number of days spent in the preflexion larval stage being 10 days compared to observed duration of 13 days. The modeled mean growth rate of flexion larvae deviated most from observations, with the model producing a growth rate of 0.16 mm day^{-1} compared to the observed growth rate of 0.08 mm day^{-1}. The average number of model days spent in the flexion larval stage was six compared to the observed duration of 12 days. Postflexion larval mean growth rate estimated in the model was 0.52 mm day^{-1} compared to the observed growth rate of 0.45 mm day^{-1}. The duration of time spent in the postflexion larval stage was 44 model days compared to the observed duration of 47 days. Finally, pelagic juvenile growth predicted by the model was 0.44 mm day^{-1} relative to an observed growth rate of 0.51

mm day^{-1}. In the model, Shortbelly metamorphosed to the pelagic juvenile stage by day 59, on average, compared to Laidig's estimate of day 73.

Across years, length-at-age trajectories averaged over the model domain (3,750 grid cells) showed interannual variability in growth relative to the observed length-at-age curve of Laidig et al. (1991) and the grand mean of simulated length-at-age (Fig. S2). Growth was fastest in 1999 and from 2002 to 2010 with the annual mean length-at-age being consistently higher than the grand mean (1988-2010). In contrast, growth was relatively slow in 1989, 1992, 1994-1995, and 1998 with the daily mean length-at-age being consistently lower than the daily grand mean length-at-age.

Interannual variability of size and intensity of hotspots among life stages

Growth hotspots were inversely correlated with temperature implying that cooler conditions are related to faster growth and the association is strongest for flexion and pelagic juveniles (Table 2). Greater hotspot intensity occurred for all life stages when total prey availability was high. However, pelagic juvenile growth potential intensity was not related to the availability of small zooplankton (ZS; Table 2), which is understandable since pelagic juveniles do not feed on small zooplankton within the model. Similarly, preflexion and flexion do not feed on predatory zooplankton and were not significantly related to their concentration (Table 2).

Hotspots identified by the Gi* analysis were mostly spatially contiguous (i.e. a single hotspot) for all life stages and years. For preflexion larvae, exceptions

included 2002 and 2009 when two hotspots were detected and 2006 when four

hotspots were detected. For flexion larvae, two hotspots were detected in 1988, 2002,

2006, and 2008, and three for 2009. Two hotspots were detected in 2000 and 2004 for

postflexion larvae and two hotspots were detected in 2003 and 2007 for pelagic

juveniles. No hotspot was detected in 2003 for preflexion larvae (Fig. 3).

Mean intensity and areal extent of significant hotspots were quite variable

year-to-year with little to no cycling or synchrony among life stages (Fig. 3; Table 3).

However, hotspot intensity of preflexion larvae was positively correlated with the

areal extent (size) of preflexion hotspots ($\rho = 0.52$; $p = 0.013$) and hotspot intensity of

flexion larvae ($\rho = 0.52$; $p = 0.014$). Intensity and areal extent of postflexion larvae

were positively and significantly correlated ($\rho = 0.86$; $p < 0.01$; Table 3), implying

that when growth was fast, it also occurred over larger areas.. An average and

standard deviation of life-stage specific Z-scores across all year's highlights where

hotspots tended to be located (Fig. 4) and how variable they were (Fig. 5). Growth for

all life stages was greatest just offshore of the Gulf of Farallones (outside of the San

Francisco Bay; Fig. 4) but was quite variable across years for preflexion larvae (Fig.

5a) and relatively consistent for flexion and postflexion larvae, and pelagic juveniles

(Fig. 5B-D).

Hotspots of Growth Potential Explain Interannual Recruitment

The best GAM for explaining interannual deviance in recruitment included:

preflexion hotspot intensity, flexion hotspot intensity and size, postflexion hotspot

size, and pelagic juvenile hotspot intensity (Table 4). Preflexion hotspot size and

pelagic juvenile hotspot size were not found to be significant predictors of recruitment. Since postflexion hotspot intensity and size were significantly correlated beyond the threshold to prevent concurvity (Wood, 2017; Table 2), we fit a separate model that included postflexion hotspot intensity but not size, and found that postflexion hotspot size was a better predictor based off AICc (ΔAICc = 3.1; not shown). The deviance explained by the top GAM was 78.6% and the model reproduced observed recruitment well (Fig. 6A). Model diagnostics revealed the GAM model did not violate assumptions of autocorrelation (Fig. S3) and did not violate the assumption of a Gaussian error term (Shapiro-Wilks = 0.94; p-value = 0.17).

The final GAM yielded functional relationships that were both linear and non-linear depending on life stage (Fig. 6B-F). Preflexion hotspot intensity had a negative linear relationship with recruitment (Fig. 6B). The functional relationship between hotspot intensity during the flexion larval stage was U-shaped, implying that intermediate hotspot intensity was poor for recruitment while lower and higher hotspot intensity levels were advantageous (Fig. 6C). The areal extent (size) of flexion and postflexion hotpots were positively, and linearly related to the time series of recruitment (Fig. 6D-E). Finally, the hotspot intensity of pelagic juvenile shortbelly rockfish had an asymptotic relationship with estimated recruitment (Fig. 6F).

The intensity of life stage-specific hotspots of growth potential explained more of the variance in recruitment estimates than did the areal extent (size) of hotspots. The ranking of each covariate in terms of proportional contribution to total

deviance explained by the full model (78.6%) is: (i) flexion hotspot intensity (36%), (ii) pelagic juvenile hotspot intensity (35%), (iii) preflexion hotspot intensity (27%), (iv) flexion hotspot size (19%), and (v) postflexion hotspot size (13%).

Discussion

We have shown that annual life-stage specific spatial patterns of growth potential for Shortbelly during larval and pelagic juvenile phases explains a large fraction (76%) of Shortbelly recruitment variability. Raw growth potential is determined by local and regional patterns of temperature and prey availability derived from a historical physical-biogeochemical simulation, and thus, variability in growth is implicitly environmentally driven. Growth potential estimated from our model consistently produced spatial clusters of rapid growth, or hotspots, whose intensity (growth rate) and areal extent were mostly asynchronous across the preflexion, flexion and postflexion larval stages, as well as the pelagic juvenile stage. This asynchrony suggests that spatial variation of ocean conditions differentially affects growth at each life stage. Throughout the 23-year study period (1988-2010), the abundance of pelagic juvenile Shortbelly is related to the strength and size of hotspots of growth potential across all four life stages suggesting recruitment of Shortbelly is at least partially determined by growth throughout the entire pelagic duration for this species. However, the effect of fast growth on recruitment was complex, with several of the functional relationships changing direction across ontogenetic stages. Growth during larval preflexion and flexion, as well as the pelagic juvenile stage explained the greatest fraction of observed variability in year-class strength, with the areal

extent of good growing conditions during flexion and postflexion also contributing but to a lesser degree. Below we describe these results in the context of the growth-survival hypothesis and how the relationship between growth during the pelagic duration and recruitment could differ throughout ontogeny.

The growth-survival hypothesis posits faster somatic growth during the early life stages of marine fish will lead to higher survivorship and larger year-class strength (Cushing, 1975, Houde, 1987, Anderson, 1988), however there are numerous examples of fast growth conferring higher mortality (reviewed by Robert et al., 2023). Marine fish larvae are most vulnerable to adverse advection and predation during the earliest larval stages when swimming capacity and sensory cues are minimal (Bailey and Houde, 1989). When preflexion rockfish larvae grow fast, they are in better condition to resist starvation and accrue a larger length-at-age. However, they may also have developmental constraints that limit defensive responses (Fuiman and Magurran, 1994) such as slow escape times due to underdeveloped morphological structure relative to later stage conspecifics (Downie et al., 2020). Faster swimming of larvae resulting from larger size (Kashef et al., 2014) could increase predation mortality if the encounter rate with predators increases (Rothschild and Osborn, 1988; Bailey and Houde, 1989; Sundby and Fossum, 1990). In fact, more active fish larvae are eaten more frequently by ambush-raptorial predators (e.g., chaetognaths and siphonophores) and this selectivity has been attributed to more frequent encounters (Purcell, 1981). In the context of our results, recruitment will be reduced in years when the intensity of growth hotspots for preflexion larvae is high.

Hotspot intensity is a measure of the spatial distinctness of fast growth, with higher intensity values indicating faster growth within hotspots. While our model does not explicitly account for predation, raw growth and hotspot intensity within the model is associated with the amount of food available. Preflexion larvae feed exclusively on small zooplankton and there is a strong positive association between preflexion hotspot intensity and the total amount of food available, including large zooplankton. The large zooplankton size class modeled in NEMUCSC is parameterized to represent copepods (Kishi et al., 2007), which, along with chaetognaths and other zooplankton, can be predators of fish larvae (McGowan and Miller, 1980; Bailey and Yen, 1983). If fast growth for preflexion co-occurs in regions of increased predatory copepods and other predatory zooplankton, as suggested by our model, then encounter rates with larval predators could be greater when hotspot intensity is strongest, thus yielding the predicted negative relationship between preflexion hotspot intensity and recruitment.

The relationship between intensity of hotspots during flexion and recruitment was U-shaped, suggesting that intermediate growth hotspot intensity results in weak year-class strength. Reduced recruitment at intermediate levels of growth is an interesting and somewhat puzzling result. However, examples of this have been shown empirically (e.g. Gagliano et al., 2007). An explanation for this pattern can come from an evaluation of anatomical development and energy expenditure during flexion. Larval flexion, a major milestone in development, occurs when the notochord turns upward, trunk musculature differentiates, and the caudal fin develops, which,

collectively, results in improved swimming performance (Downie et al., 2020). Mass-specific respiration is predicted by the underlying bioenergetics model of the Eulerian IBM to increase substantially during flexion, which must be offset by increased consumption in order to yield positive growth (Morales et al., in press). Fish growing rapidly during the flexion stage would exit this energetically costly period of development more quickly, in line with the stage duration hypothesis (Houde, 1989). Moreover, high intensity of growth hotspots are associated with an increased abundance of mesozooplankton and predatory zooplankton, and fish in years with high hotspot intensity would possibly be exposed to increased predation risk, albeit over a shorter duration of time and with a slight swimming advantage compared to preflexion larvae. Larvae growing at the lower end of the hotspot intensity spectrum would be at less risk of predation as described above for preflexion larvae. However simulated growth during flexion was overestimated compared to empirical growth, and therefore the model may put undue emphasis on how important growth is during this stage.

Inference on the positive relationship between the areal extent of growth hotspots for the flexion and postflexion larval stages and recruitment is somewhat intuitive given that ocean currents can disperse larvae far and wide by the time fish are in these stages of development (Petersen et al., 2010). For years with a large areal extent of growth potential hotspots, flexion and postflexion larvae would experience suitable growing conditions to resist starvation over a wide array of dispersal trajectories. One reason why preflexion hotspot size might not be as important as

flexion and postflexion hotspot size has to do with the spatial patterns of reproduction for Shortbelly rockfish (Ralston et al., 2003). Peak reproduction for Shortbelly along the central California coast occurs along the shelf break between Point Reyes and Monterey Bay (Macfarlane and Norton, 1999; Ralston et al., 2003), which overlaps spatially with the highest mean hotspot intensity values for preflexion. However, growth hotspot intensities for preflexion larvae are quite variable from year-to-year in this area and the total area of a preflexion growth hotspot will not relate to Shortbelly recruitment if hotspots do not overlap with reproductive sites in some years. For flexion and postflexion larvae, the location of growth hotspots are more persistent meaning when ocean currents transport larvae away from their birth (parturition) site. When the size of flexion hotspots are large, there is a greater chance of larvae dispersing to areas favorable for growth.

The functional relationship between the intensity of pelagic juvenile growth hotspots and subsequent recruitment is asymptotic. As hotspot intensity increases, there are diminishing returns to recruitment because as growth increases during the highly mobile pelagic juvenile phase, encounter rates with prey vary little and are insignificant compared to capture success by predators (Juanes and Conover, 1994; Sogard, 1997). Intensity of a significant hotspot is related to the degree of clustering of the variable of interest, so when intensity is high, the variable of interest is spatially clustered with uniquely high values relative to the values outside of its neighborhood (Getis and Ord, 1992). So, at increasing intensities, the realized distribution of pelagic juvenile Shortbelly may become more aggregated within a

hotspot if pelagic juveniles can target good growing conditions by directed movement to habitat favorable to growth. If pelagic juvenile rockfish are aggregated in higher densities in regions of fast growth, they may be more susceptible to predation by visual predators and thus have diminishing returns at increasingly high growth potential hotspot intensities. Alternatively, it could be that pelagic juveniles reach a point of saturation in consumption and additional increases to food will not lead to additional growth, or by association, recruitment.

Pelagic juvenile rockfish are the leading forage group within the CCS, being preyed upon by a wide diversity of predators compared to any other species or group (Szoboszlai et al., 2015). Wells et al. (2017) showed a positive relationship between the proportion of juvenile rockfish in the diets of common murre (*Uria aalge*) nesting at the Farallon Islands and the abundance of juvenile rockfish caught by the RREAS. Furthermore , the foraging trip duration of common murre's returning to nests with pelagic juvenile rockfish was half that compared to when birds returned with alternative prey (mainly northern anchovy (*Engraulis mordax*)), implying that when rockfish are in high abundance, they are also distributed closer to the Farallon Islands (Wells et al., 2017). Located downstream of the Point Reyes upwelling plume, the Gulf of Farallones is a known retention zone (Wing et al., 1998) that concentrates recently upwelled water enriched with nutrients required for primary production (Fiechter et al., 2018), and is a hotspot for krill aggregations (Santora et al., 2011; Cimino et al., 2020; Fiechter et al., 2020; Messié et al., 2022), which are known prey of pelagic juvenile shortbelly (Chess et al., 1988; Reilly et al., 1992). Here we

showed that growth hotspots for pelagic juvenile Shortbelly are collocated near the

Farallon Islands (Fig. 4d) and that these hotspots are persistent (i.e. low interannual

variability; Fig. 5d). The intensity of growth potential in the Gulf of Farallones is

related to cooler waters and increased secondary production, with faster growth

potential being advantageous to recruitment strength.

One interesting result from our study is that no single life stage-specific

attribute of ELS shortbelly growth potential could explain the recruitment time series

alone. Instead, attributes of growth potential across all pelagic ELS's cumulatively

explained 78.6% of interannual recruitment variability. Patterns of growth potential

during ELS integrate physical and biological conditions across pelagic life stages to

determine eventual year-class strength. Studies examining the influence of ocean

conditions on rockfish recruitment point to large-scale physical mechanisms, but here

we argue that a biological mechanism, combined growth over all pre-recruitment

stages, has explanatory power that rivals other rockfish recruitment studies. For

example, mean sea surface temperature (SST) during January-March, the period of

peak parturition (Wyllie-Echeverria, 1987;), had a dome-shaped relationship to the

abundance of pelagic juvenile stages and settled juveniles of blue rockfish (*Sebastes

mystinus*) and yellowtail rockfish (*Sebastes flavidus*) (Ralston and Howard, 1995).

The authors concluded that recruitment was set before the late pelagic juvenile stage,

with interannual recruitment variability being mediated by temperature, but noted

SST is a proxy for more complicated physical mechanisms (Ralston and Howard,

1995). In another study, lagged sea level height anomalies (SLA) during February-

May were negatively correlated with the abundance of rockfish species in May-June (1983-2010) and the strongest correlations occurred during April-May ($\rho = 0.57$) which, on average, would correspond to the pelagic juvenile stage (Ralston et al., 2013). However, in a follow up study, the correlation with SLA deteriorated when more data were added that covered the North Pacific marine heatwave of 2014-2016, a period of high SLA and high rockfish catches (Schroeder et al., 2019). Instead, a better indicator of source water transport, the 'spiciness index', explained rockfish recruitment and that the strength of correlations increased from January-May with mean April-May spiciness values explaining 81% of interannual recruitment variation (Schroeder et al., 2019). The interpretation of these results from Ralston et al. (2013) and Schroeder et al. (2019) is that a greater influx of Pacific Subarctic Upper Water (PSUW) is beneficial for rockfish productivity, but the biological mechanism is still unclear. Other studies have noted the importance of PSUW intrusion for fish production (Chelton et al., 1982; Schirripa and Colbert 2006; Stachura et al. 2014; Tolimieri et al., 2018; Haltuch et al., 2020; Vestfalls et al., 2023). The overarching hypothesized biological mechanism is that an increase flux of Pacific subarctic water to the CCS is enriched with oxygen (Meinville and Johnson, 2013) and supports a greater abundance of lipid-rich subarctic copepods (Keister et al., 2011), which would be beneficial to the ELS rockfishes (Peterson et al., 2014). This analysis advances upon these studies by mechanistically modeling growth based on first principles (i.e. temperature-dependent physiology and prey abundance) and finds similar explanatory power compared to studies using oceanic proxies.

Next steps to unraveling a mechanistic understanding of rockfish recruitment via Eulerian IBMs could include gaining a better understanding of growth potential hotspot formation and its relationship to large scale oceanographic forcing, such as the influence of PSUW intrusion into the CCS. Empirically, growth rate variability for the ELS of northeast Pacific rockfishes is mediated by environmental conditions (Ralston, 1995; Crane, 2014; Wheeler et al., 2017; Fennie et al., 2023a; 2023b). ELS growth of three deep dwelling species, chilipepper rockfish (*Sebastes goodei*), widow rockfish (*S. entomelas*), and yellowtail rockfish (*S. flavidus*), captured in the RREAS, are positively correlated with SST (Crane, 2014). Similar findings were seen for black rockfish (*S. melanops*) that settled in kelp forests of central Oregon (Fennie et al., 2023a). Meanwhile, for two nearshore species, copper rockfish (*S. caurinus*) and gopher rockfish (*S. carnatus*), SST was negatively related to growth (Wheeler et al., 2017), which is similar to the results of scenario experiments performed on the underlying ontogenetic bioenergetics model of Shortbelly rockfish (Morales et al., *in press*). Growth potential hotspot intensity from the Eulerian IBM analyzed here is negatively correlated with simulated temperatures from ROMS at 30m depth. Considering growth during the four life stages modeled here contributes to the magnitude of recruitment in different ways, the conflicting relationships between SST and backcalculated larval growth of fish that survived to either the pelagic juvenile phase (Crane, 2014) or settled to benthic habitat (Wheeler et al., 2017; Fennie et al., 2023a) could be confounded by not accounting for life stage-dependency effects of growth on survival.

While describing the mechanisms of stage-specific hotspot formation in detail was outside the scope of this paper, it is worth noting that, for example, 1998 was one of the lowest recruitment years on record, while hotspot intensity was relatively high and the average temperature within a hotspot was relatively low (as indicated by the negative association between temperature and hotspot intensity). The strongest El Niño within our 23-year study occurred in 1998, and temperatures throughout the central CCS were, in general, significantly warmer than normal (Thompson et al., 2022). However, thermal refugia with elevated food availability were likely responsible for generating growth hotspots in 1998 and these refugia were likely advantageous to the fish that recruited in 1998. Indeed, MacFarlane et al. (2005) showed that growth of juvenile Chinook Salmon (*Oncorhynchus tshawytscha*) was faster in 1998 (compared to 1999) and fast growth was associated with greater zooplankton abundance in the Gulf of Farallones which emphasizes the importance of local-scale oceanographic variability on fish growth. However, 1998 ended up being a poor year for salmon survival in the Gulf of Farallones region (Henderson et al., 2019). In Oregon, Fennie et al. (2023a) showed that high SST in their study region predicted fast growth of blue rockfish, but fast growth did not predict high survival. They note that fish who survived the pelagic larval duration and settled in 2015 grew the fastest, yet the magnitude of settlement was the lowest over the four-year time series (Fennie et al., 2023a). Empirical approaches to testing the growth-survival hypothesis on recruitment can be prone to sampling biases. The major sampling bias comes in recognizing that while the overall magnitude of recruitment can be low, fish that did survive to settlement, and whose characteristics were realized, were those

who grew the fastest while most individuals in the cohort grew slow and did not survive to settlement. Our approach bypasses these constraints by characterizing the potential for growth within ELS Shortbelly, mediated by ocean conditions, and then relates growth to recruitment by taking into consideration only the regions that experienced fast growth (and their associated ocean conditions).

Our approach, however, has its limitations. First, the underlying bioenergetics model overestimates early larval growth when exposed to novel conditions. The bioenergetics model was trained on spatially invariant climatological conditions during parameterization (Morales et al., *in press*). However, expansion of the model to a spatial climatology of temperature and food availability produced spatial patterns of high growth potential for preflexion larvae that overlapped with historical spawning grounds as well as produced regions of fast growth potential that were similar to spatial patterns of catches from the RREAS (Morales et al., *in press*). Our baseline bioenergetics model could be improved with new physiological data for early larval stages and a better understanding of feeding rates, which should improve predictions of growth during preflexion, flexion and postflexion larval stages when exposed to novel and/or highly dynamic conditions. Second, our interpretation of the functional relationships between life stage-explicit growth presented here are largely based on the assumption that growth is tightly coupled with predation mortality, which is the primary assumption in the growth-survival hypothesis (Robert et al., 2023). Incorporation of predation mortality into the shortbelly IBM would greatly enhance our understanding of rockfish recruitment. Efforts are underway to

characterize larval predator-prey assemblages for the CCS using eDNA techniques (Andrew Thompson, *personal communication*) and coupling these efforts within a mechanistic IBM framework could fill the missing link. For pelagic juvenile rockfish, a dominant prey group to higher trophic level predators within the CCS (Thayer et al., 2014; Warzybok et al., 2018; Lowry et al., 2022), the incorporation of predation mortality within an IBM framework could follow the approach outlined by Vasbinder et al. (2023). There they imposed top-down predation mortality from a seabird on modeled juvenile Chinook salmon given size-dependent predation thresholds (mediated by simulated salmon growth), dynamic seabird abundance and distribution, and annual variability of diet composition. Finally, we did not incorporate larval dispersal via ocean currents, which would determine the fate of larvae during the earliest developmental stages (i.e. preflexion and flexion), and perhaps beyond. Advective losses of larvae is Hjort's second hypothesis for explaining year-class success and separating food web dependency from transport dependency via a Lagrangian IBM could further tease out mechanisms of recruitment fluctuations for this ecologically important species.

Conclusion

Our modeling efforts have revealed that the relationships between growth during four distinct ELS's of Shortbelly rockfish and recruitment are complex with the direction of growth-mediated recruitment variability changing across ontogenetic stages. The preponderance of growth contributing to recruitment is, overall, in line with the growth-survival hypothesis since growth across all four pre-recruitment

stages explains a high degree of incoming year-class strength. Identifying mechanisms of recruitment variation for Shortbelly rockfish, and the many other species of commercially and recreationally important rockfishes who covary with them, has the potential to greatly improve forecasting and management of rockfish productivity throughout the California Current. An improved understanding of these mechanisms also illuminates the complex interplay between physical variability, primary and secondary production, forage fish availability, the diverse suite of predators, and the human community that interacts with the system. In doing so, we can move closer to an operational ecosystem-based management approach for this productive marine ecosystem.

Tables and Figures

Table 1. Sample sizes of pelagic juvenile Shortbelly rockfish (*Sebastes jordani*) used for ageing caught in the Rockfish Recruitment and Ecosystem Assessment Survey through otolith microstructure analysis and the sample size of standard length (SL) measurements used for back-calculating birthdate frequency distributions. Mean, median, and standard deviation (Std Dev) of back-calculated birthdates of pelagic juvenile Shortbelly caught in the RREAS as well as pelagic juvenile growth rate (mm/day) based off the slope of linear length-at-age regressions are provided.

Year	Otolith Sample Size	SL Sample Size	Mean	Median	Std Dev	Pelagic Juvenile Growth Rate (mm/day)
1988	91[a]	3921[a]	1-Feb[a]	28-Jan[a]	24.37[a]	0.5735[a]
1989	57[b]	584[b]	13-Feb[b]	3-Feb[b]	35.59[b]	0.5253[b]
1990	34	1149	23-Feb	23-Feb	10.33	0.5804
1991	36	658	10-Mar	12-Mar	28.15	0.5852
1992	32	467	9-Apr	9-Apr	6.17	0.5343
1993	35	1668	10-Mar	17-Mar	22.8	0.4763
1994	42	44	3-Apr	11-Apr	26.41	0.5317
1995	15	94	27-Mar	31-Mar	19.67	0.5042
1996	29	457	13-Apr	17-Apr	13.66	0.4282
1997	37	360	23-Mar	23-Mar	14.97	0.5666
1998	27	32	29-Mar	30-Mar	6.71	0.4353
1999	0	NA	20-Mar	21-Mar	14.47	NA
2000	0	NA	30-Mar	30-Mar	10.87	NA
2001	44	1120	13-Mar	14-Mar	19.46	0.5462
2002	0	NA	12-Feb	11-Feb	14.26	NA
2003	38	107	9-Feb	5-Feb	16.04	0.6224

2004	10	356	13-Mar	16-Mar	21.21	0.4677
2005	7	4	20-Mar	16-Mar	14.03	0.4082
2006	11	44	31-Mar	2-Apr	6	0.5888
2007	7	159	22-Mar	21-Mar	11.84	0.5708
2008	0	0	NA	NA	NA	NA
2009	3	289	17-Mar	14-Mar	13.65	0.6454
2010	11	135	16-Mar	16-Mar	16.15	0.5251
1988-2010	566	7143	13-Mar	16-Mar	24.17	0.556

[a] Woodbury and Ralston (1991)

[b] Lenarz et al. (1995)

Table 2. Correlation between life stage explicit growth potential intensity (Gi*
values) and raw growth, temperature, small zooplankton (ZS), large zooplankton
(ZL), krill (ZP), and total food (sum of ZS, ZL, and ZP). * indicates p-value < 0.05.

| Life Stage	Growth	Temperature	Total Food	ZS	ZL	ZP
Preflexion	**0.58**	-0.17	**0.42**	**0.45**	**0.36**	0.11
Flexion	**0.59**	**-0.29**	**0.41**	**0.35**	**0.41**	0.19
Postflexion	**0.74**	-0.15	**0.63**	**0.38**	**0.68**	**0.4**
Pelagic Juvenile	**0.62**	**-0.51**	**0.48**	-0.09	**0.56**	**0.62**

Table 3. Correlation matrix of growth potential hotspot intensity and areal extent (size). Upper triangle are Pearson correlation coefficients and lower triangle are associated p-values. Bold values indicate significance at the p < 0.05 level.

|	Preflexion Intensity	Preflexion Size	Flexion Intensity	Flexion Size	Postflexion Intensity	Postflexion Size	Juvenile Intensity
Preflexion Intensity		**0.52**	**0.52**	0.41	0.39	0.31	0.16
Preflexion Size	**0.013**		-0.32	0.31	-0.18	-0.11	0.089
Flexion Intensity	**0.014**	0.13		0.1	0.38	0.11	0.074
Flexion Size	0.058	0.16	0.65		-0.22	-0.24	0.056
Postflexion Intensity	0.073	0.4	0.07	0.32		**0.86**	0.28
Postflexion Size	0.16	0.63	0.62	0.27	**1.32E-07**		0.34
Juvenile Intensity	0.47	0.68	0.74	0.8	0.2	0.12	
Juvenile Size	0.99	0.75	0.69	0.86	0.74	0.17	0.003

Table 4. Summary statistics for the generalized additive model for explaining interannual deviance in Shortbelly recruitment showing model types, model formulation, p-value of model covariates, generalized cross validation (GCV), deviance explained (%), Akaike Information Criterion corrected for small sample size (AICc), and the difference of AICc between top model and single covariate models (ΔAICc). Hot spot (HS).

Model Type	Model	p-value	GCV	Deviance Explained	AICc	ΔAICc
Top Model	s(preflexion HS intensity) + s(flexion HS intensity) + s(flexion HS size) + s(postflexion HS size) + s(juvenile HS intensity)	all predictors significant @ $p < 0.05$	0.632	78.60%	49.92	0
Single Covariate Model	s(preflexion HS intensity)	0.432	1.13	11.20%	60.7	16.79
	s(preflexion HS size)	0.143	1.03	9.91%	67.85	17.93
	s(flexion HS intensity)	0.112	0.951	54.30%	60.65	10.73
	s(flexion HS size)	0.195	1.02	39.50%	63.53	13.61
	s(postflexion HS intensity)	0.41	1.16	3.42%	67.47	17.55
	s(postflexion HS size)	0.138	1.07	10.70%	65.75	15.84

|					
s(juvenile HS intensity)	0.09	0.944	28.70%	62.73	12.81
s(juvenile HS size)	0.06	0.959	21.80%	63.28	13.36
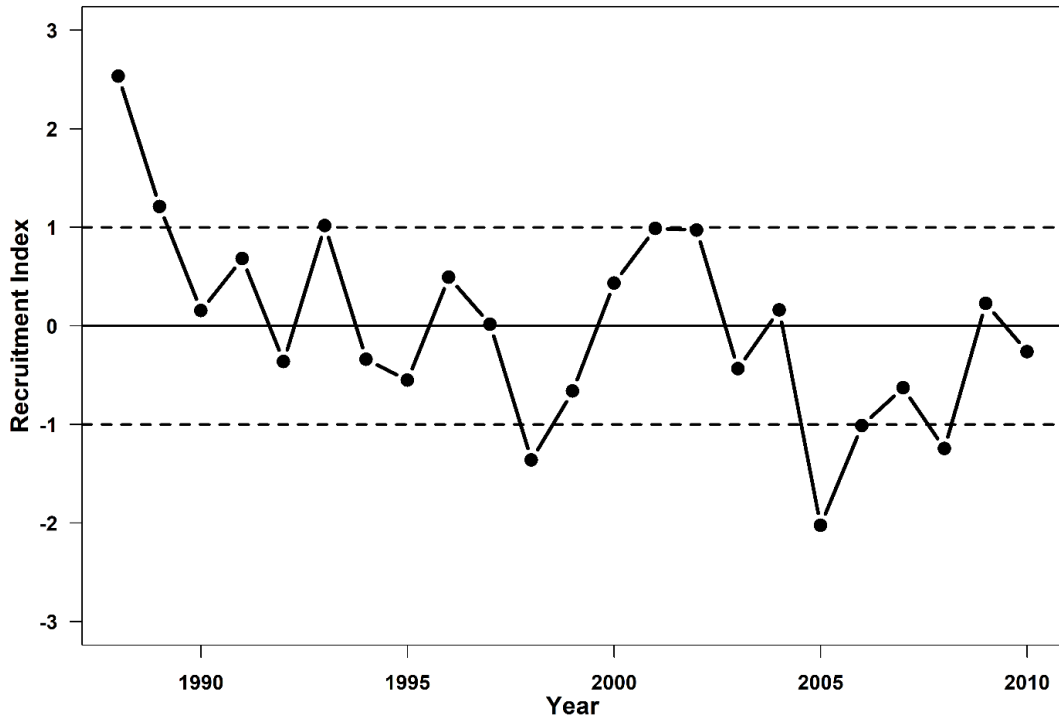
Figure 1. Standardized recruitment anomalies of pelagic juvenile shortbelly rockfish (*Sebastes jordani*) from the Rockfish Recruitment and Ecosystem Assessment Survey (RREAS).
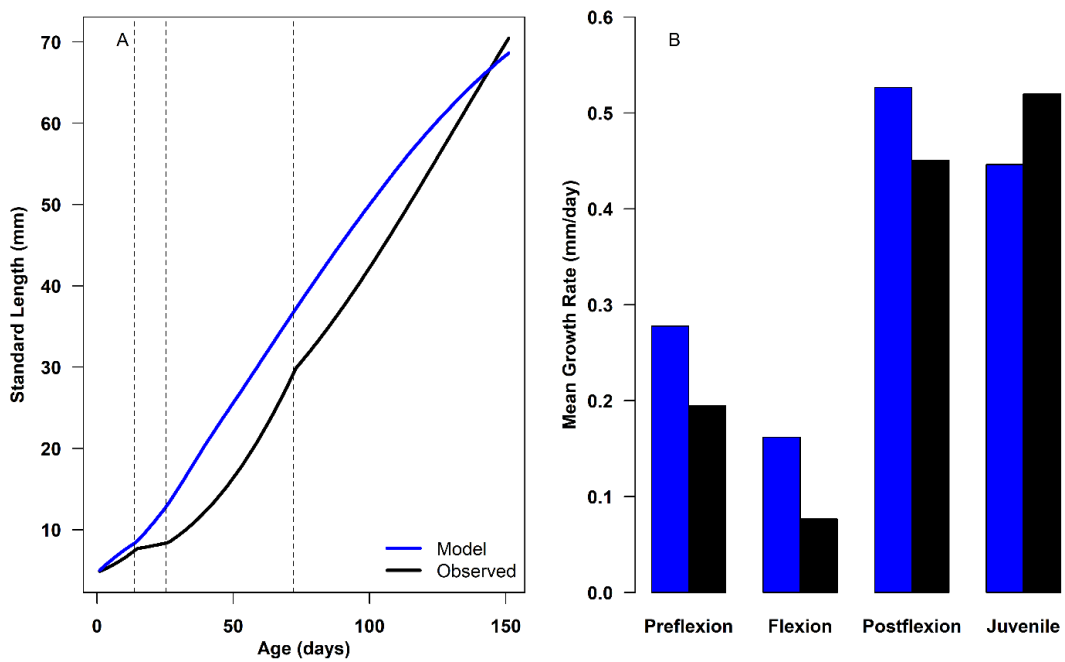
Figure 2. Modeled growth potential from the Shortbelly rockfish Eulerian IBM
relative to observed growth. (A) Modeled grand mean (1988-2010) of standard length
of fish (mm) vs. age (days) (blue line) relative to observations (black line) of Laidig
et al. (1991).Vertical dashed lines denote observed life stage transitions for preflexion,
flexion and postflexion larval stages, and the pelagic juvenile stage. (B) Modeled
grand mean growth rate (mm/day) (blue bars) relative to observed growth rate (black
bars).
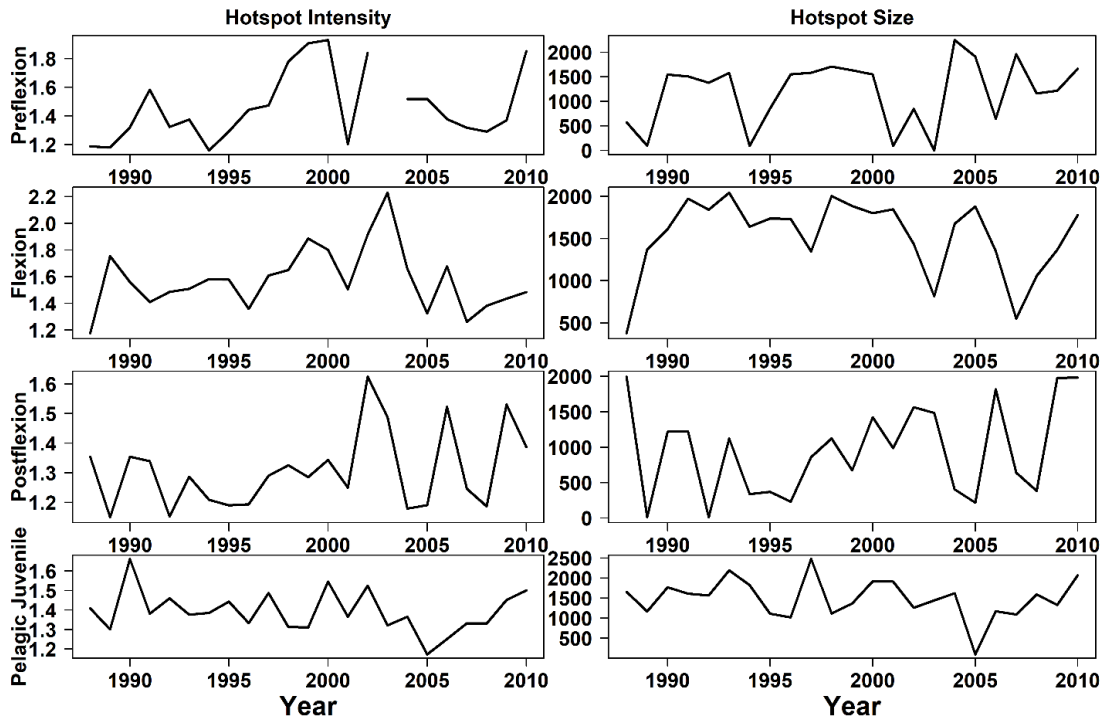
Figure 3. Time series of mean growth potential hotspot intensity (1st column) and areal extent (size) (2nd column) of significant hotspots for each life stage (rows). No significant growth potential hotspot was detected for preflexion larvae in 2003.
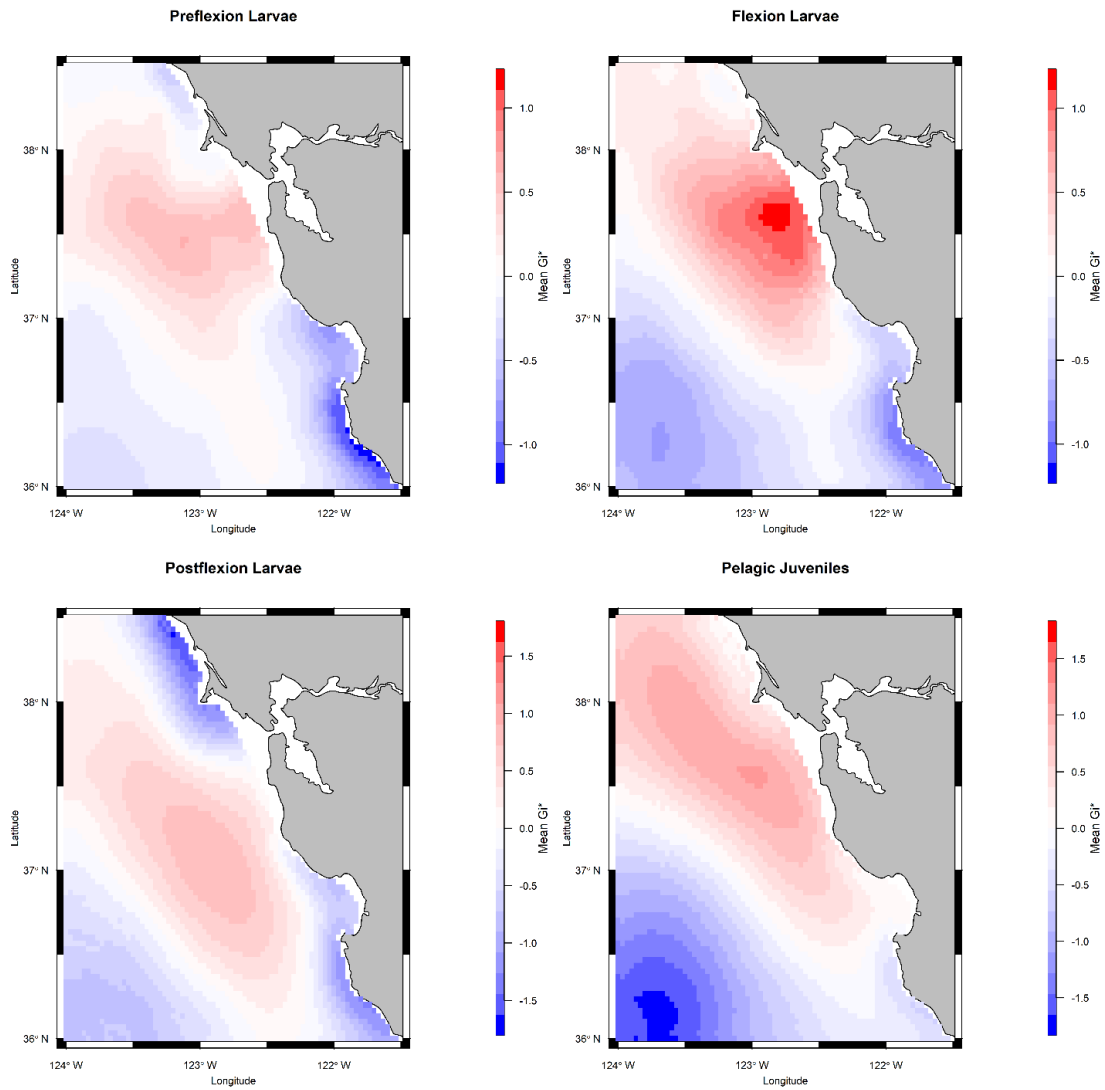
Figure 4. Mean growth potential hotspot intensity (Gi* values) (1988-2010) maps for

preflexion, flexion and postflexion larval, and pelagic juvenile stages.
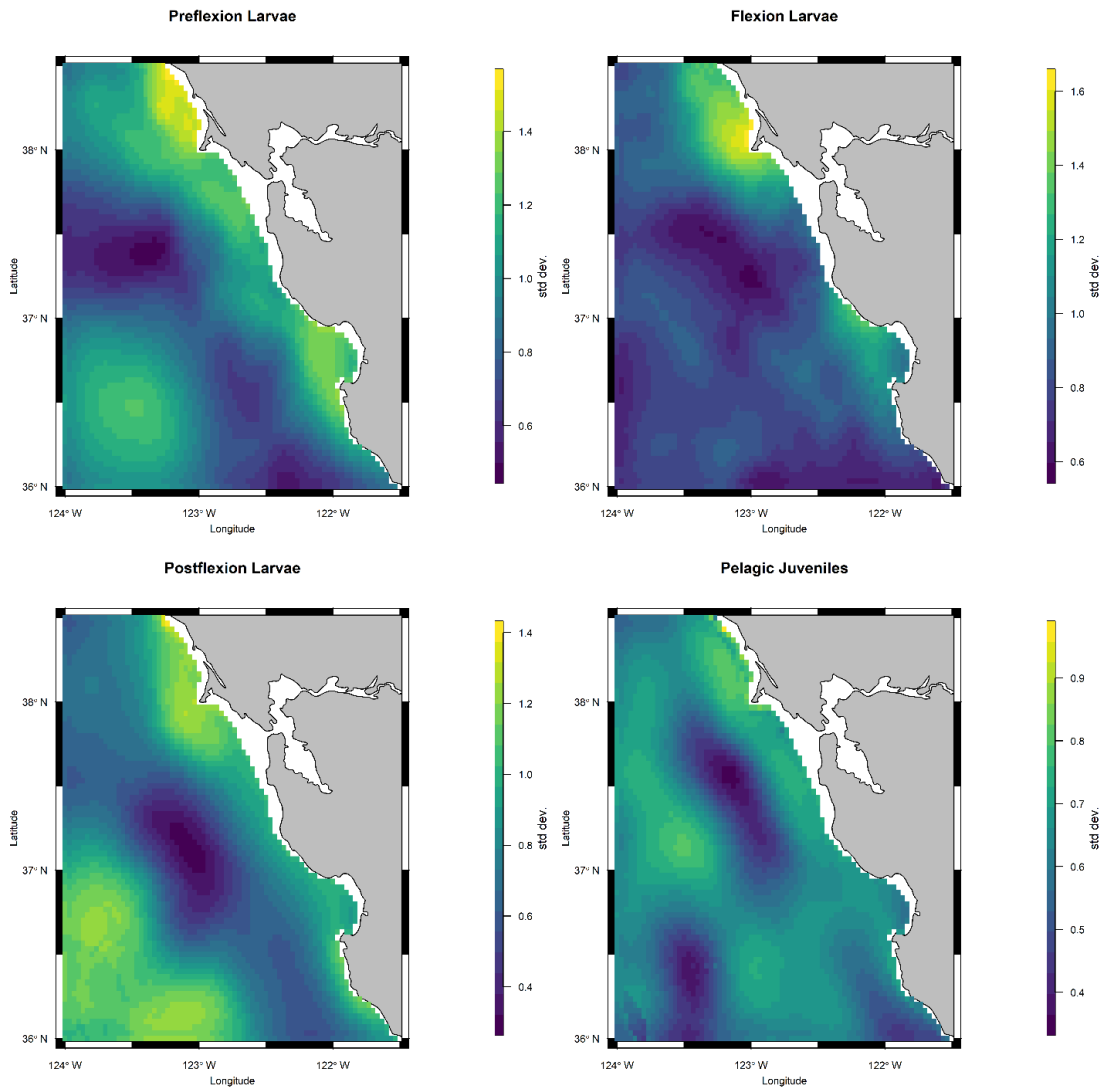
Figure 5. Temporal variation **(**standard deviation) of hotspot intensity over 1988-
2010 for preflexion, flexion and postflexion larval, and pelagic juvenile stages.
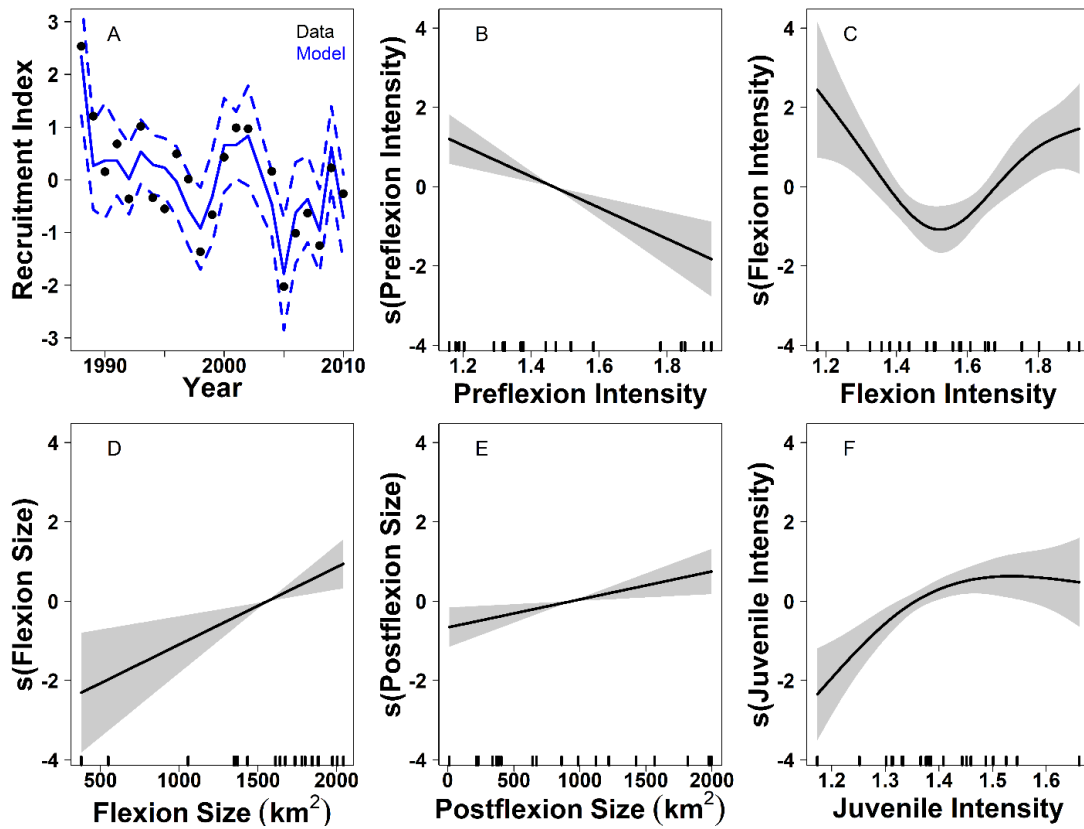
**Figure 6.** Results of generalized additive model for explaining Shortbelly rockfish recruitment with growth potential hotspot attributes. (A) Modeled recruitment (blue line) and delta-GLM standardized recruitment (black points??) of pelagic juvenile shortbelly abundance from the Rockfish Recruitment and Ecosystem Assessment Survey (RREAS). (B-F) Generalized additive model results for evaluating the functional relationship between Shortbelly recruitment and (B) preflexion intensity, (C) flexion intensity, (D) areal extent of hotspot (size; km^2) for flexion and (E) postflexion larvae, (F) pelagic juvenile hotspot intensity.

107
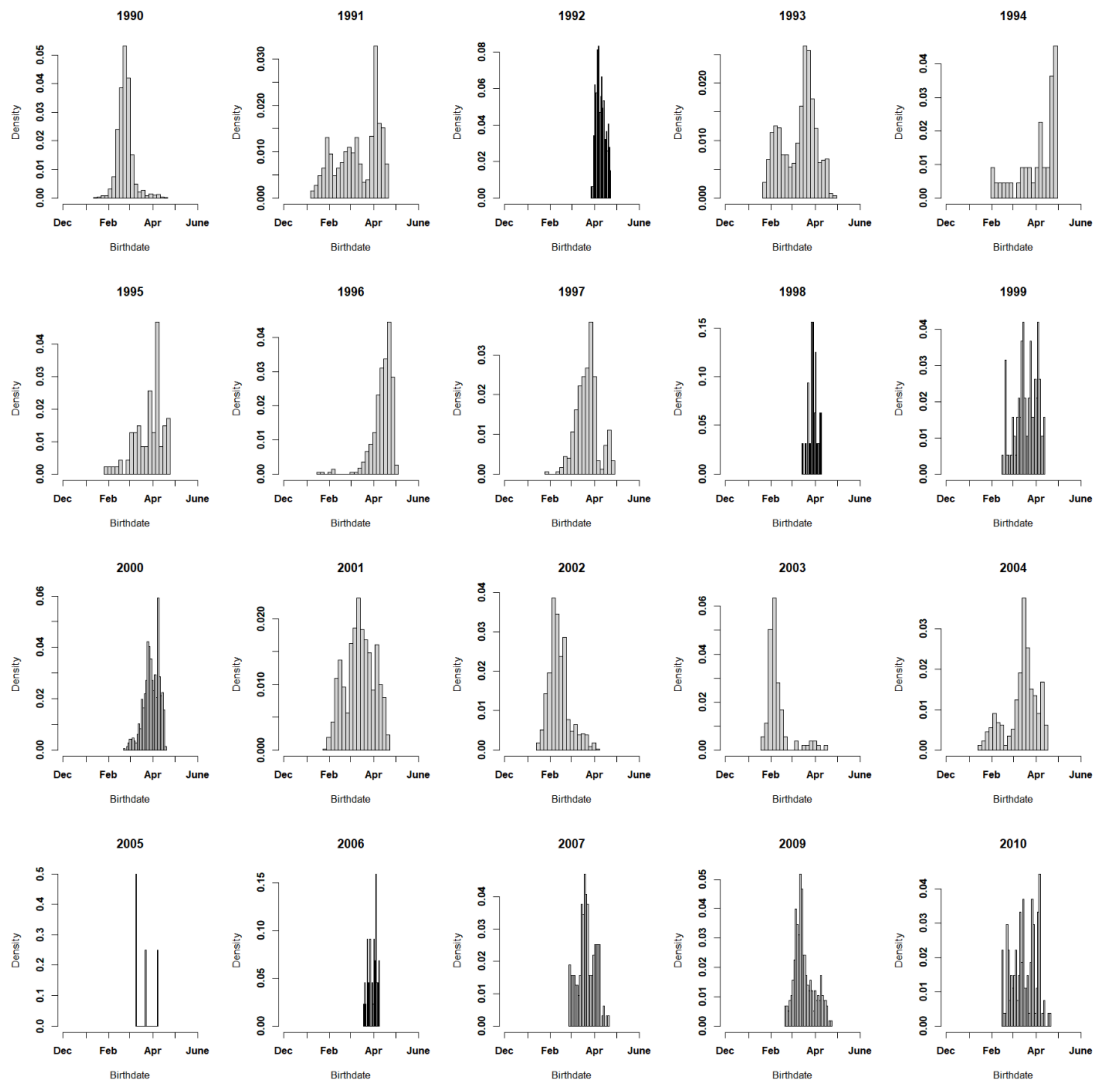
Figure S1. Back-calculated birthdate frequency distributions of pelagic juvenile shortbelly rockfish for 1990-2010.
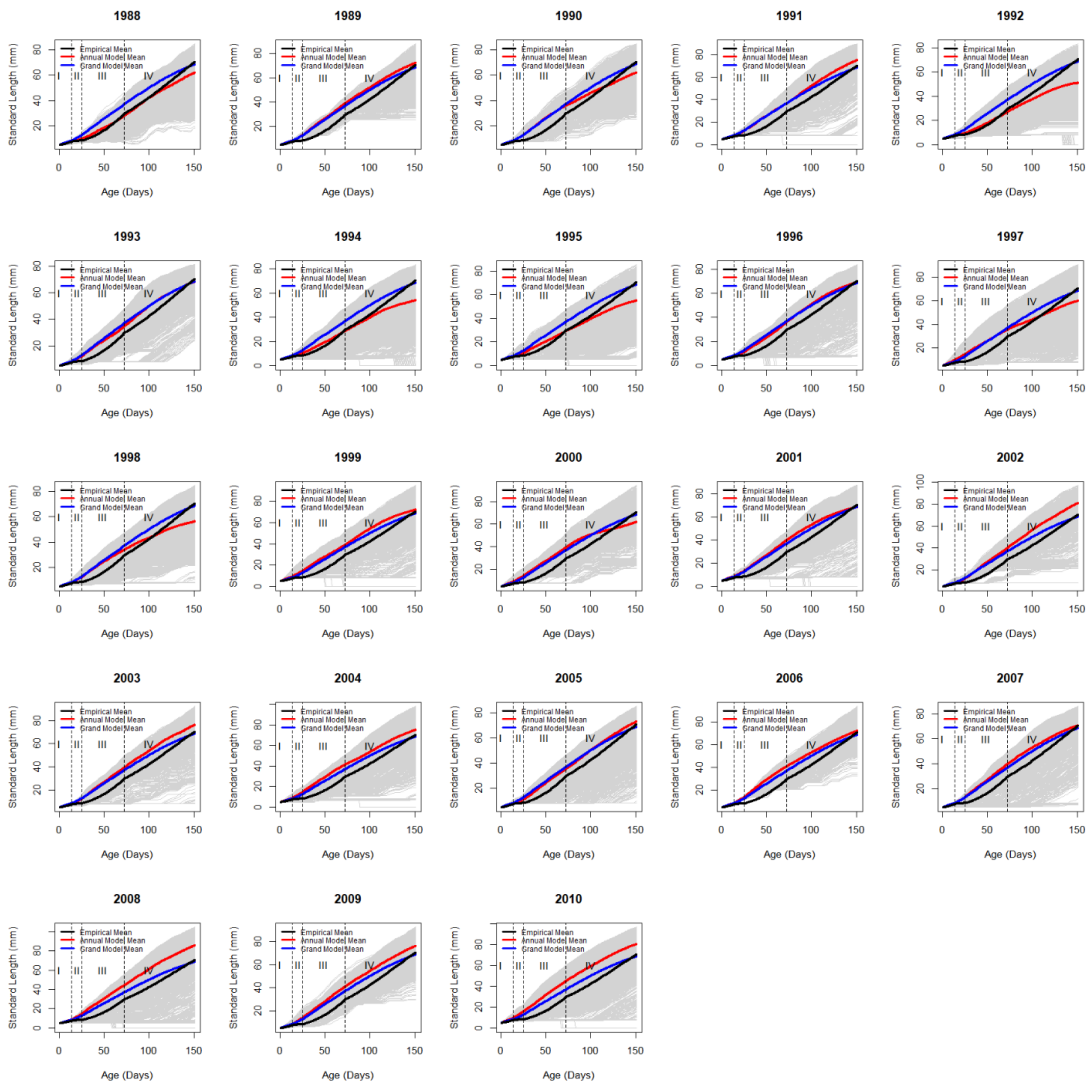
Figure S2. Modeled annual standard length-at-age curves for all individuals in model domain (grey lines) relative to empirical mean (black; Laidig et al., 1991), annual mean of individuals (red) and the grand mean (blue; 1988-2010).

Series residuals(mod3_v2)
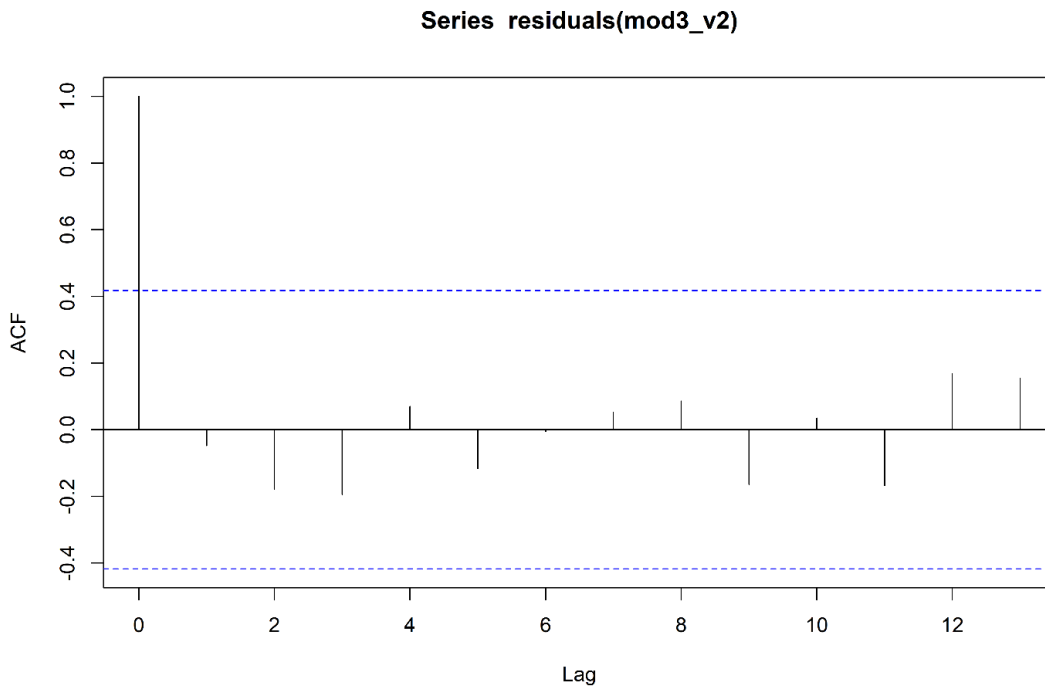
Figure S3. Autocorrelation of the top generalized additive model. Bars extending beyond broken lines indicate significant autocorrelation (p < 0.05).

Chapter 3

Context matters: mechanisms of recruitment dynamics associated with contrasting ENSO events in the California Current

Abstract

Understanding biophysical drivers of year-to-year changes in the replenishment of marine fish populations (i.e., recruitment) is crucial for effective single species and ecosystem-based fisheries management (EBFM). Mechanistic models grounded in first principles (i.e., physiology) when coupled to ocean circulation models are useful to retrospectively test recruitment hypotheses. Here, a coupled biophysical individual-based model for Shortbelly rockfish (*Sebastes jordani*), a non-commercial, yet ecologically important species of the California Current System, is used to evaluate the relative influence of starvation mortality and advective losses on recruitment across El Niño Southern Oscillation events. Starvation should dominate over transport processes because during an El Niño event, temperature is warm leading to increased metabolic cost and food availability leading to decreased consumption. In contrast, increased upwelling during La Niña events will lead to cooler conditions and increased prey production (thus reducing starvation), but larvae would be advected offshore and away from habitat favorable to settlement (nearshore). Leveraging biological data from a fisheries-independent survey along with model output, I show that starvation had a larger effect on modeled recruitment than did retention during El Niño events ($\beta_{\text{Starvation, El Niño}}$ = -0.84 vs. $\beta_{\text{Retention, El Niño}}$ = 0.27), and both starvation and modeled recruitment explain the timing and magnitude of observed recruitment

(ρ = -0.67 and ρ = 0.68, respectively). In contrast, retention over the continental shelf had a larger effect on modeled recruitment than did starvation during La Niña events ($\beta_{\text{Retention, La Niña}}$ = 0.95 vs. $\beta_{\text{Starvation, La Niña}}$ = -0.049), but while retention alone could not explain the timing of observed recruitment, modeled recruitment was positively associated with observed recruitment for one of the two La Niña years (1999) (ρ = 0.66) and when both years (1989 and 1999) were combined (ρ = 0.44). The preponderance of recruitment variability being differentially driven by food web-dependent and transport-dependent processes amongst a backdrop of contrasting environmental conditions (ENSO events) emphasizes the importance of context-dependency when studying mechanisms of recruitment variability.

Introduction

Marine fish populations fluctuate over broad spatial and temporal scales (e.g., Lluch-belda et al., 1999). Annual recruitment variability is a main driver of adult fish population fluctuations (Hjort, 1914). Recruitment is the number of larval fish that survive to become adults, and for exploited marine fish species, is the number of fish that enter the fishery (Ricker, 1954; Beverton and Holt, 1957). Fisheries oceanographers have strived for over a century to understand the biophysical drivers of recruitment success (Houde, 2008). Johan Hjort proposed two hypotheses to explain large amplitude fluctuations in annual recruitment (Hjort, 1914; 1926). The first mechanism proposed was the Critical Period hypothesis which posits that young larvae must acquire suitable food before their yolk sacs (or oil globules) have become fully absorbed or else mass mortality will occur due to starvation. Hjort's second

mechanism was the Aberrant Drift hypothesis which predicts recruitment strength is determined by larval dispersal via ocean currents. For example, if fish are transported away from their adult populations and/or nursery grounds then recruitment will be low (Harden-Jones, 1968). Several extensions of Hjort's hypothesized mechanisms of recruitment variability have been made since his seminal articles and these extensions can be broadly categorized into either food web-dependent or transport-dependent mechanisms (Figure 1). Some authors of these extensions argued their stance in the literature, proposing food limitation overrides transport effects, or vice versa (e.g., Sinclair and Illes, 1985; Cushing, 1986). However, rather than recruitment being determined solely by food web-dependent or transport-dependent mechanisms, both could operate on year class success of the same species, with each category of mechanisms being important in different places and at different times (Cury and Roy, 1989).

Context dependence occurs when ecological relationships vary in magnitude or sign depending on differing abiotic and/or biotic conditions (Catford et al., 2022). Physical variability of the California Current System (CCS), one of the four major eastern boundary upwelling systems (Fréon et al., 2009), operates over multiple scales (Checkley and Barth, 2009). The dominant modes of variability for the central CCS (Cape Mendocino to Point Conception) occur at intraseasonal and interannual timescales (Chavez and Messié, 2009). At intraseasonal timescales, synoptic upwelling events can vary in frequency and magnitude, which in turn can impact the delivery of fish larvae to nursery sites (Hobson and Chess, 1988; Bakun, 1996), can

have significant impacts on lower trophic level production (Garcia-Reyes et al., 2014), and can modulate larval fish feeding success and survival (Lasker, 1975; 1978). At interannual timescales, the El Niño Southern Oscillation (ENSO), with a periodicity of ~3-7 years, can modify surface winds and subsequent upwelling through Rossby waves that strengthen and displace the Aleutian low (Alexander et al., 2002; Schwing et al., 2002). Furthermore, during an El Nino event, coastal Kelvin waves deepen the nutricline, which together with decreased upwelling favorable winds, leads to decreased primary productivity (Palacios et al., 2004; Jacox et al., 2015). The influence of ENSO on upwelling dynamics can affect the composition, distribution, and abundance of zooplankton (Santora et al., 2014; Lilly and Ohman, 2018; Cimino et al., 2020) and transport of marine fish larvae (Bashevkin et al., 2020). These food web-dependent and transport-dependent processes significantly impact recruitment dynamics of coastal marine fishes, but the relative influence of the two mechanisms together have not been fully investigated under contrasting environmental conditions.

Rockfishes (*Sebastes spp.*) of the northeast Pacific are a highly speciose genus of fishes with commercial, recreational, ecological, and cultural significance (Love et al., 2002). The Rockfish Recruitment and Ecosystem Assessment Survey (RREAS) has sampled the micronekton assemblage in central California (36.5°N-38.5°N) using a midwater trawl since 1983 with the goal to assess recruitment of winter-born rockfishes (Sakuma *et al*., 2016; Field et al. 2021). Annual indices of abundance for young-of-the-year rockfish species are used in statistical catch-at-age stock

assessments to estimate incoming year-class strength (recruitment) and reduce uncertainty in biological reference points used in fisheries management (Field et al., 2021). Importantly, the indices represent the abundance of a species after most of the density-independent processes have occurred (Field et al., 2010) and are a close approximation to 'realized' recruitment (Ralston et al., 2013). Deviations between recruitment estimates from the RREAS and 'realized' recruitment estimated from stock assessments can be driven by density-dependent mortality after fish have settled to adult benthic habitat (Ralston et al., 2013). Additionally, differences between the RREAS recruitment indices and realized recruitment are due to sampling bias in the RREAS and uncertainty in realized recruitment from assessments. For example, during a strong La Niña year, intense and persisting upwelling throughout the reproductive window can transport larvae offshore and outside of the sampling area, leading to an underestimation of recruitment in the assessment if larval survival and subsequent recruitment is high. Conversely, during a strong El Niño year, weakened or delayed upwelling could lead to low productivity of phytoplankton and zooplankton and lead to mass mortality of the early life stages of rockfishes. However, reduced offshore Ekman transport should lead to greater retention of young-of-the-year rockfish near the coast and reduce sampling bias, albeit at relatively lower levels of abundance. Hence, the interplay between food web-dependent vs. transport-dependent mechanisms of recruitment variability, and the detectability of incoming year class strength in recruitment surveys, should be context dependent.

I predict that recruitment of rockfish will disproportionately be driven by food web-dependent mechanisms (i.e., starvation mortality) during El Niño events and transport-dependent mechanisms during La Niña events. Individual-based models (IBMs) are useful tools to evaluate mechanisms of fish recruitment (Peck and Hufnagl, 2012). I test these predictions using a coupled biophysical individual-based model (CBP-IBM) across two El Niño years and two La Niña years by comparing starvation mortality and coastal retention of early life stage (ELS) Shortbelly across years. I then investigate intra-annual variation of each mechanism by comparing the timing and magnitude of observed recruitment (estimated by birthdates of surviving pelagic juveniles captured in the RREAS) with sub-cohort level starvation mortality and retention indices predicted by the CBP-IBM under differing larval release dates.

Materials

Shortbelly rockfish

This study focuses on Shortbelly rockfish (*Sebastes jordani*), which are the most abundant species of rockfish on the U.S. West Coast, but are most abundant in central California along the continental shelf break between Point Reyes (~38°N) and the northern end of Monterey Bay (~37°N) (Love et al., 2002; Field et al., 2007). As adults, they are found from 90 to 500 m in depth and form dense schools at night on the bottom, but disperse at night to feed on krill in shallower depths (Love et al., 2002). Shortbelly are early to mature (50% of females mature by age 2, 99% by age 3 or 20 cm standard length) and have a relatively high natural mortality rate (Field et al., 2007), making them more 'forage fish like' compared to other species of genus

Sebastes (Love et al., 2002). Females can produce as many as 50,000 eggs per reproductive bout (Love et al., 2002), and parturate (give birth to) live larvae over a broad reproductive window that begins as early as December, ends in late April, but peaks in February (Wyllie-Echeverria, 1987; Woodbury and Ralston, 1991; Lenarz et al., 1995). Larvae and pelagic juveniles spend up to 150 days in the coastal pelagic environment before recruiting to nearshore rocky reefs from June-August (Love et al., 2002). Shortbelly exhibit drastic fluctuations in recruitment lending them ideal for tests of Hjort's hypotheses (Field et al., 2007). While Shortbelly are not targeted directly by commercial or recreational fisheries, they are an essential component of the CCS forage assemblage (Thayer et al., 2014; Warzybok et al., 2018; Lowry et al., 2022). Recently, there has been an increase in the incidental take (i.e., bycatch) of Shortbelly in Pacific Hake (*Merluccius productus*) fisheries, which almost closed the profitable fishery without adaptive management (PFMC 2022). Due to their ecological importance, recent challenges to fisheries management, and numerical dominance in the RREAS (Field et al., 2021), I use Shortbelly as a model species to test the hypothesis that mechanisms of recruitment variability differ between ENSO years (i.e., context dependent).

Coupled Biophysical Individual-Based Model – Model Structure Overview

The CBP-IBM for the ELS of Shortbelly rockfish was implemented by coupling four separate models (Figure 2). First, the Regional Ocean Modeling System (ROMS; Shchepetkin & McWilliams, 2005; Haidvogel et al., 2008) at 3 km horizontal resolution is used here to simulate temperature and horizontal velocity

117

fields (Fiechter et al., 2018; 2020). NEMUCSC, a customized version of the North Pacific Ecosystem Model for Understanding Regional Oceanography (NEMURO; Kishi et al., 2007), which is coupled to ROMS, is used to simulate the concentrations of three zooplankton size classes (Fiechter et al., 2018; 2020). The ROMS-NEMUCSC domain used here was subsampled from its original configuration (32-44°N, 129-116°W) to focus on the region encompassing Cape Mendocino to Point Conception (34.5-40.5°N) and from the coast to 300 km offshore. This reduced domain was chosen because Cape Mendocino to Point Conception represents the latitudinal extent of the central CCS (Checkley and Barth, 2009), which encompasses important habitat and spawning grounds for Shortbelly. Temperatures from ROMS and zooplankton concentrations from NEMUCSC were used to force a highly resolved ontogenetic bioenergetics growth model for the larval and pelagic juvenile stages of Shortbelly (Chapter 1). Horizontal velocity fields (i.e., gridded zonal and meridional current velocities) from ROMS, in combination with a Lagrangian particle tracking model, were used to simulate ELS dispersal trajectories.

Lagrangian Particle Tracking Model

Larval dispersal in the CBP-IBM was implemented with a customized Lagrangian particle tracking algorithm developed for this chapter. Coupling was performed offline, using stored output from ROMS-NEMUCSC. Offline coupling is less computationally intensive compared to online coupling (tracking trajectories simultaneously with ROMS calculations) but does not allow for feedback between lower trophic level biology and ELS fish consumption (i.e., top-down control on

zooplankton). The particle tracking algorithm calculates Lagrangian trajectories from daily Eulerian velocity fields at 30m depth using a first order Euler integration scheme with an internal time step of ~26 minutes (55 internal time steps per day). The choice of internal time steps was determined by solving the inequality $\Delta t < \Delta x / U$, where Δt is the internal time step of discretization (in seconds), Δx is the model resolution (3km in this case), and U the expected maximum velocity (1.44 m/s) across the entire model domain for a particular depth (30 m here). Linear interpolation of ocean currents was conducted to estimate velocities at any location within a grid cell (ROMS calculate velocities at the center of each grid cell). The decision to track ELS dispersal in 2D (depth invariant) rather than 3D was threefold: (i) 30 m is the depth of maximum density for larval and pelagic juvenile Shortbelly (Moser and Boehlert, 1991; Ross and Larson, 2003); 30 m is the target depth of the RREAS midwater trawls (Field et al., 2021); and (iii) 2D particle tracking is not as computationally intensive as 3D (North et al., 2009). Furthermore, ELS Shortbelly were tracked as passive drifters, which is a simplifying assumption because evidence from laboratory experiments suggests that even the smallest rockfish larvae (i.e., preflexion larval stages) are capable of swimming at speeds that could counteract ocean currents (Kashef et al., 2014). However, ELS swimming behavior is poorly understood, particularly because it is unclear how long they can maintain a swimming speed, and any directed swimming implemented in the CBP-IBM would introduce uncertainty in dispersal trajectories. If a particle reached any boundary of the domain (northern, coast, south, or offshore (300km from coast)), the particle would 'stick' until it was transported back into the domain. The particle tracking algorithm was implemented in

the R Programming Language (v3.6.1) using the doParallel (v1.0.15) and ncdf4

(v1.17) packages.

Parturition Module

Ralston et al. (2003) reported the spatial location of larvae age 0-2d (Figure

3). I use this as a proxy for the spatial location of reproduction to assemble a spatial

parturition module by assuming that recently born larvae are found near their

birthplace (Figure 4). The highest density of early staged larvae occurred near Pioneer

Canyon and Ascension Canyon, with decreasing density to north and south. A total of

5,000 individual particles were released for each parturition bout (n = 507 grid cells),

with 3,000 individuals being released near the two canyon structures (n = 154 grid

cells). The decision to standardize the number of larvae that were introduced to each

model simulation within and between years was to compare the relative effects of

food web-dependent and transport-dependent processes without confounding the

model with differential larval production within a season or across years.

Timing of peak parturition is believed to be fixed in time (i.e., February; Field,

unpublished data), but considerable interannual variability in birthdate frequencies of

surviving pelagic juveniles captured in the RREAS suggests mortality occurs

differentially on larvae throughout a given cohort (Woodbury and Ralston, 1991;

Lenarz et al., 1995; Chapter 2). For this reason, I initialized eight 'subcohorts' within

a given year over 1988-2010 to understand the influence of within year variability of

food web- and transport-dependent processes on recruitment. Within-year model

initializations occurred on the 1st and 15th day of the month from January-April, or

roughly every 14-17 days. Preliminary analysis of daily water velocities averaged over the parturition grounds at 30 m depth in central California showed current reversals occurred at a frequency of ~2 weeks, and thus my decision to initialize eight reproductive bouts at ~2-week intervals was sufficient to account for intraseasonal upwelling variability.

Oceanic Niño Index and Modeled Biophysical Conditions

While the full CBP-IBM simulation covered 1988-2010, I selected the two largest La Niña and El Niño events over this period using the Oceanic Niño Index (ONI). The decision to select two years for each event was so that only "strong" or "very strong" events were included in the analysis for greatest contrast. ONI data were downloaded from the California Current Integrated Ecosystem Assessment website (https://www.integratedecosystemassessment.noaa.gov/regions/california-current/california-current-iea-indicators).

Zonal and meridional velocities, temperature, and zooplankton concentration (ZS, ZL, and ZP) at 30m depth were qualitatively compared across the four ENSO years to characterize the biophysical conditions experienced by individuals along their drift routes. Anomalies of mass-specific respiration, proportional consumption, and mass-specific growth were calculated by finding the grand mean and standard deviation of each biophysical variable by averaging across all individuals, days, subcohort batches, and years (1988-2010). Standardized anomalies (z-scores) for each of the four ENSO years were calculated as, $(\underline{x}_{i,t} - \mu_i) / s_i$, where $\underline{x}_{i,t}$ is the annual mean of variable i in year t, μ_i is the grand mean (1988-2010) of variable i, and s_i is the

grand standard deviation (1988-2010) of variable i. The interplay of respiration and consumption determines growth, and growth determines the susceptibility of starvation (see section on Modeled Starvation Mortality and Retention Indices). Proportional consumption represents the proportion of realized consumption relative to maximum consumption (Chapter 1). Realized consumption is a proportion of maximum consumption determined by the amount of food available at a given place and time. Maximum consumption is determined by an allometric relationship (between weight and consumption) and is offset by a dome shaped temperature-dependence function. Since the baseline bioenergetics model accounts for ontogenetic changes in dietary preferences and feeding rates (half saturation coefficients), proportional consumption was calculated for each of the four life stages in the growth model (i.e., preflexion, flexion, and postflexion larvae, and pelagic juveniles).Similarly, growth rate varies by life-stage (Chapter 1), so ontogenetic mass-specific annual growth (g fish $\cdot$ g fish^{-1} $\cdot$ day^{-1}) anomalies were calculated to characterize the effect of ENSO on growth rate. Respiration parameters are fixed across life stages and so annual anomalies across life stages are reported for simplicity.

Modeled Starvation Mortality, Retention, and Recruitment Indices

Starvation mortality was selected as a proxy for the food web-dependent processes that can operate on the magnitude of recruitment. While many marine mammals, seabirds and piscivorous fish feed on ELS shortbelly (Lowry et al., 2022; Warzybok et al., 2018; Thayer et al., 2014), I ignore the influence of top-down

controls on the strength of recruitment in this chapter because I was interested in understanding the influence of bottom-up drivers on ELS Shortbelly recruitment (Figure 1) across El Niño and La Niña years. Starvation mortality was determined from a bioenergetics growth model (Chapter 1). Along an individual's drift route, spatiotemporal variation in temperature and food availability from ROMS-NEMUCSC causes individual growth rate variability and starvation was imposed if an individual fell below 50% of their expected weight-at-age during larval stages and 40% during the pelagic juvenile stage. The expected weight-at-age was from Norton et al. (2001). Importantly, fish were not allowed to shrink in length, but could only lose weight. This allowed for the bookkeeping of ELS condition and prevented individuals from transitioning back to an earlier life stage since ontogenetic transitions were length-based (Chapter 1). Both annual (mean over eight within year reproductive bouts) and subannual (individual reproductive bouts) starvation indices were defined as the proportion of total larvae (n = 40,000 or 5,000, respectively) that 'died' of starvation.

Retention within the RREAS sampling area was selected as a proxy for the transport-dependent processes that can operate on the magnitude of recruitment (Figure 1). Shortbelly rockfish recruit to kelp beds and other nearshore areas, but sometimes recruit to deeper rocky reefs during the summer months (June-August) (Love et al., 2002). To encompass these areas, but more importantly to compare the CBP-IBM results with empirical data from the RREAS, I defined retention as the proportion of individuals that were within the RREAS sampling area (Figure 5) on

123

the median date of sampling (May 25th). With this definition of retention, model results could be directly compared with observed recruitment from the RREAS.

Modeled recruitment was defined as the proportion of individuals who survived and were retained within the RREAS survey (Figure 5) on the median date of sampling. Similarly, using the survey area at the time of sampling to define recruitment, modeled and observed recruitment could be directly compared.

Timing and Magnitude of Observed Recruitment

Back-calculation of pelagic juvenile Shortbelly birthdates from otolith microstructure analysis have been described in detail in Chapter 1 and Chapter 2. Here I binned birthdates of surviving juveniles corresponding to an equal number of days preceding and following each model simulation start date (1st and 15th day of January-April). The proportion of total fish born within a particular bin was defined as the timing and magnitude of observed recruitment and was used for intra-annual comparison with starvation mortality, retention, and modeled recruitment indices.

Analysis

Three sets of statistical analyses were conducted on the CBP-IBM output to understand whether ENSO modulates the relative influence of food web-dependent and transport-dependent drivers of Shortbelly rockfish recruitment variability. The first analysis employed a linear mixed effects model to determine if the annual mean starvation mortality, retention, or modeled recruitment differed across ENSO events (two El Niños and two La Niñas). The 'lmer' function from the 'lmtest' package

(v0.9.40) in the R Programming Language (v4.2.0) was used to fit the linear mixed effects model. Either starvation mortality, retention, or modeled recruitment were the response variable and ENSO category (El Niño and La Niña as factors) was included as a fixed effect with year as a random variable. P-value's less than 0.05 were considered statistically significant. Additionally, a pairwise Student's t-test was used to determine differences between ungrouped years, and to account for multiple comparisons, used a threshold p-value of 0.001 to infer significance.

The second analysis looked at subannual starvation mortality, retention, and modeled recruitment over the different modeled start times within a year relative to the timing and magnitude of observed recruitment indicated by birthdate frequencies of surviving pelagic juveniles. Spearman rank correlation coefficients were conducted on the association of the timing and magnitude of observed recruitment and subannual starvation mortality, retention, and recruitment from the model. P-values less than 0.05 were considered statistically significant.

The third analysis quantified the relative effect of subannual starvation mortality and retention on modeled recruitment. Six separate multiple linear regression models (one for each of the four ENSO events, and two for combined ENSO events) were employed with modeled recruitment as the response variable, and starvation mortality and retention as the predictor variables. Standardized coefficients of predictors were used to quantify the relative effect of starvation and retention on modeled recruitment. P-values less than 0.05 were considered significant.

Results

ENSO Impacts on Biophysical Conditions

1989 and 1999 were selected as the two strongest La Niña events (< -1.5 ONI) and 1992 and 1998 were the two strongest El Niño events (>1.5 ONI) over the period of the full CBP-IBM simulation (1988-2010) according to the ONI index (https://origin.cpc.ncep.noaa.gov/products/analysis_monitoring/ensostuff/ONI_v5.php).

Biophysical oceanographic conditions experienced by individuals ("realized conditions") along drift trajectories varied greatly between El Niño (1992 and 1999) and La Niña (1989 and 1999) events (Figure 6). Individuals experienced less offshore advection (less negative zonal velocity) in the two El Niño years and one of the two La Niña years (1989) compared to 1999 (Figure 6A). Meridional velocities (north-south component) experienced by individuals were similar for both El Niño years and in 1999, but meridional velocities differed considerably in 1989 with more northward flow (positive meridional velocity) (Figure 6B).

In general, temperatures were cooler (warmer) and zooplankton concentrations were higher (lower) for the two La Niña (El Niño) years (Figure 6C-F). The contrasting temperatures and zooplankton concentrations across ENSO years caused differential metabolic costs, consumption rates, and subsequent growth rates (Figures 7-9). Respiration was near the long-term average (1988-2010) during La Niña events but was very high during El Niño events (Figure 7). Increased metabolic loss during El Niño and not La Niña events reflects the elevated temperatures experienced by ELS during El Niño events whereas temperatures were relatively

closer to the long-term average during La Niña events (Figure 6C). Proportional

consumption, on average, was anomalously high in La Niña years and low in El Niño

years, however, life-stage specific differences were evident within a given year

(Figure 8). In 1989, consumption was near the long-term average for preflexion (stage

1; Figure 8A) and flexion larvae (stage 2; Figure 8B) but was slightly above average

for postflexion (stage 3; Figure 8C) and the pelagic juvenile stage (stage 4; Figure

8D). For the two El Niño years, consumption was low for all stages (Figure 8A-D)

except for pelagic juveniles which had a relatively average consumption rate in 1992

(Figure 8D). During the 1999 La Niña, individuals were consistently feeding above

average for all life stages (Figure 8A-D). The interactive effect of respiration and

consumption led to differential growth rates across ENSO years (Figure 9). Growth

rate during all life stages was anomalously low during El Niño events, except for

pelagic juveniles in 1992 who grew anomalously fast (Figure 9A-D). In contrast,

growth was fast during La Niña events, but more so in 1999 relative to 1989 (Figure

9A-D).

ENSO Effects on Cohort-level Modeled Starvation Morality, Retention and
Recruitment

The interplay between respiration, consumption, and growth determined

cumulative starvation mortality of a cohort. Mean cumulative starvation mortality

over preflexion, flexion, and postflexion larval stages and the pelagic juvenile stage

was 21% in 1989, 98% in 1992, 86% in 1998, and 15% in 1999 (Figure 10A). El

Niño (La Niña) had a strong, positive (negative) effect on starvation mortality

(F(2,30) = 123.85; p < 0.001; Figure 10A). However, ENSO did not have a significant effect on mean cohort-level retention (F(2,30) = 0.12; p = 0.45; Figure 10B). This was due to 1989 having relatively high retention (33.7%) compared to 1999 (8.2%), and the high retention in 1989 was more comparable to El Niño events (1992 (33.6%) and 1998 (32%)). Retention in 1999, however, was significantly lower compared to all other years (F(3,28) = 10.68; p < 0.01).

Annual mean starvation mortality and retention interacted to determine modeled annual recruitment (Figure 10C), however, modeled recruitment was not related to ENSO (F(2,30) = 0.41; p = 0.59). This was primarily because modeled recruitment was high in 1989 and low in 1999. The high recruitment in 1989 was due to the combination of low starvation mortality and high retention (Figure 10A-C). In contrast, recruitment was low in 1999 despite starvation mortality being the lowest over the four-year comparative period (Figure 10A&C). This was because retention near the coast and within the RREAS survey area was also the lowest over the four-period (Figure 10B) as well as the full simulation period (not shown). In summary, ENSO, when grouped across years, can significantly explain mean starvation mortality for an entire cohort, but not retention or modeled recruitment.

ENSO Effects on Subcohort-level Starvation Mortality, Retention, and Modeled and Empirical Recruitment

Effects of ENSO on subcohort-level starvation mortality, retention, and recruitment within a year were qualitatively apparent (Fig. 12). El Niño events coincided with high cumulative starvation mortality (~90-100%) for fish born early in

the reproductive window (January-March; Figure 11B-C). In contrast, there was no discernable pattern in subcohort-level starvation in 1989 (La Niña) but rather mortality was consistently low (15-30%) for fish born throughout the reproductive season (Figure 11A). Cumulative starvation mortality in 1999 (La Niña) was very low (<10%) throughout the reproductive season until mortality levels increased (~30-60%) for fish that were born in April (Figure 11D). There was little qualitative effect of ENSO on subcohort-level retention (Figure 11E-H), however, retention did slightly increase for later reproductive bouts in 1999 (Figure 11H). Higher modeled recruitment occurred for fish born later in 1992, 1998, and 1999 while recruitment in 1989 was relatively constant, albeit with slightly reduced recruitment in January (Figure 11I-L). Observed recruitment was spread over the reproductive period in 1989 as indicated by back-calculated birthdate frequency of surviving juvenile Shortbelly caught in the RREAS (Figure 11M). In contrast, observed recruitment came from fish that were born later in the reproductive season (late March-April), during the two ENSO years (Figure 11N-O), and fish that recruited in 1999 were born in mid-February through April.

Quantitatively, the timing and magnitude of cumulative starvation mortality was negatively associated with the timing and magnitude of observed recruitment from the RREAS for both El Niño years combined ($\rho = -0.67$; p-value = 0.002) and individually for 1992 ($\rho = -0.67$; p-value = 0.0343) and 1998 ($\rho = -0.80$; p-value = 0.009) (Table 1). The timing and magnitude of retention was not related to observed recruitment in either El Niño years, nor when the two years were combined (Table 1).

129

Modeled recruitment was positively associated with the timing and magnitude of observed recruitment during El Niño years and starvation mortality had a larger effect on the modeled recruitment signal than did retention (Table 2).

The association between modeled starvation mortality, retention, and modeled recruitment with observed recruitment were more nuanced during La Niña events compared to El Niño events (Table 1). None of the modeled indicators were associated with observed recruitment in 1989 (Table 1). For 1999, neither starvation nor retention alone were sufficient to explain observed recruitment, but modeled recruitment, which combines survival (1-starvation mortality) with retention, was positively associated with observed recruitment ($\rho = 0.66$; p-value = 0.038; Table 1). A similar result can be shown when the two La Niña events were combined; starvation mortality and retention were unrelated to observed recruitment, but modeled recruitment was significantly, and positively, associated with observed recruitment ($\rho = 0.48$; p-value = 0.028). Taken together, modeled recruitment was positively associated with observed recruitment (excluding 1989), and retention had a larger effect on modeled recruitment than did starvation mortality during La Niña years (Table 2).

Discussion

The objective of this study was to test the hypothesis that mechanisms of recruitment variability are context-dependent with a numerical model grounded in first principles (i.e., physiology and physics) and fisheries-independent data. The CBP-IBM revealed that the effects of food web-dependent processes on recruitment

strength are more pronounced during El Niño events as demonstrated by the strong association between starvation mortality and observed recruitment. In contrast, the effects of transport-dependent processes on observed recruitment were mediated by retention through modeled recruitment during La Niña events, rather than retention alone being directly related to observed recruitment. These results suggest that at least for the current version of the CBP-IBM, mechanisms of Shortbelly rockfish recruitment variability are more apparent for weak recruitment years (El Niño events) compared to strong recruitment years (La Niña events). The propensity to characterize drivers of poor recruitment more easily is consistent with a recent study that showed more skill in forecasting poor recruitment because it required only one predictor variable to be extreme rather than good recruitment requiring all biophysical predictors to align (Gross et al., 2022). Nevertheless, the results support the hypothesis that Shortbelly recruitment variability is differentially driven by food web- and transport-dependent processes amongst a backdrop of contrasting environmental conditions (i.e., ENSO).

Over the duration of the full CBP-IBM (1988-2010), 1989 and 1999 were two of the largest year classes on record for Shortbelly rockfish, as indicated by pre-recruitment indices from the RREAS and realized recruitment from age-structured stock assessments (Chapter 2; Ralston et al., 2013). However, for 1999, the signal of the large year class was not detected in the RREAS (Ralston et al., 2013) and this study suggests that strong offshore transport of ELS rockfish throughout their pelagic larval and juvenile duration left propagules outside of the survey area (indexed by

131

low retention) at the time of sampling. The timing of parturition for fish that did not starve and were within the survey area at the time of sampling (i.e., modeled recruitment) closely matched the timing and magnitude of observed recruitment, as indicated by birthdate frequency distributions. Given the sequence of events revealed by the model, why then was realized recruitment from stock assessment so high in 1999 but not detected in the survey? The model suggested a reduced metabolic cost because of the existence of cooler water temperatures as well as elevated consumption rates due to increased prey availability which resulted in a large proportion of modeled fish being in good condition (large weight-to-length ratio). While not directly explored here, good body condition could have provided pelagic juveniles with the energy reserves to offset strong offshore Ekman transport through directed swimming towards shore (Bjorkstedt, unpublished). Alternatively, settlement to nearshore nursery grounds could have occurred earlier in the year because fish would have reached settlement size at an earlier age as result of their fast growth. This latter possibility was not directly assessed in this study because settlement-at-size was not included as an agent of recruitment, though this would be a useful scenario to explore in future iterations of the model. However, care would need to be taken when comparing the modeled results to observed recruitment which does not take into account settlement-at-size.

Interestingly, despite 1989 being a strong La Niña year, retention was high along with the expected low starvation mortality. In the context of the CBP-IBM, this resulted in high modeled recruitment, and retention contributed disproportionately to

modeled recruitment. However, the timing and magnitude of modeled recruitment was not associated with the timing and magnitude of observed recruitment. Despite a lack of correlation between modeled and observed recruitment, 1989 was the second largest year class over the 1988-2010 observed recruitment record (Chapter 2) and this is consistent with the high recruitment predicted by the model. While elucidating the physical basis of advection being advantageous for retention during 1989 was outside the scope of this study (e.g., frontogenesis), it is worth noting that the 1989 La Niña event occurred at a time when the Pacific Decadal Oscillation (PDO; Mantua et al., 1997) had been in a positive state since 1977 (Hare and Mantua, 2002). Since the manifestation of the PDO on the physical oceanography of the CCS is similar to ENSO (Jacox et al., 2014), but operating with a periodicity of 40-76 years instead of 3-7 years, respectively, it is possible that the opposing signs of the two dominant modes of interannual variability for the CCS during the time period of this study could have had canceling effects which lead to increased retention of ELS rockfish. Indeed, upwelling in the central CCS is strongly negatively correlated with ENSO and the PDO (Jacox et al., 2014), and if the two modes of variability are out of phase with each other like they were in 1989, then upwelling should have been close to the long-term average and recruitment would not be limited by retention. This is in fact what the CBP-IBM suggests; zonal velocities (east-west component) experienced by individuals along their drift routes were close to the 1988-2010 average. Importantly, the modeled recruitment signal in 1989 was still more strongly influenced by retention than starvation whereas starvation had a larger effect on modeled recruitment for both El Niño years. Importantly, the PDO and ENSO were in phase

with each other during the 1992 and 1998 El Niño events, as well as during the 1999 La Niña event, which likely explains why the timing and magnitude of modeled recruitment in these years had a stronger association with starvation mortality and retention, respectively.

This study emphasizes the difficulty of elucidating recruitment mechanisms and underscores why they have challenged fisheries oceanographers for over a century by highlighting that biophysical mechanisms can alternate in importance depending on the physical state of the system (i.e., ENSO), and at times confounded by multiple scales of variability operating against each other (e.g., PDO and ENSO). It is now acknowledged in fisheries oceanography that multiple hypotheses of recruitment should be tested but comparing and linking multiple hypotheses together in a context dependent fashion is difficult and seldom done (Hare, 2014). This is partially because most studies of recruitment mechanisms use correlative analyses that relate the full record of a time series to a suite of environmental indicators that are a proxy for a more biologically realistic process that affects the strength of recruitment. For example, temperature has been used in the management of Pacific sardine (*Sardinops sagax*) in the CCS as a proxy for the physical-biological interactions that drive recruitment fluctuations (Jacobson and MacCall, 1995; Lindegren and Checkley, 2013) despite the recognition that the mechanisms controlling the fluctuations are more complicated (Rykaczewski and Checkley, 2008; Lindegren et al., 2013; Fiechter et al., 2015; Politikos et al., 2018). Furthermore, correlative analyses of environment-recruitment relationships are prone to break

down over time due to spurious correlations (Meyers et al., 1998; McClatchie et al., 2010; Zwolinski and Demer, 2019) or be susceptible to non-stationary relationships between climate and biological time series (Litzow et al., 2020). For example, the importance of the PDO has waned in recent years while the contribution of the North Pacific Gyre Oscillation (NPGO; Di Lorenzo et al., 2008) has increased (Litzow et al., 2020). Nonstationarity of basin climate indices, if not accounted for in regression models, led to a longstanding temperature-salmon production and PDO-salmon production relationship declining to 0 (Litzow et al., 2020). Even if nonstationary relationships are accounted for in correlative studies, they still typically rely on proxies for more complicated physical-biological interactions (e.g., PDO, NPGO, and ENSO). In what is now a classic review of fish recruitment hypotheses, Houde (2008) acknowledged that it is likely that fish recruitment is determined by multiple mechanisms, and different mechanisms are likely to be important at different times depending on conditions. I show here based on simulations from a CBP-IBM for Shortbelly that starvation mortality and retention are important for recruitment and their relative contribution to recruitment is dependent on the physical state of the system (i.e., context dependent).

Another reason that context dependency of recruitment drivers is often not explored is because developing IBMs for the ELS of marine fishes to mechanistically test hypotheses is a time consuming and data intensive endeavor that requires careful assessment of parameter and model structure uncertainty through sensitivity and scenario testing (Chapter 1). For this reason, they are not as commonly used

compared to other process-based modeling approaches (e.g., models of intermediate complexity; Collie et al., 2014), despite the potential for IBMs to tell us why most larvae in the ocean die (Peck and Hufnagl, 2012). Typically, IBMs rely on modeling one fish species in great detail, and with this increased realism comes increased uncertainty (Collie et al., 2014).

Despite the CBP-IBM used here being relatively complex, I still took many simplifying assumptions that are worth discussing. First, the Lagrangian particle tracking model was a 1st order Euler integration scheme which is relatively simple and computationally efficient compared to more advanced methods like a 4th order Runge-Kutta integration scheme. Increasing the complexity of the particle tracking algorithm however would improve the precision of particle trajectories rather than promote more bias (Press, 2007) and this method should be used in future iterations of the Shortbelly CBP-IBM. Second, I assumed that ELS dispersal was passive (no directed swimming) and depth-invariant (so that model output could be directly compared with observational data). While Ross and Larson (2003) show that the peak abundance for Shortbelly was at 30m, there was still considerable biomass above and below this depth. Ekman velocities also decrease and change in orientation with depth (Talley, 2011) and several studies have shown the implications of vertical shear on larval dispersal using ocean circulation models in the CCS (e.g., Petersen et al., 2010). A future direction of this model could implement multiple depths, or even allow for physically- or biologically induced depth migrations based on an optimization routine that maximizes growth as function of depth, bounded by the full

136

depth range of larvae and pelagic juveniles (Humston et al., 2000; 2004). Third, reproduction was spatially invariant because the spawning module was based on the distribution of very young larvae in central California, which was assumed fixed across years (Ralston et al., 2003). Improved monitoring of gravid (pregnant) female Shortbelly would aid in determining if, and to what extent, reproduction was spatially dynamic. Furthermore, Shortbelly are also quite abundant in the Southern California Bight (Field et al., 2007) and I did not account for any source-sink dynamics between the central and southern CCS population. Finally, maternal effects are known to influence the condition and survival of rockfish larvae (Sogard et al., 2008; Fennie et al., 2023b), yet this was also ignored in this study. Improved understanding of these factors, albeit through field or laboratory experiments, would increase the ecological realism of the CBP-IBM and possibly have implications for the relative importance of food web- and transport-dependent processes on Shortbelly recruitment.

The RREAS is a unique program because it is one of the few fisheries-independent surveys that directly estimates recruitment of commercially important fish species and includes the data directly into stock assessments to derive harvest control rules for sustainable fisheries management (Field et al., 2021). While Shortbelly are not of commercial importance, they are a significant component of the ecosystem, comprising a large proportion of the diets of many seabirds, marine mammals and piscivorous fishes (Thayer et al., 2014; Warzybok et al., 2018; Lowry et al., 2022). Using an unfished species also allows for a more direct examination of the recruitment dynamics independent of a human-induced mortality signal. Taking a

similar approach to a fished species could help disentangle climate and fishing impacts on a stock (Essington et al., 2015) The model presented here is parameterized to represent Shortbelly but the recruitment dynamics of many species of rockfish are strongly correlated with each other which suggests that factors that control recruitment of rockfish in the central CCS operate similarly across species (Ralston et al., 2013; Schroeder et al., 2019). Therefore, the mechanisms identified to be important for the recruitment of Shortbelly could be extended to other species of rockfish. Because of the slow growing and late to mature life history of most commercially important rockfish species (Love et al., 2002) the survey-derived recruitment indices are quite informative in stock assessments (Field et al., unpublished). For example, Chilipepper rockfish (*Sebastes goodei*) recruit to the fishery around 4-5 years of age, and given the large recruitment event that occurred in 1999 that was not detected in the survey, projected adult biomass of Chillipepper rockfish in 2004 was severely underestimated which meant that groundfish fisheries had maximum sustainable yield quotas that were significantly lower than they should have been (Field et al., 2015). A model such as the one presented here could be extended to include more recent years (e.g., 2018-2019 at the time of writing) and compared with recruitment from RREAS to adjust any bias in the adult biomass projections (e.g., 2023). Similarly, IBMs, when coupled to downscaled climate projections (Pozo-Buil et al., 2021), can be used to assess long term recruitment impacts resulting from climate change (Fiechter et al., 2021). Such applications would be a significant improvement to fisheries management and to ecosystem-based

138

fisheries management given the ecological role of Shortbelly rockfish and

commercial importance of other rockfish species.

Tables and Figures

Table 1. Spearman rank correlation coefficients (ρ) evaluating the association between subcohort-level cumulative starvation mortality, retention, and modeled recruitment on the observed timing and magnitude of recruitment from the Rockfish Recruitment and Ecosystem Assessment Survey (RREAS). Significant correlations are indicated in bold and defined by p-value < 0.05.

ENSO Category	Year(s)	Process	ρ	p-val
El Niño (Combined)	1992 & 1998	**Starvation**	**-0.67**	**0.002**
		Retention	0.18	0.258
		Recruitment	**0.67**	**0.002**
La Niña (Combined)	1989 & 1999	Starvation	0.25	0.83
		Retention	0.26	0.16
		Recruitment	**0.48**	**0.028**
La Niña	1989	Starvation	0.02	0.52
		Retention	0.00	0.72
		Recruitment	0.25	0.274
El Niño	1992	**Starvation**	**-0.67**	**0.0343**
		Retention	0.08	0.427
		Recruitment	**0.67**	**0.034**
El Niño	1998	**Starvation**	**-0.80**	**0.009**
		Retention	0.44	0.14
		Recruitment	**0.81**	**0.007**
La Niña	1999	Starvation	-0.15	0.36
		Retention	0.22	0.3
		Recruitment	**0.66**	**0.038**

Table 2. Multiple linear regression results showing the effect of subcohort-level cumulative starvation mortality and retention (predictors) on modeled recruitment (response). The predictor with the higher absolute effect size is indicated in bold.

| ENSO Category	Year(s)	Response	Predictor	Standardized Coefficient (β)	p-value	R^2
El Niño (Combined)	1992 & 1998	Modeled Recruitment	**Starvation**	**-0.84**	**< 0.001**	0.93
			Retention	0.27	0.0035	
La Niña (Combined)	1989 & 1999	Modeled Recruitment	Starvation	-0.049	0.66	0.867
			Retention	**0.95**	**< 0.0001**	
La Niña	1989	Modeled Recruitment	Starvation	-0.56	0.052	0.81
			Retention	**1.01**	**0.007**	
El Niño	1992	Modeled Recruitment	**Starvation**	**-0.99**	**< 0.001**	0.97
			Retention	-0.019	0.822	
El Niño	1998	Modeled Recruitment	**Starvation**	**-0.67**	**<0.001**	0.82
			Retention	0.47	0.002	
La Niña	1999	Modeled Recruitment	Starvation	0.25	0.38	0.82
			Retention	**0.72**	**0.039**	
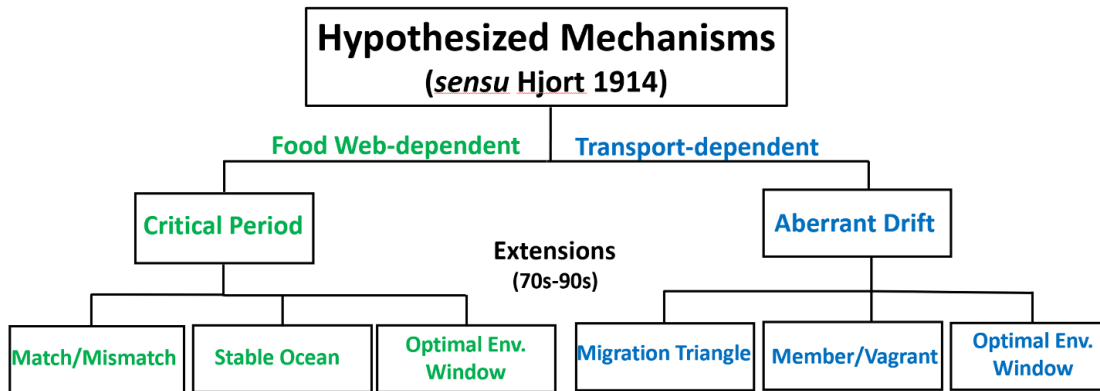
Figure 1. Hypotheses of recruitment variability categorized by food web-dependent (green) and transport-dependent (blue) mechanisms. The "Critical Period Hypothesis" and the "Aberrant Drift Hypothesis" (Hjort, 1914) and their extensions: "Match-Mismatch" (Cushing 1969; 1990), "Stable Ocean" (Lasker, 1975; 1978); "Optimal Environmental Window" (Cury and Roy, 1989); "Migration Triangle" (Harden-Jones, 1968); and "Member/Vagrant" (Sinclair, 1988). Note: the "Optimal Environmental Window" appears on both sides.
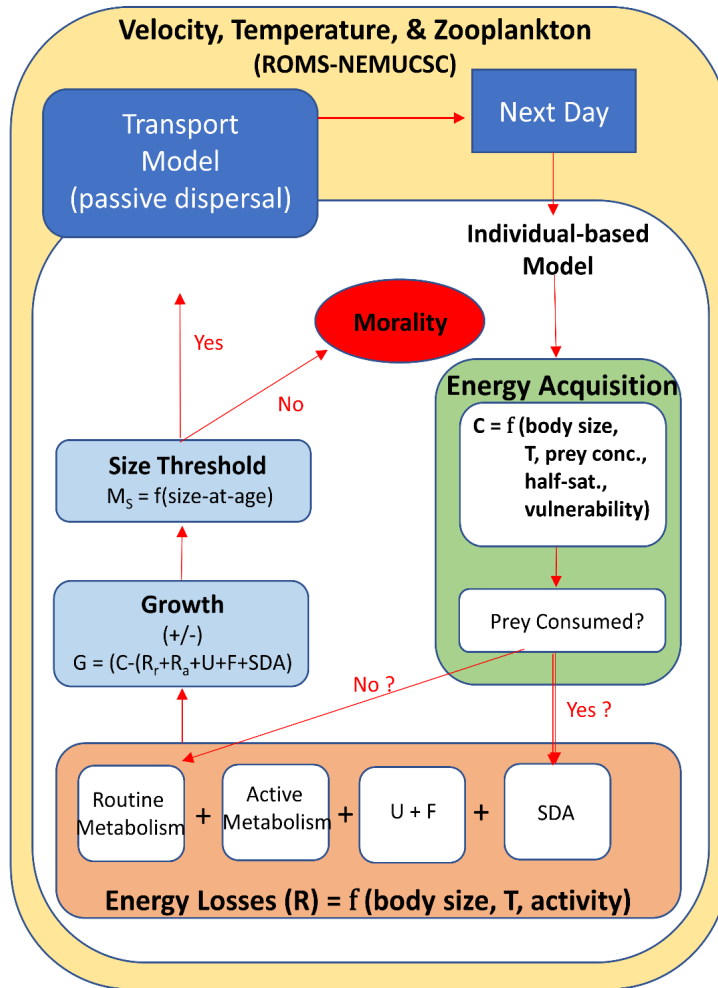
Figure 2. Schematic of model structure for the coupled biophysical individual-based model (CBP-IBM) showing the four separate models (Model 1 and 2 = ROMS-NEMUCSC (yellow); Model 3 = Energy Acquisition, Energy Losses, Growth, and Starvation Mortality Size Threshold (green, peach, light blue); Model 4 = Transport Model (Lagrangian Particle Tracking Model; dark blue)). The IBM (somatic growth model for an individual fish) is imbedded within ROMS-NEMUCSC (offline) and coupled to a Lagrangian particle tracking algorithm (also offline). Simulations report daily values of state variables: location, temperature (T), prey concentration ('prey

conc.'), consumption (C; parameters are half saturation coefficients ('half sat.') and prey vulnerability (Chapter 1)), metabolism, excretion (U), egestion (F), specific dynamic action (cost of digestion; SDA), and growth in weight ('body size'). Starvation mortality (M_S) is determined as a function of size-at-age. If an individual does not starve on a given day, then the Lagrangian particle tracking algorithm updates the individual's location and the IBM calculation repeat. Note: 'active dispersal' was not implemented in this chapter. This figure was adapted from Peck and Hufnagl (2012).
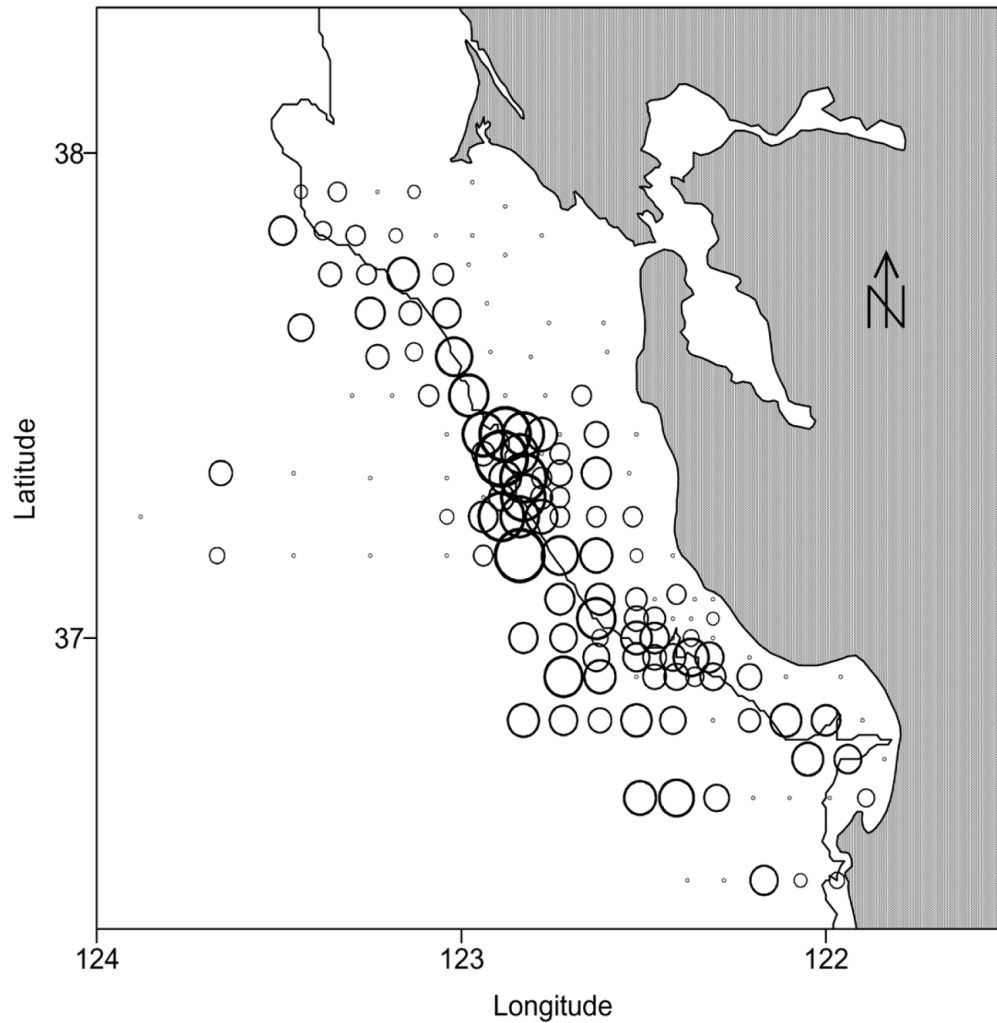
Figure 3. Map showing the spatial distribution of very young (0-2 d) Shortbelly rockfish larvae used as a proxy for the spatial reproduction patterns to inform the parturition module. The size of the circles is proportionate to catch. This map was originally published in Ralston et al., 2003.
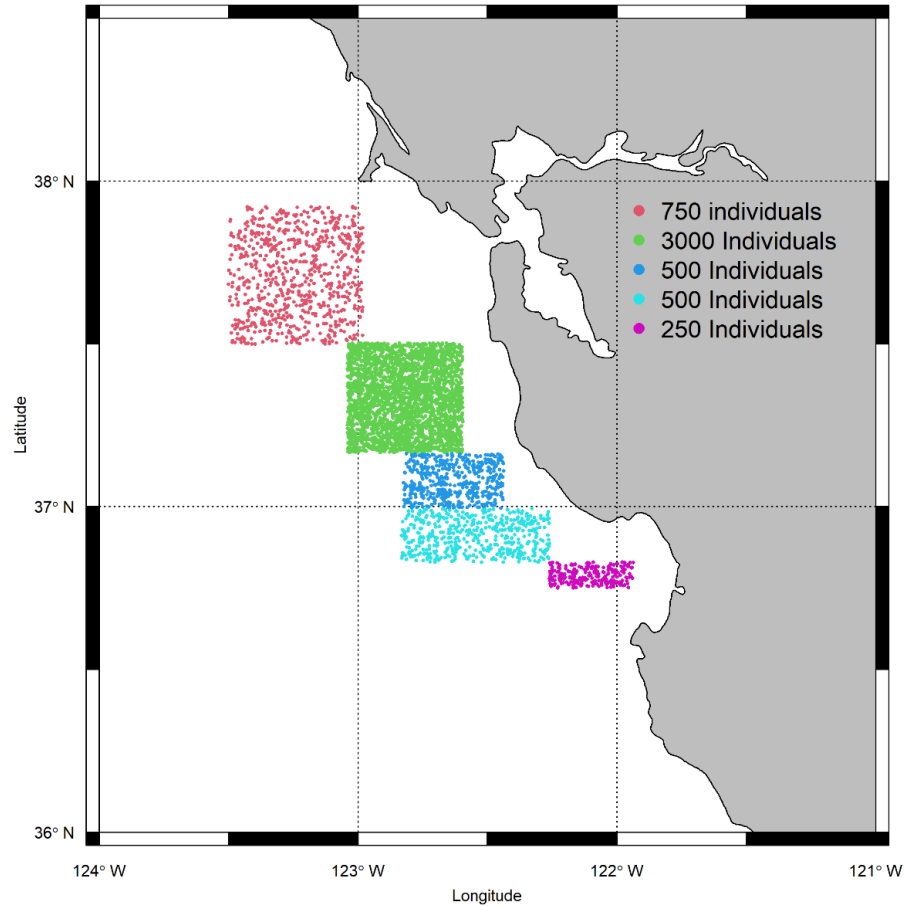
Figure 4. Spatial distribution of reproduction in the parturition module that seeds preflexion larvae into the domain of the CBP-IBM. The number of grid cells released in each spawning region are shown on map. 507 ROMS grid cells are implemented over the five spawning regions (region 1(red dots) = 195 grid cells; region 2 (green dots) = 154 grid cells; region 3 (dark blue dots) = 55 grid cells; region 4 (light blue dots) = 85 grid cells; region 5 (violet dots) = 18 grid cells).
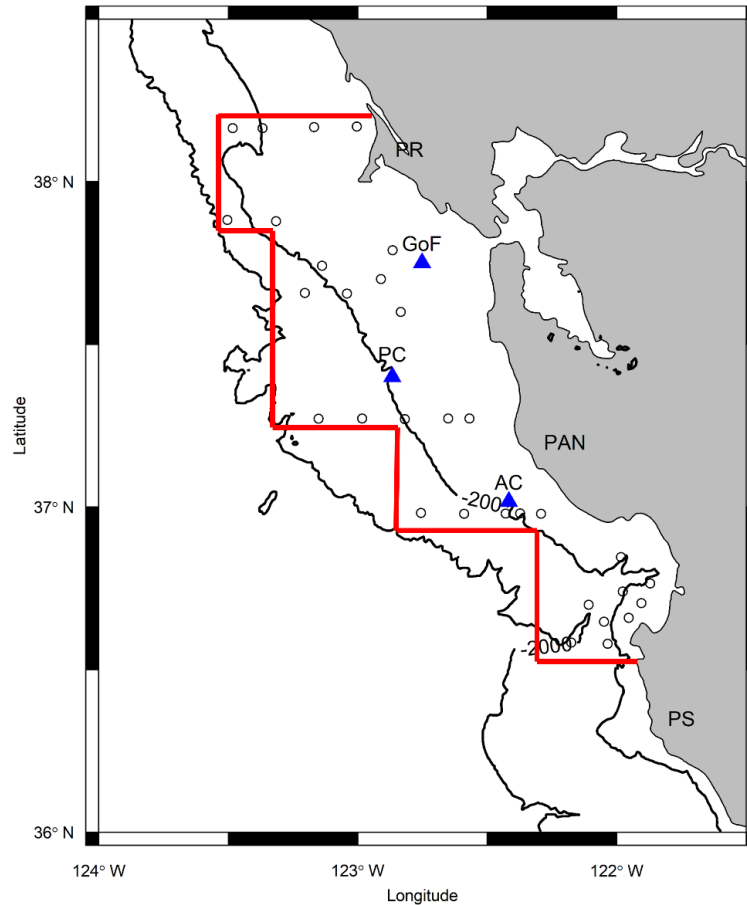
Figure 5. Map showing the location of the Rockfish Recruitment and Ecosystem Assessment Survey midwater trawl location (circles) bounded by the region of 'retention' (red). Two submarine canyons important for both reproduction and recruitment of Shortbelly rockfish (blue triangles); Pioneer Canyon (PC) and Ascension Canyon (AC). The Gulf of Farallones (GoF), which is a large breeding ground for seabirds that feed on pelagic juvenile Shortbelly (blue triangle). 200m and 2,000m isobaths are shown to denote the shelf-break (~200m) and the shelf slope
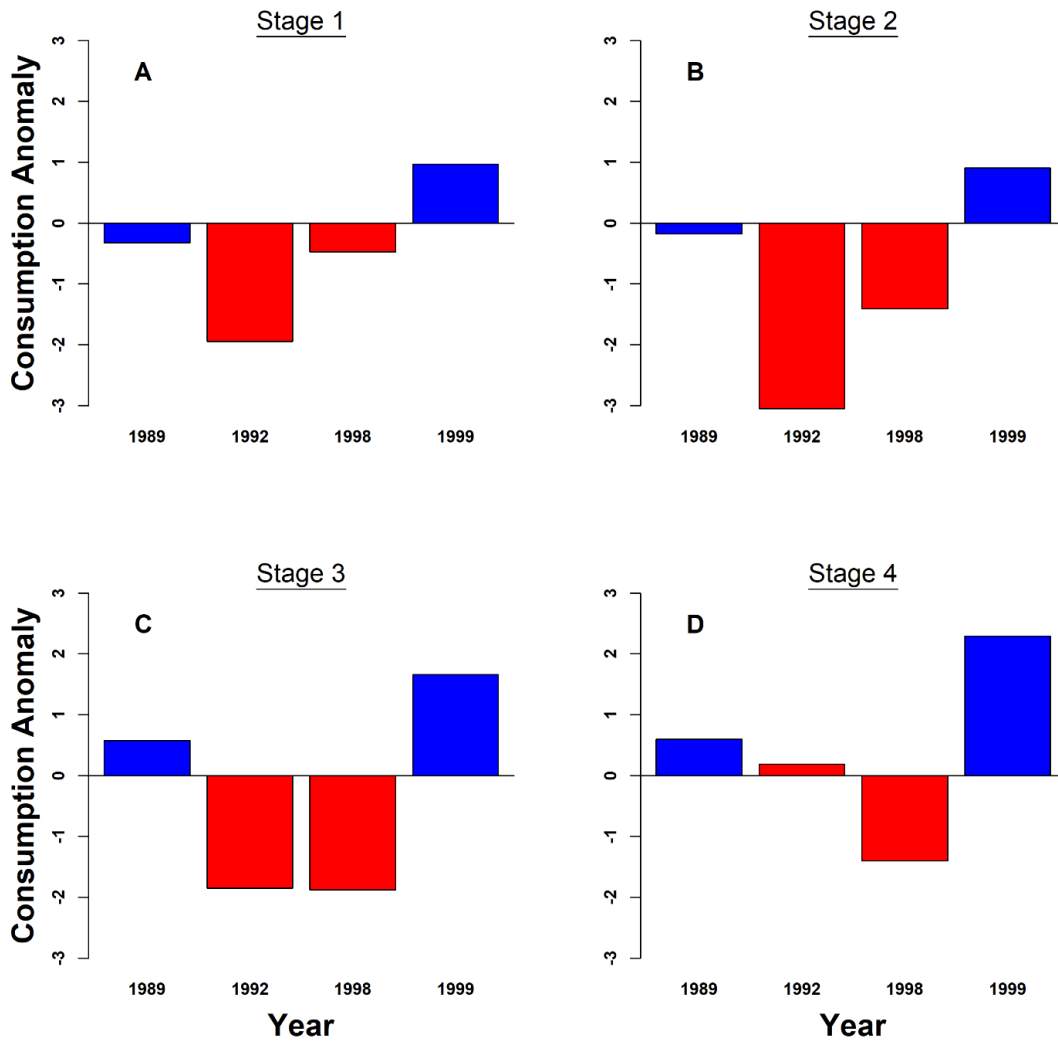
(~200-2,000m). Notable coastal promontories are shown; Point Reyes (PR), Point

Año Nuevo (PAN), and Point Sur (PS).
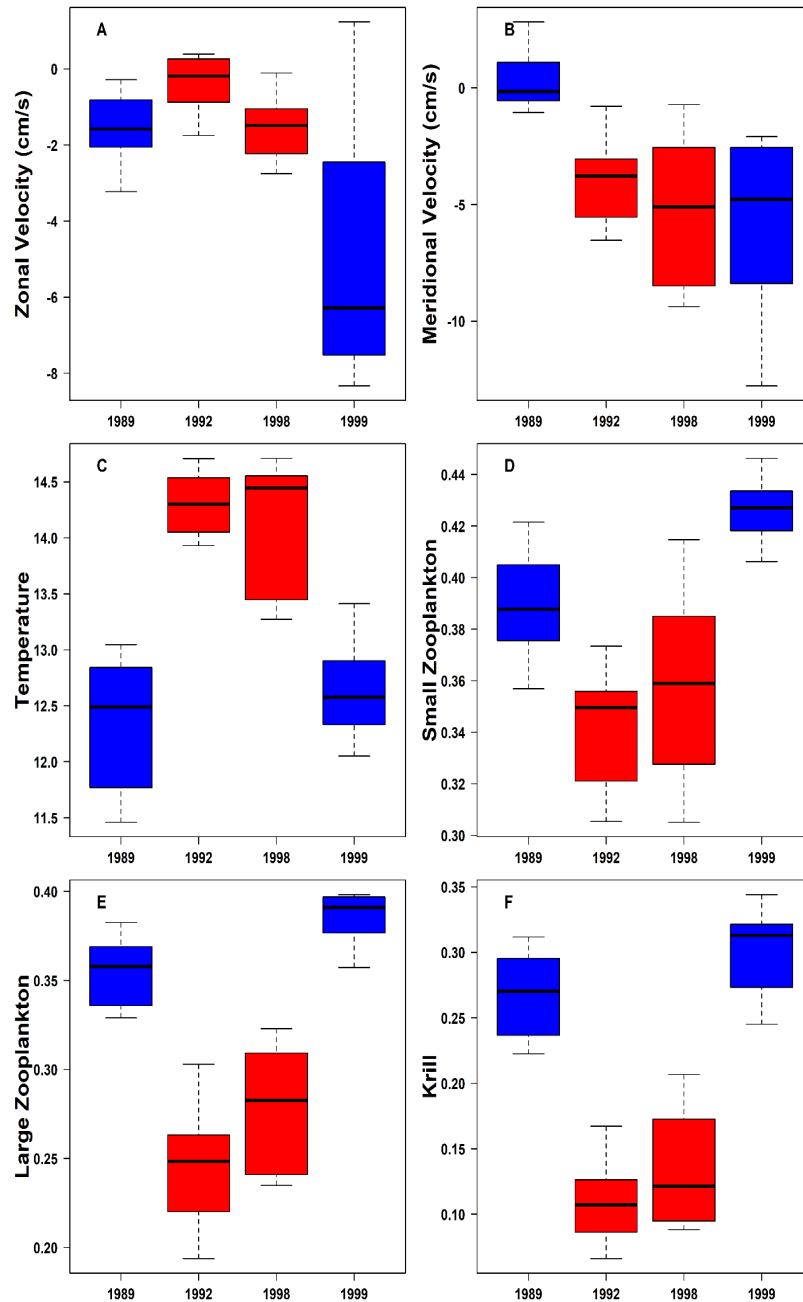
Figure 6. Biophysical conditions experienced by individuals across two La Niña

years (blue) and two El Niño years (red).
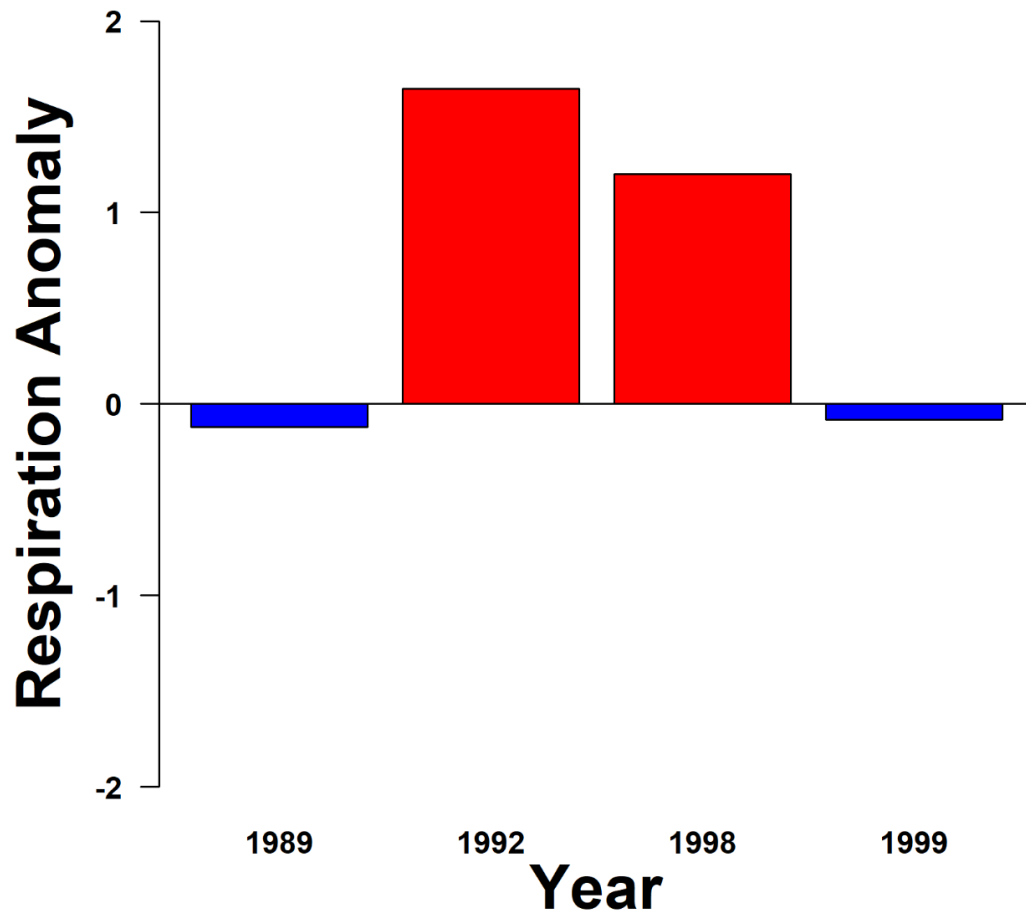
Figure 7. Mass-specific respiration standardized anomalies (relative to 1988-2010) across La Niña (blue) and El Niño (red) years.

Figure 8. Life stage-specific proportional consumption standardized anomalies (relative to 1988-2010) across La Niña (blue) and El Niño (red) years. Stage 1 = preflexion larvae; Stage 2 = flexion larvae; Stage 3 = postflexion larvae; Stage 4 = pelagic juvenile.
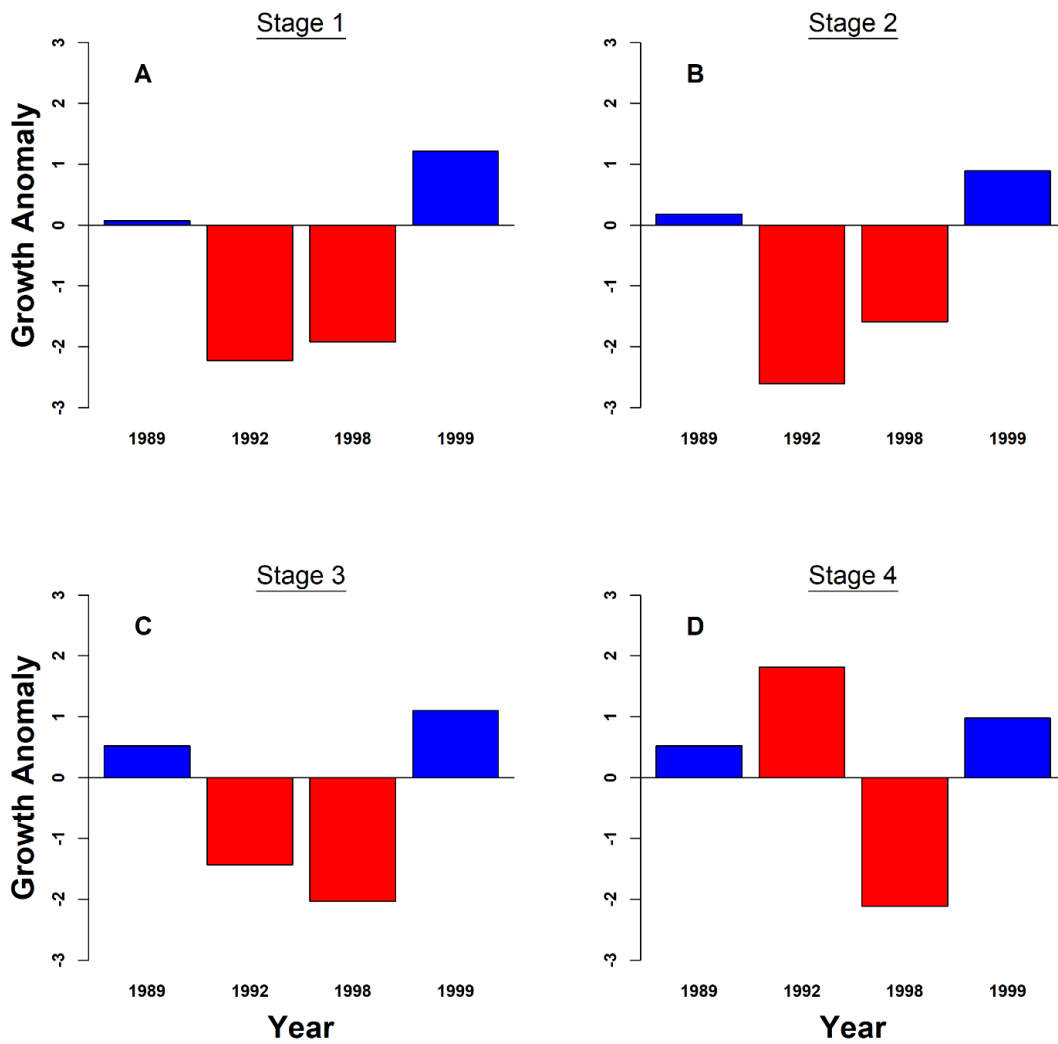
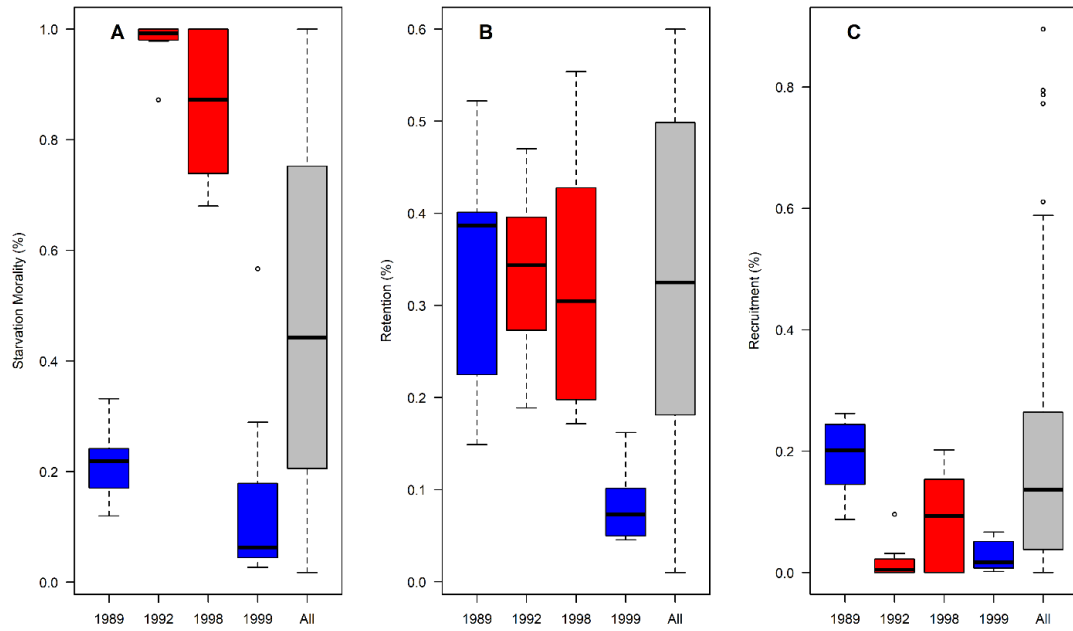**Figure 9.** Ontogenetic mass-specific growth standardized anomalies (relative to 1988-2010) across La Niña (blue) and El Niño (red) years. Stage 1 = preflexion larvae; Stage 2 = flexion larvae; Stage 3 = postflexion larvae; Stage 4 = pelagic juvenile.

151

Figure 10. Modeled (A) starvation mortality, (B) retention, and (C) recruitment for each of the 8 reproductive bouts during La Niña (blue) and El Niño (red) years. All years are shown for comparison (1988-2010; grey).
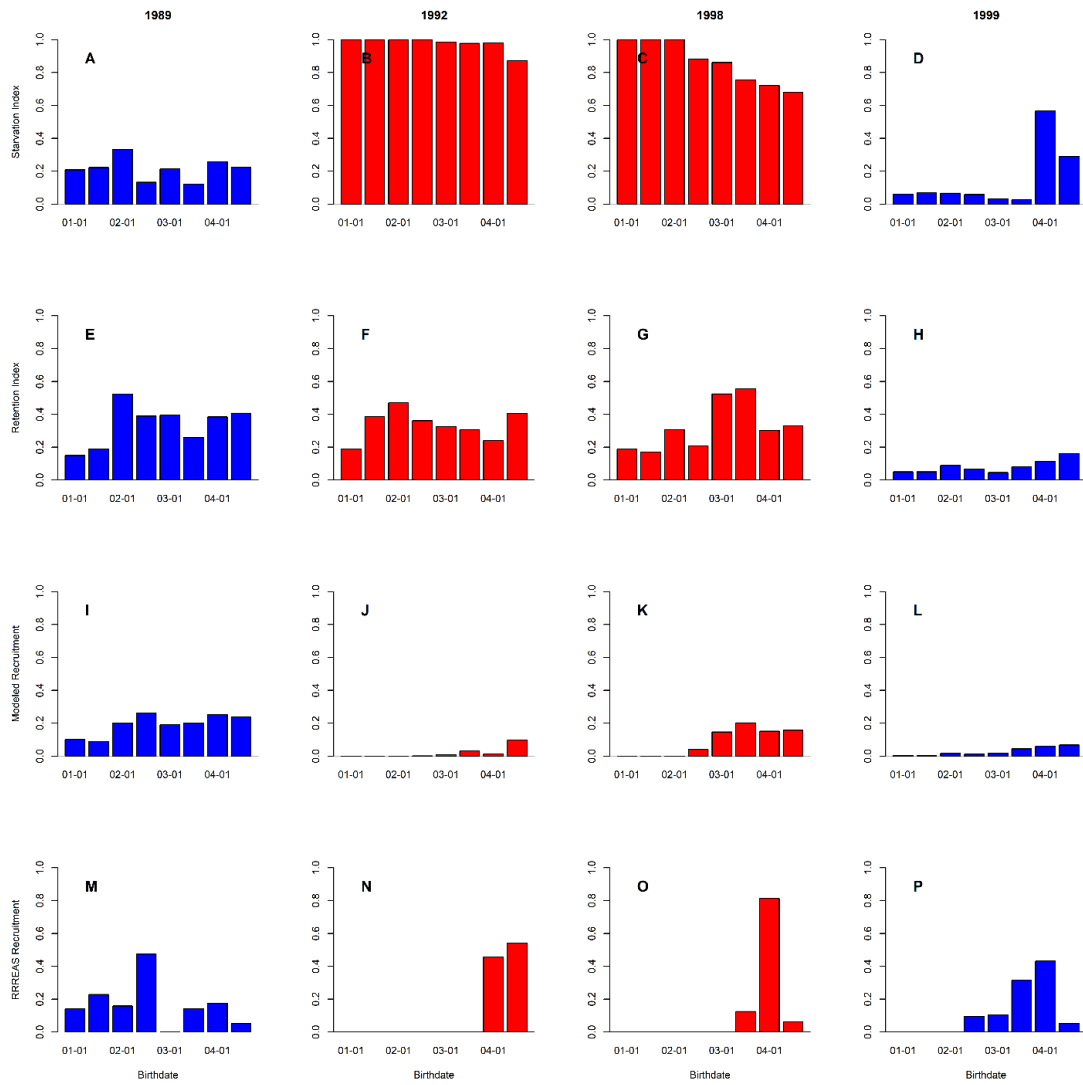
Figure 11. Cohort-level (A-D) starvation mortality, (E-H) retention, (I-L) modeled recruitment, and (M-P) observed recruitment from the Rockfish Recruitment and Ecosystem Assessment Survey (RREAS) across La Niña (blue) and El Niño (red) years.

Conclusion

One of the biggest challenges in marine fisheries management is understanding recruitment variability. Beginning with the seminal work of Johan Hjort (1914), two separate classes of mechanisms are hypothesized to control recruitment strength. While several extensions of Hjort's hypotheses have been made, food web- and transport-dependent mechanisms are still believed to be the underlying drivers of year-to-year changes in the strength of recruitment (Houde, 2016). The central tenant of food web-dependent mechanisms of recruitment variability is that the early life stages (ELS) of fish must find and acquire food in sufficient quantity to outgrow the highly vulnerable larval stages or else poor body condition will result in starvation or increased risk of predation. The central tenant of transport-dependent mechanisms of recruitment variability is that ocean currents can disperse larvae to habitat that is either favorable or unfavorable for growth, and for fish with a bipartite life cycle, ocean currents must also facilitate transport to suitable nursery habitat or settlement sites. Since production at the base of pelagic food webs in the marine environment and larval dispersal is determined by physical oceanographic processes (e.g., the delivery of nutrients to the sunlit waters), the two hypothesized mechanisms of recruitment variability must inherently consider physical environmental variability over multiple spatial and temporal scales.

Climate change will have many interactive effects on the physical environment such as increased water temperatures, increased stratification, shoaling oxygen minimum zones, ocean acidification, and rising sea levels which will directly

impact marine organisms through physiological responses and redistributions and indirectly through changes in species interactions and population connectivity (Doney et al., 2012). Therefore, better understanding the environmental drivers of recruitment variability will allow resource managers to make more informed decisions and be situated to for climate-ready fisheries management. This is particularly true for the California Current System (CCS) which supports numerous commercially important fisheries and many threatened marine seabirds and mammals that require healthy populations of fish to feed on. While the exact fate of the CCS is still uncertain, recent advances in numerical modeling have increased the spatial resolution of projected changes to the physical and chemical environment to better resolve mescoscale processes important to the ELS of marine fishes (Pozo Buil et al., 2021), and when coupled to biological models, climate impacts will undoubtedly lead to changes in fish distribution and population productivity (Smith et al., 2023).

In this dissertation I sought to better understand the biophysical factors that determine recruitment variability for an ecologically important marine fish species in the California Current System (CCS), the Shortbelly Rockfish (*Sebastes jordani*). Recognizing the importance of somatic growth to recruitment, and that growth integrates environmental conditions across multiple ELS's that can differentially influence the overall magnitude of recruitment, I developed a highly resolved ontogenetic bioenergetics model for ELS Shortbelly that allows for growth rate to vary in response to changing temperature and prey availability (Chapter 1). This model, when coupled to a highly resolved physical-biogeochemical model of the CCS

155

was able to reproduce observed growth with high precision over multiple pre-recruitment life stages. As a proof of concept, the model was applied in a spatial context, under a historical climatological forcing scenario, and produced a highly heterogenous spatial pattern of growth potential for the earliest larval stage that indicated Shortbelly reproduce where larval growth will be maximized. This was a compelling result in that in provides evidence that on average, fish reproduction is an adaptive strategy that places young (preflexion) larvae in habitat that is suitable for rapid growth to quickly exit the highly vulnerable preflexion stage. Interestingly, intermediate larval stages (postflexion), on average, experienced rapid growth over a broad homogenous area, indicating that multiple larval dispersal pathways can result in sufficient growth potential and possibly promote survival. Finally, spatial patterns of growth potential for the pelagic juvenile stage were closely associated with the distribution and abundance of pelagic juvenile Shortbelly from a fisheries-independent survey, suggesting pelagic juvenile Shortbelly aggregate in areas suitable for faster growth.

To understand how interannual variability of ocean conditions affects growth, and how growth rate variability relates to Shortbelly recruitment, I expanded the baseline bioenergetics model from Chapter 1 to include temporal variability of temperature and prey availability by performing spatial simulations of growth potential over the period 1988-2010 in Chapter 2. Hotspots of spatiotemporal growth potential (spatial regions of elevated growth) was able to explain a large proportion of observed Shortbelly recruitment variance (78.6%). An interesting result of this

156

analysis was that no single life stage could explain recruitment alone, but rather growth potential across all life stages cumulatively explained recruitment, and that relationship between growth and recruitment was life stage specific. These results illuminated the importance of food web-dependent processes on the strength of recruitment, in line with the growth-survival hypothesis (Robert et al., 2023), but did not seek to incorporate transport-dependent mechanisms of recruitment.

In Chapter 3 I coupled a larval dispersal model to the bioenergetics growth model to better resolve the relative influence of food web- and transport-dependent processes on determining recruitment strength. Here I hypothesized that the relative importance of the two mechanisms should depend on background environmental conditions, which is to say that there should be context-dependency. The El Niño Southern Oscillation (ENSO) modulates upwelling dynamics, and in turn influences temperature and primary and secondary production in the CCS. Under contrasting environmental conditions (El Niño vs. La Niña), I predicted that food web-dependent mechanisms (i.e., starvation) should dominate during an El Niño year when upwelling is weakened, and prey availability is reduced. In contrast, I predicted that transport-dependent mechanisms (i.e., retention near the coast) should dominate over starvation during a La Niña year when upwelling is intensified (i.e., more offshore transport), and prey availability is high. The results of this chapter support the general hypothesis that mechanisms of recruitment variability are context dependent, and more specifically, that recruitment will be limited by food web-dependent processes during low productivity regimes and transport-dependent processes will limit recruitment

during high productivity regimes. These results partially highlight why elucidating mechanisms of recruitment variability can be challenging if researchers do not account for changing ecological interactions under differing environmental conditions.

Taken together, this dissertation developed and employed a mechanistic ecosystem modeling approach, grounded in first principles (i.e., physics and physiology) to elucidate the factors important for the recruitment of an ecologically important fish species of the CCS. In doing so, this dissertation assumed bottom-up drivers are the controlling mechanisms of recruitment fluctuations and did not account for top-down controls on recruitment strength. Recognizing that Shortbelly are a key component of the forage community in the CCS, next steps could include adding predation mortality as a module with the ecosystem model to understand the role of top-down influences on recruitment strength and to assess the influence of Shortbelly on higher trophic level population dynamics and foraging behavior. In addition, since the mechanisms controlling Shortbelly productivity are believed to be similar other commercially important rockfish species (Ralston et al., 2013), the modeling framework presented here can easily be adapted to other species to aid in improving fisheries management. Finally, the modeling framework for Shortbelly can be extended to understand the influence of climate change on population dynamics as new regional forecasting products become available (e.g., Pozo Buil et al., 2021).

Literature Cited

Ainley, D.G., Sydeman, W.J., Parrish, R.H. and Lenarz, W.H., 1993. Oceanic factors influencing distribution of young rockfish (Sebastes) in central California: a predator's perspective. California Cooperative Oceanic Fisheries Investigations Reports, 34, pp.133-139.

Ainley, D.G., Sydeman, W.J., Parrish, R.H. and Lenarz, W.H., 1993. Oceanic factors influencing distribution of young rockfish (Sebastes) in central California: a predator's perspective. California Cooperative Oceanic Fisheries Investigations Reports, 34, pp.133-139.

Alexander, M.A., Bladé, I., Newman, M., Lanzante, J.R., Lau, N.C. and Scott, J.D., 2002. The atmospheric bridge: The influence of ENSO teleconnections on air-sea interaction over the global oceans. Journal of climate, 15(16), pp.2205-2231.

Anderson, J.T., 1988. A review of size dependent survival during pre-recruit stages of fishes in relation to recruitment. Journal of Northwest Atlantic Fishery Science, 8, pp.55-66.

Auth, T.D., Brodeur, R.D. and Fisher, K.M., 2007. Diel variation in vertical distribution of an offshore ichthyoplankton community off the Oregon coast. Fishery Bulletin, 105(3), pp.313-327.

Bailey, K.M. and Houde, E.D., 1989. Predation on eggs and larvae of marine fishes and the recruitment problem. In Advances in marine biology (Vol. 25, pp. 1-83). Academic press. https://doi.org/10.1016/S0065-2881(08)60187-X

Bailey, K.M. and Yen, J., 1983. Predation by a carnivorous marine copepod, Euchaeta elongata Esterly, on eggs and larvae of the Pacific hake, Merluccius productus. Journal of Plankton Research, 5(1), pp.71-82. https://doi.org/10.1093/plankt/5.1.71

Bakun, A.. 1996. Patterns in the ocean: ocean processes and marine population dynamics. California Sea Grant College System, San Diego, California, USA.

Bartell, S.M., Breck, J.E., Gardner, R.H. and Brenkert, A.L., 1986. Individual parameter perturbation and error analysis of fish bioenergetics models. Canadian Journal of Fisheries and Aquatic Sciences, 43(1), pp.160-168. https://doi.org/10.1139/f86-018

Bashevkin, S.M., Dibble, C.D., Dunn, R.P., Hollarsmith, J.A., Ng, G., Satterthwaite, E.V. and Morgan, S.G., 2020. Larval dispersal in a changing ocean with an emphasis on upwelling regions. Ecosphere, 11(1), p.e03015.

Beverton, R.J. and Holt, S.J., 2012. On the dynamics of exploited fish populations (Vol. 11). Springer Science & Business Media.

Bi, H., Peterson, W.T. and Strub, P.T., 2011. Transport and coastal zooplankton communities in the northern California Current system. Geophysical Research Letters, 38(12). https://doi.org/10.1029/2011GL047927

Bjørnstad, O.N., Nisbet, R.M. and Fromentin, J.M., 2004. Trends and cohort resonant effects in age-structured populations. Journal of animal ecology, pp.1157-1167.

Black, B.A., Schroeder, I.D., Sydeman, W.J., Bograd, S.J. and Lawson, P.W., 2010. Wintertime ocean conditions synchronize rockfish growth and seabird reproduction in the central California Current ecosystem. Canadian Journal of Fisheries and Aquatic Sciences, 67(7), pp.1149-1158. https://doi.org/10.1139/F10-055

Blaxter, J.T., 1969. 4 development: eggs and larvae. In Fish physiology (Vol. 3, pp. 177-252). Academic Press. https://doi.org/10.1016/S1546-5098(08)60114-4

Boehlert, G.W. and Yoklavich, M.M., 1983. Effects of temperature, ration, and fish size on growth of juvenile black rockfish, Sebastes melanops. Environmental Biology of Fishes, 8, pp.17-28. https://doi.org/10.1007/BF00004942

Boehlert, G.W., 1978. Changes in the oxygen consumption of prejuvenile rockfish, Sebastes diploproa, prior to migration from the surface to deep water. Physiological Zoology, 51(1), pp.56-67.

Boehlert, G.W., 1981. The role of temperature and photoperiod on the ontogenic migration of pre-juvenile Sebastes diploproa. Calif. Fish Game, 67, pp.164-175.

Bograd, S.J., Hazen, E.L., Howell, E.A. and Hollowed, A.B., 2014. The fate of fisheries oceanography: Introduction to the special issue. Oceanography, 27(4), pp.21-25.

Bograd, S.J., Schroeder, I., Sarkar, N., Qiu, X., Sydeman, W.J. and Schwing, F.B., 2009. Phenology of coastal upwelling in the California Current. Geophysical Research Letters, 36(1). https://doi.org/10.1029/2008GL035933

Bosley, K.L., Miller, T.W., Brodeur, R.D., Bosley, K.M., Van Gaest, A. and Elz, A., 2014. Feeding ecology of juvenile rockfishes off Oregon and Washington based on stomach content and stable isotope analyses. Marine biology, 161, pp.2381-2393. https://doi.org/10.1007/s00227-014-2513-8

Brandt, S.B. and Kirsch, J.A.Y., 1993. Spatially explicit models of striped bass growth potential in Chesapeake Bay. Transactions of the American Fisheries Society, 122(5), pp.845-869. https://doi.org/10.1577/1548-8659(1993)122<0845:SEMOSB>2.3.CO;2

Brandt, S.B., Mason, D.M. and Patrick, E.V., 1992. Spatially-explicit models of fish growth rate. Fisheries, 17(2), pp.23-35. https://doi.org/10.1577/1548-8446(1992)017<0023:SMOFGR>2.0.CO;2

Brodie, S., Taylor, M.D., Smith, J.A., Suthers, I.M., Gray, C.A. and Payne, N.L., 2016. Improving consumption rate estimates by incorporating wild activity into a bioenergetics model. Ecology and Evolution, 6(8), pp.2262-2274. https://doi.org/10.1002/ece3.2027

Browman, H.I., 2014. Commemorating 100 years since Hjort's 1914 treatise on fluctuations in the great fisheries of northern Europe: where we have been, where we are, and where we are going. ICES Journal of Marine Science, 71(8), pp.1989-1992. https://doi.org/10.1093/icesjms/fsu159

Brown, J.H., Gillooly, J.F., Allen, A.P., Savage, V.M. and West, G.B., 2004. Toward a metabolic theory of ecology. Ecology, 85(7), pp.1771-1789. https://doi.org/10.1890/03-9000

Caselle, J.E., Wilson, J.R., Carr, M.H., Malone, D.P. and Wendt, D.E., 2010. Can we predict interannual and regional variation in delivery of pelagic juveniles to nearshore populations of rockfishes (Genus Sebastes) using simple proxies of ocean conditions? California Cooperative Oceanic Fisheries Investigations Reports, 51, pp.91-105.

Caswell, H., 2001. Matrix population models (Vol. 1). Sunderland, MA: Sinauer.

Catford, J.A., Wilson, J.R., Pyšek, P., Hulme, P.E. and Duncan, R.P., 2022. Addressing context dependence in ecology. Trends in Ecology & Evolution, 37(2), pp.158-170.

Chavez, F.P. and Messié, M., 2009. A comparison of eastern boundary upwelling ecosystems. Progress in Oceanography, 83(1-4), pp.80-96. https://doi.org/10.1016/j.pocean.2009.07.032

Chavez, F.P., Collins, C.A., Huyer, A., Mackas, D. (Eds.), 2002a. El Niño along the west coast of North America. Progress in Oceanography 54 (1-4), 1-511.

Chavez, F.P., Pennington, J.T., Castro, C.G., Ryan, J.P., Michisaki, R.P., Schlining, B., Walz, P., Buck, K.R., McFadyen, A., Collins, C.A., 2002b. Biological and chemical consequences of the 1997-1998 El Niño in central California waters. Progress in Oceanography 54 (1-4), 205-232.

Checkley Jr, D.M. and Barth, J.A., 2009. Patterns and processes in the California Current System. Progress in Oceanography, 83(1-4), pp.49-64. https://doi.org/10.1016/j.pocean.2009.07.028

Chelton, D.B., Bernal, P.A. and McGowan, J.A., 1982. Large-scale interannual physical and biological interaction in the California Current. Journal of Marine Research, 40, p.4.

Cheresh, J. and Fiechter, J., 2020. Physical and biogeochemical drivers of alongshore pH and oxygen variability in the California Current System. Geophysical Research Letters, 47(19), p.e2020GL089553. https://doi.org/10.1029/2020GL089553

Cheresh, J., Kroeker, K.J. and Fiechter, J., 2023. Upwelling intensity and source water properties drive high interannual variability of corrosive events in the California Current. Scientific Reports, 13(1), p.13013. https://doi.org/10.1038/s41598-023-39691-5

Chess, J.R., Smith, S.E. and Fischer, P.C., 1988. Trophic relationships of the shortbelly rockfish, Sebastes jordani, off central California. CalCOFI Rep, 29, pp.129-136.

Chipps, S.R. and Wahl, D.H., 2008. Bioenergetics modeling in the 21st century: reviewing new insights and revisiting old constraints. Transactions of the American Fisheries Society, 137(1), pp.298-313. https://doi.org/10.1577/T05-236.1

Cimino, M.A., Santora, J.A., Schroeder, I., Sydeman, W., Jacox, M.G., Hazen, E.L. and Bograd, S.J., 2020. Essential krill species habitat resolved by seasonal upwelling and ocean circulation models within the large marine ecosystem of the California Current System. Ecography, 43(10), pp.1536-1549. https://doi.org/10.1111/ecog.05204

Collie, J.S., Botsford, L.W., Hastings, A., Kaplan, I.C., Largier, J.L., Livingston, P.A., Plagányi, É., Rose, K.A., Wells, B.K. and Werner, F.E., 2016. Ecosystem models for fisheries management: finding the sweet spot. Fish and Fisheries, 17(1), pp.101-125.

Crane, K.E., 2014. Environmental effects on growth of early life history stages of rockfishes (Sebastes) off Central California based on analysis of otolith growth patterns. Humboldt State University.

Cury, P. and Roy, C., 1989. Optimal environmental window and pelagic fish recruitment success in upwelling areas. Canadian Journal of Fisheries and Aquatic Sciences, 46(4), pp.670-680. https://doi.org/10.1139/f89-086

Cury, P.M., Shin, Y.J., Planque, B., Durant, J.M., Fromentin, J.M., Kramer-Schadt, S., Stenseth, N.C., Travers, M. and Grimm, V., 2008. Ecosystem oceanography

for global change in fisheries. Trends in Ecology & Evolution, 23(6), pp.338-346.

Cushing, D. H., 1975. Marine Ecology and Fisheries. Cambridge Univ. Press. 278 pp.

Cushing, D.H., 1969. The regularity of the spawning season of some fishes. ICES Journal of Marine Science, 33(1), pp.81-92. https://doi.org/10.1093/icesjms/33.1.81

Cushing, D.H., 1982. Climate and Fisheries. Academic Press, London. 373 pp. https://doi.org/10.1016/0025-326X(83)90049-8

Cushing, D.H., 1986. The migration of larval and juvenile fish from spawning ground to nursery ground. ICES Journal of Marine Science, 43(1), pp.43-49.

Cushing, D.H., 1990. Plankton production and year-class strength in fish populations: an update of the match/mismatch hypothesis. In Advances in marine biology (Vol. 26, pp. 249-293). Academic Press. https://doi.org/10.1016/S0065-2881(08)60202-3

Deslauriers, D., Chipps, S.R., Breck, J.E., Rice, J.A. and Madenjian, C.P., 2017. Fish bioenergetics 4.0: an R-based modeling application. Fisheries, 42(11), pp.586-596. https://doi.org/10.1080/03632415.2017.1377558

Di Lorenzo, E., Schneider, N., Cobb, K.M., Franks, P.J.S., Chhak, K., Miller, A.J., McWilliams, J.C., Bograd, S.J., Arango, H., Curchitser, E. and Powell, T.M.,

2008. North Pacific Gyre Oscillation links ocean climate and ecosystem change. Geophysical research letters, 35(8).

Dick, E.J., 2004. Beyond 'lognormal versus gamma': discrimination among error distributions for generalized linear models. Fisheries Research, 70(2-3), pp.351-366. https://doi.org/10.1016/j.fishres.2004.08.013

Dick, E.J., Beyer, S., Mangel, M. and Ralston, S., 2017. A meta-analysis of fecundity in rockfishes (genus Sebastes). Fisheries Research, 187, pp.73-85. https://doi.org/10.1016/j.fishres.2016.11.009

Doney, S.C., Ruckelshaus, M., Emmett Duffy, J., Barry, J.P., Chan, F., English, C.A., Galindo, H.M., Grebmeier, J.M., Hollowed, A.B., Knowlton, N. and Polovina, J., 2012. Climate change impacts on marine ecosystems. Annual review of marine science, 4, pp.11-37.

Downie, A.T., Illing, B., Faria, A.M. and Rummer, J.L., 2020. Swimming performance of marine fish larvae: review of a universal trait under ecological and environmental pressure. Reviews in Fish Biology and Fisheries, 30, pp.93-108. https://doi.org/10.1007/s11160-019-09592-w

Durant, J.M., Hjermann, D.Ø., Anker?Nilssen, T., Beaugrand, G., Mysterud, A., Pettorelli, N. and Stenseth, N.C., 2005. Timing and abundance as key mechanisms affecting trophic interactions in variable environments. Ecology Letters, 8(9), pp.952-958. https://doi.org/10.1111/j.1461-0248.2005.00798.x

Durant, J.M., Hjermann, D.Ø., Falkenhaug, T., Gifford, D.J., Naustvoll, L.J., Sullivan, B.K., Beaugrand, G. and Stenseth, N.C., 2013. Extension of the match-mismatch hypothesis to predator-controlled systems. Marine Ecology Progress Series, 474, pp.43-52. https://doi.org/10.3354/meps10089

Durant, J.M., Hjermann, D.Ø., Ottersen, G. and Stenseth, N.C., 2007. Climate and the match or mismatch between predator requirements and resource availability. Climate research, 33(3), pp.271-283. https://doi.org/10.3354/cr033271

Durant, J.M., Molinero, J.C., Ottersen, G., Reygondeau, G., Stige, L.C. and Langangen, Ø., 2019. Contrasting effects of rising temperatures on trophic interactions in marine ecosystems. Scientific Reports, 9(1), p.15213. https://doi.org/10.1038/s41598-019-51607-w

Ellertsen, B., Fossum, P., Solemdal, P. & Sundby, S., 1989. Relation between temperature and survival of eggs and first-feeding larvae of northeast Arctic cod (Gadus morhua L.). Rapport et Proces-verbaux des Réunions du Conseil international pour l'Exploration de la Mer, 191, 209-219.

Essington, T.E., Moriarty, P.E., Froehlich, H.E., Hodgson, E.E., Koehn, L.E., Oken, K.L., Siple, M.C. and Stawitz, C.C., 2015. Fishing amplifies forage fish population collapses. Proceedings of the National Academy of Sciences, 112(21), pp.6648-6652.

Fennie, H.W., Ben Aderet, N., Bograd, S.J., Kwan, G.T., Santora, J.A., Schroeder, I.D. and Thompson, A.R., 2023b. Momma's larvae: Maternal oceanographic

experience and larval size influence early survival of rockfishes. Fisheries Oceanography.

Fennie, H.W., Grorud-Colvert, K. and Sponaugle, S., 2023a. Larval rockfish growth and survival in response to anomalous ocean conditions. Scientific Reports, 13(1), p.4089.

Fennie, H.W., Sponaugle, S., Daly, E.A. and Brodeur, R.D., 2020. Prey tell: what quillback rockfish early life history traits reveal about their survival in encounters with juvenile coho salmon. Marine Ecology Progress Series, 650, pp.7-18. https://doi.org/10.3354/meps13300

Fiechter, J., Curchitser, E.N., Edwards, C.A., Chai, F., Goebel, N.L. and Chavez, F.P., 2014. Air?sea CO2 fluxes in the California Current: Impacts of model resolution and coastal topography. Global Biogeochemical Cycles, 28(4), pp.371-385. https://doi.org/10.1002/2013GB004683

Fiechter, J., Edwards, C.A. and Moore, A.M., 2018. Wind, circulation, and topographic effects on alongshore phytoplankton variability in the California Current. Geophysical Research Letters, 45(7), pp.3238-3245. https://doi.org/10.1002/2017GL076839

Fiechter, J., Pozo Buil, M., Jacox, M.G., Alexander, M.A. and Rose, K.A., 2021. Projected shifts in 21st century sardine distribution and catch in the California Current. Frontiers in Marine Science, p.874. https://doi.org/10.3389/fmars.2021.685241

Fiechter, J., Rose, K.A., Curchitser, E.N. and Hedstrom, K.S., 2015. The role of environmental controls in determining sardine and anchovy population cycles in the California Current: Analysis of an end-to-end model. Progress in Oceanography, 138, pp.381-398.

Fiechter, J., Santora, J.A., Chavez, F., Northcott, D. and Messié, M., 2020. Krill hotspot formation and phenology in the California Current Ecosystem. Geophysical research letters, 47(13), p.e2020GL088039. https://doi.org/10.1029/2020GL088039

Field, J.C., Beyer, S. and He, X., 2017. Status of the chilipepper rockfish, Sebastes goodei, in the California Current for 2015. Pacific Fishery Management Council, Portland, OR.

Field, J.C., Dick, E.J., Key, M., Lowry, M., Lucero, Y., MacCall, A., Pearson, D., Ralston, S., Sydeman, W. and Thayer, J., 2007. Population dynamics of an unexploited rockfish (Sebastes jordani) in the California Current. Biology, Assessment, and Management of North Pacific Rockfishes, pp.451-472.

Field, J.C., MacCall, A.D., Bradley, R.W. and Sydeman, W.J., 2010. Estimating the impacts of fishing on dependent predators: a case study in the California Current. Ecological Applications, 20(8), pp.2223-2236.

Field, J.C., MacCall, A.D., Ralston, S., Love, M.S. and Miller, E.F., 2010. Bocaccionomics: the effectiveness of pre-recruit indices for assessment and

management of bocaccio. Calif. Coop. Oceanic Fish. Invest. Rep, 51, pp.77-90.

Field, J.C., Miller, R.R., Santora, J.A., Tolimieri, N., Haltuch, M.A., Brodeur, R.D., Auth, T.D., Dick, E.J., Monk, M.H., Sakuma, K.M. and Wells, B.K., 2021. Spatiotemporal patterns of variability in the abundance and distribution of winter-spawned pelagic juvenile rockfish in the California Current. PloS one, 16(5), p.e0251638.

Free, C.M., Anderson, S.C., Hellmers, E.A., Muhling, B.A., Navarro, M.O., Richerson, K., Rogers, L.A., Satterthwaite, W.H., Thompson, A.R., Burt, J.M. and Gaines, S.D., 2023. Impact of the 2014-2016 marine heatwave on US and Canada West Coast fisheries: Surprises and lessons from key case studies. Fish and Fisheries. https://doi.org/10.1111/faf.12753

Fréon, P., Barange, M. and Arístegui, J., 2009. Eastern boundary upwelling ecosystems: integrative and comparative approaches. Progress in Oceanography, 83(1-4), pp.1-14.

Friedman, W.R., Santora, J.A., Schroeder, I.D., Huff, D.D., Brodeur, R.D., Field, J.C. and Wells, B.K., 2018. Environmental and geographic relationships among salmon forage assemblages along the continental shelf of the California Current. Marine Ecology Progress Series, 596, pp.181-198. DOI: https://doi.org/10.3354/meps12598

Fry, F.E.J., 1971. The effect of environmental factor on the physiology of fish. In: Hoar, W.S., Randell, D.J. (Eds.), Fish Physiology: Environment Relation and Behaviour. Academic Press, New York, pp. 1-98.

Fuiman, L.A. and Magurran, A.E., 1994. Development of predator defences in fishes. Reviews in Fish Biology and Fisheries, 4, pp.145-183. https://doi.org/10.1007/BF00044127

Gagliano, M., McCormick, M.I. and Meekan, M.G., 2007. Survival against the odds: ontogenetic changes in selective pressure mediate growth-mortality trade-offs in a marine fish. Proceedings of the Royal Society B: Biological Sciences, 274(1618), pp.1575-1582. https://doi.org/10.1098/rspb.2007.0242

García-Reyes, M., Largier, J.L. and Sydeman, W.J., 2014. Synoptic-scale upwelling indices and predictions of phyto-and zooplankton populations. Progress in Oceanography, 120, pp.177-188.

Getis, A. and Ord, J.K., 1992. The analysis of spatial association by use of distance statistics. Geographical analysis, 24(3), pp.189-206. https://doi.org/10.1111/j.1538-4632.1992.tb00261.x

Giménez, L., 2011. Exploring mechanisms linking temperature increase and larval phenology: the importance of variance effects. Journal of Experimental Marine Biology and Ecology, 400(1-2), pp.227-235. https://doi.org/10.1016/j.jembe.2011.02.036

Gross, J.M., Sadler, P. and Hoenig, J.M., 2022. Evaluating a possible new paradigm for recruitment dynamics: predicting poor recruitment for striped bass (Morone saxatilis) from an environmental variable. Fisheries Research, 252, p.106329.

Haidvogel, D.B., Arango, H., Budgell, W.P., Cornuelle, B.D., Curchitser, E., Di Lorenzo, E., Fennel, K., Geyer, W.R., Hermann, A.J., Lanerolle, L. and Levin, J., 2008. Ocean forecasting in terrain-following coordinates: Formulation and skill assessment of the Regional Ocean Modeling System. Journal of computational physics, 227(7), pp.3595-3624.

Haltuch, M.A., Tolimieri, N., Lee, Q. and Jacox, M.G., 2020. Oceanographic drivers of petrale sole recruitment in the California Current Ecosystem. Fisheries Oceanography, 29(2), pp.122-136. https://doi.org/10.1111/fog.12459

Hamilton, S.L., Logan, C.A., Fennie, H.W., Sogard, S.M., Barry, J.P., Makukhov, A.D., Tobosa, L.R., Boyer, K., Lovera, C.F. and Bernardi, G., 2017. Species-specific responses of juvenile rockfish to elevated p CO2: from behavior to genomics. PLoS One, 12(1), p.e0169670. https://doi.org/10.1371/journal.pone.0169670

Hanson, P.C., Johnson, T.B., Schindler, D.E., Kitchell, J.F., 1997. Fish Bioenergetics 3.0 for Windows. Technical Report WISCU-T-97-001. University of Wisconsin Sea Grant Institute, Madison, Wisconsin.

Harden Jones, F.R., 1968. Fish migration. Edward Arnold, London

Hare, J.A. and Cowen, R.K., 1995. Effect of age, growth rate, and ontogeny on the otolith size-fish size relationship in bluefish, Pomatomus saltatrix, and the implications for back-calculation of size in fish early life history stages. Canadian Journal of Fisheries and Aquatic Sciences, 52(9), pp.1909-1922. https://doi.org/10.1139/f95-783

Hare, J.A., 2014. The future of fisheries oceanography lies in the pursuit of multiple hypotheses. ICES Journal of Marine Science, 71(8), pp.2343-2356.

Hare, S.R. and Mantua, N.J., 2000. Empirical evidence for North Pacific regime shifts in 1977 and 1989. Progress in oceanography, 47(2-4), pp.103-145.

Hartman, K.J. and Kitchell, J.F., 2008. Bioenergetics modeling: progress since the 1992 symposium. Transactions of the American Fisheries Society, 137(1), pp.216-223. https://doi.org/10.1577/T07-040.1

Harvey, C. J., 2005. Effects of El Niño events on energy demand and egg production of rockfish (Scorpaenidae: Sebastes): A bioenergetics approach. Fish. Bull. 103:71-83.

Harvey, C.J., 2005. Effects of El Nino events on energy demand and egg production of rockfish (Scorpaenidae: Sebastes): a bioenergetics approach. Fishery Bulletin, 103, 71-83.

Harvey, C.J., 2009. Effects of temperature change on demersal fishes in the California Current: a bioenergetics approach. Canadian Journal of Fisheries and Aquatic Sciences, 66(9), pp.1449-1461. https://doi.org/10.1139/F09-087

Harvey, C.J., Field, J.C., Beyer, S.G. and Sogard, S.M., 2011. Modeling growth and reproduction of chilipepper rockfish under variable environmental conditions. Fisheries Research, 109(1), pp.187-200. https://doi.org/10.1016/j.fishres.2011.02.004

Hazen, E.L., Jorgensen, S., Rykaczewski, R.R., Bograd, S.J., Foley, D.G., Jonsen, I.D., Shaffer, S.A., Dunne, J.P., Costa, D.P., Crowder, L.B. and Block, B.A., 2013. Predicted habitat shifts of Pacific top predators in a changing climate. Nature Climate Change, 3(3), pp.234-238. https://doi.org/10.1038/nclimate1686

Henderson, M., Fiechter, J., Huff, D.D. and Wells, B.K., 2019. Spatial variability in ocean?mediated growth potential is linked to Chinook salmon survival. Fisheries Oceanography, 28(3), pp.334-344. https://doi.org/10.1111/fog.12415

Henderson, M., Fiechter, J., Huff, D.D. and Wells, B.K., 2019. Spatial variability in ocean?mediated growth potential is linked to Chinook salmon survival. Fisheries Oceanography, 28(3), pp.334-344. https://doi.org/10.1111/fog.12415

Hewett, S.W., Johnson, B.L., 1987. A generalized bioenergetics model of fish growth for microcomputers. Technical Report No. WIS-SG-87-245. University of Wisconsin Sea Grant Institute, Madison, WI.

Hewett, S.W., Johnson, B.L., 1992. Fish Bioenergetics 2 Model. Technical Report No. WIS-SG-91-250. University of Wisconsin Sea Grant Institute, Madison, WI.

Hixon, M.A., Johnson, D.W. and Sogard, S.M., 2014. BOFFFFs: on the importance of conserving old growth age structure in fishery populations. ICES Journal of Marine Science, 71(8), pp.2171-2185. 10.1093/icesjms/fst200

Hjort, J., 1914. Fluctuations in the great fisheries of northern Europe. Rapports Procès Verbaux des Réunions Conseil Permanent International l'Exploration Mer 20, 1.

Hjort, J., 1926. Fluctuations in the year classes of important food fishes. ICES Journal of Marine Science, 1(1), pp.5-38. https://doi.org/10.1093/icesjms/1.1.5

Hobson, E.S. and Chess, J.R., 1993. Trophic relations of the blue rockfish, Sebastes mystinus, in a coastal upwelling system off northern California. Collected Reprints, 1(4).

Hollowed, A.B., Aydin, K.Y., Essington, T.E., Ianelli, J.N., Megrey, B.A., Punt, A.E. and Smith, A.D., 2011. Experience with quantitative ecosystem assessment tools in the northeast Pacific. Fish and Fisheries, 12(2), pp.189-208. https://doi.org/10.1111/j.1467-2979.2011.00413.x

Holsman, K. and Danner, E., 2016. Numerical integration of temperature-dependent functions in bioenergetics models to avoid overestimation of fish growth. Transactions of the American Fisheries Society, 145(2), pp.334-347. https://doi.org/10.1080/00028487.2015.1094129

Houde, E. D., 2016. Recruitment variability. In Reproductive Biology of Fishes: Implications for Assessment and Management, 2nd Edn, eds T. Jakobsen, M.

Fogarty, B. Megrey, and E. Moksness (Hoboken, NJ: John Wiley & Sons, Ltd), 98-187. doi: 10.1002/9781118752739.ch3

Houde, E.D., 1987. Fish early life dynamics and recruitment variability. In Am. Fish. Soc. Symp. (Vol. 2, pp. 17-29).

Houde, E.D., 1989. Subtleties and episodes in the early life of fishes. Journal of Fish Biology, 35, pp.29-38. https://doi.org/10.1111/j.1095-8649.1989.tb03043.x

Houde, E.D., 1997. Patterns and consequences of selective processes in teleost early life histories. In Early life history and recruitment in fish populations (pp. 173-196). Dordrecht: Springer Netherlands.

Houde, E.D., 2008. Emerging from Hjort's shadow. Journal of Northwest Atlantic Fishery Science, 41. DOI:10.2960/J.v41.m634

Houde, E.D., 2016. Recruitment variability. Fish reproductive biology: implications for assessment and management, pp.98-187.

Humston, R., Ault, J.S., Lutcavage, M. and Olson, D.B., 2000. Schooling and migration of large pelagic fishes relative to environmental cues. Fisheries Oceanography, 9(2), pp.136-146.

Humston, R., Olson, D.B. and Ault, J.S., 2004. Behavioral assumptions in models of fish movement and their influence on population dynamics. Transactions of the American Fisheries Society, 133(6), pp.1304-1328.

Huyer, A., Kosro, P.M., Fleischbein, J., Ramp, S.R., Stanton, T., Washburn, L., Chavez, F.P., Cowles, T.J., Pierce, S.D. and Smith, R.L., 1991. Currents and water masses of the coastal transition zone off northern California, June to August 1988. Journal of Geophysical Research: Oceans, 96(C8), pp.14809-14831.

Ishihara, T., Watai, M., Ohshimo, S. and Abe, O., 2019. Differences in larval growth of Pacific bluefin tuna (Thunnus orientalis) between two spawning areas, and an evaluation of the growth-dependent mortality hypothesis. Environmental Biology of Fishes, 102(4), pp.581-594. https://doi.org/10.1007/s10641-019-00855-w

Ito, S.I., Kishi, M.J., Kurita, Y., Oozeki, Y., Yamanaka, Y., Megrey, B.A. and Werner, F.E., 2004. Initial design for a fish bioenergetics model of Pacific saury coupled to a lower trophic ecosystem model. Fisheries Oceanography, 13, pp.111-124. https://doi.org/10.1111/j.1365-2419.2004.00307.x

Jacobson, L.D. and MacCall, A.D., 1995. Stock-recruitment models for Pacific sardine (Sardinops sagax). Canadian Journal of Fisheries and Aquatic Sciences, 52(3), pp.566-577.

Jacox, M.G., Fiechter, J., Moore, A.M. and Edwards, C.A., 2015. ENSO and the California Current coastal upwelling response. Journal of Geophysical Research: Oceans, 120(3), pp.1691-1702.

Jacox, M.G., Hazen, E.L., Zaba, K.D., Rudnick, D.L., Edwards, C.A., Moore, A.M. and Bograd, S.J., 2016. Impacts of the 2015-2016 El Niño on the California Current System: Early assessment and comparison to past events. Geophysical Research Letters, 43(13), pp.7072-7080.

Jacox, M.G., Moore, A.M., Edwards, C.A. and Fiechter, J., 2014. Spatially resolved upwelling in the LenarzCalifornia Current System and its connections to climate variability. Geophysical Research Letters, 41(9), pp.3189-3196.

Ji, R., Edwards, M., Mackas, D.L., Runge, J.A. and Thomas, A.C., 2010. Marine plankton phenology and life history in a changing climate: current research and future directions. Journal of plankton research, 32(10), pp.1355-1368. https://doi.org/10.1093/plankt/fbq062

Johnson, K.A., Yoklavich, M.M. and Cailliet, G.M., 2001. Recruitment of three species of juvenile rockfish (Sebastes spp.) on soft benthic habitat in Monterey Bay, California. California Cooperative Oceanic Fisheries Investigations Report, pp.153-166.

Jørgensen, C., Enberg, K. and Mangel, M., 2016. Modelling and interpreting fish bioenergetics: a role for behaviour, life?history traits and survival trade?offs. Journal of fish biology, 88(1), pp.389-402. https://doi.org/10.1111/jfb.12834

Juanes, F. and Conover, D.O., 1994. Piscivory and prey size selection in youngof-the-year bluefish: predator preference or size-dependent capture success?. Marine Ecology Progress Series, 114, pp.59-69.

Kashef, N.S., Sogard, S.M., Fisher, R. and Largier, J.L., 2014. Ontogeny of critical swimming speeds for larval and pelagic juvenile rockfishes (Sebastes spp., family Scorpaenidae). Marine Ecology Progress Series, 500, pp.231-243. https://doi.org/10.3354/meps10669

Keister, J.E., Di Lorenzo, E., Morgan, C.A., Combes, V. and Peterson, W.T., 2011. Zooplankton species composition is linked to ocean transport in the Northern California Current. Global Change Biology, 17(7), pp.2498-2511. https://doi.org/10.1111/j.1365-2486.2010.02383.x

King, J.R., Agostini, V.N., Harvey, C.J., McFarlane, G.A., Foreman, M.G., Overland, J.E., Di Lorenzo, E., Bond, N.A. and Aydin, K.Y., 2011. Climate forcing and the California Current ecosystem. ICES Journal of Marine Science, 68(6), pp.1199-1216.

Kishi, M.J., Kashiwai, M., Ware, D.M., Megrey, B.A., Eslinger, D.L., Werner, F.E., Noguchi-Aita, M., Azumaya, T., Fujii, M., Hashimoto, S. and Huang, D., 2007. NEMURO-a lower trophic level model for the North Pacific marine ecosystem. Ecological Modelling, 202(1-2), pp.12-25.

Kitchell, J.F., Stewart, D.J. and Weininger, D., 1977. Applications of a bioenergetics model to yellow perch (Perca flavescens) and walleye (Stizostedion vitreum vitreum). Journal of the Fisheries Board of Canada, 34(10), pp.1922-1935. https://doi.org/10.1139/f77-258

Kjesbu, O.S., Marshall, C.T., Nash, R.D., Sundby, S., Rothschild, B.J. and Sinclair, M., 2016. Johan Hjort Symposium on recruitment dynamics and stock variability. Canadian Journal of Fisheries and Aquatic Sciences, 73(2), pp.vii-xi. https://doi.org/10.1139/cjfas-2015-0491

Koenigstein, S., Jacox, M.G., Pozo Buil, M., Fiechter, J., Muhling, B.A., Brodie, S., Kuriyama, P.T., Auth, T.D., Hazen, E.L., Bograd, S.J. and Tommasi, D., 2022. Population projections of Pacific sardine driven by ocean warming and changing food availability in the California Current. ICES Journal of Marine Science, 79(9), pp.2510-2523. https://doi.org/10.1093/icesjms/fsac191

Kooijman, B. and Kooijman, S.A.L.M., 2010. Dynamic energy budget theory for metabolic organisation. (3rd Ed.) Cambridge University Press. https://doi.org/10.1017/CBO9780511805400

Laidig, T.E., 2010. Influence of ocean conditions on the timing of early life history events for blue rockfish (Sebastes mystinus) off California. Fishery Bulletin, 108(4), pp.442-449.

Laidig, T.E., Chess, J.R. and Howard, D.F., 2007. Relationship between abundance of juvenile rockfishes (Sebastes spp.) and environmental variables documented off northern California and potential mechanisms for the covariation. Fishery Bulletin, 105(1), pp.39-49.

Laidig, T.E., Ralston, S., and Bence, J.R., 1991. Dynamics of growth in the early life history of shortbelly rockfish Sebastes jordani. Fish. Bull., 89, pp.611-621.

Larson, R.J., Lenarz, W.H. and Ralston, S.T.E.P.H.E.N., 1994. The distribution of pelagic juvenile rockfish of the genus Sebastes in the upwelling region off central California. Calif. Coop. Ocean. Fish. Investig. Rep, 35, pp.175-221.

Lasker, R., 1975. Field criteria for survival of anchovy larvae: the relation between inshore chlorophyll maximum layers and successful first feeding. Fish. Bull., 73, pp.453-462.

Lasker, R., 1981. The role of a stable ocean in larval fish survival and subsequent recruitment. Marine fish larvae: morphology, ecology and relation to fisheries, 1, pp.80-89.

Leis, J.M., 2007. Behaviour as input for modelling dispersal of fish larvae: behaviour, biogeography, hydrodynamics, ontogeny, physiology and phylogeny meet hydrography. Marine Ecology Progress Series, 347, pp.185-193. DOI: https://doi.org/10.3354/meps06977

Lenarz, W.H., Ven Tresca, D.A., Montrose Graham, W., Schwing, F.B. and Chavez, F., 1995. Explorations of El Ni o Events and Associated Biological Population Dynamics off Central California. California Cooperative Oceanic Fisheries Investigations Report, pp.106-119.

Lilly, L.E. and Ohman, M.D., 2018. CCE IV: El Niño-related zooplankton variability in the southern California Current System. Deep Sea Research Part I: Oceanographic Research Papers, 140, pp.36-51.

Lindegren, M. and Checkley Jr, D.M., 2013. Temperature dependence of Pacific

    sardine (Sardinops sagax) recruitment in the California Current Ecosystem

    revisited and revised. Canadian Journal of Fisheries and Aquatic Sciences,

    70(2), pp.245-252.

Lindegren, M., Checkley Jr, D.M., Rouyer, T., MacCall, A.D. and Stenseth, N.C.,

    2013. Climate, fishing, and fluctuations of sardine and anchovy in the

    California Current. Proceedings of the National Academy of Sciences,

    110(33), pp.13672-13677.

Litvak, M. K., & Leggett, W. C., 1992. Age and size-selective predation on larval

    fishes: The bigger-is-better hypothesis revisited. Marine Ecology Progress

    Series, 81(1), 13-24.

Litzow, M.A., Hunsicker, M.E., Bond, N.A., Burke, B.J., Cunningham, C.J.,

    Gosselin, J.L., Norton, E.L., Ward, E.J. and Zador, S.G., 2020. The changing

    physical and ecological meanings of North Pacific Ocean climate indices.

    Proceedings of the National Academy of Sciences, 117(14), pp.7665-7671.

Lluch-Belda, D.R.J.M., Crawford, R.J., Kawasaki, T., MacCall, A.D., Parrish, R.H.,

    Schwartzlose, R.A. and Smith, P.E., 1989. World-wide fluctuations of sardine

    and anchovy stocks: the regime problem. South African Journal of Marine

    Science, 8(1), pp.195-205.

Love, M.S., Yoklavich, M. and Thorsteinson, L.K., 2002. The rockfishes of the

    northeast Pacific. Univ of California Press, Los Angeles 414 pp.

Lowry, M.S., Nehasil, S.E. and Moore, J.E., 2022. Spatio-temporal diet variability of the California sea lion Zalophus californianus in the southern California current ecosystem. Marine Ecology Progress Series, 692, pp.1-21.

MacFarlane, R.B., and Norton, E.C., 1999. Nutritional dynamics during embryonic development in the viviparous genus Sebastes and their application to the assessment of reproductive success. Fish. Bull., 97, pp.273-281.

Mantua, N.J. and Hare, S.R., 2002. The Pacific decadal oscillation. Journal of oceanography, 58(1), pp.35-44.

Mantua, N.J., Hare, S.R., Zhang, Y., Wallace, J.M. and Francis, R.C., 1997. A Pacific interdecadal climate oscillation with impacts on salmon production. Bulletin of the american Meteorological Society, 78(6), pp.1069-1080.

Maunder, M.N. and Punt, A.E., 2004. Standardizing catch and effort data: a review of recent approaches. Fisheries research, 70(2-3), pp.141-159. https://doi.org/10.1016/j.fishres.2004.08.002

McClatchie, S., Goericke, R., Auad, G. and Hill, K., 2010. Re-assessment of the stock-recruit and temperature-recruit relationships for Pacific sardine (Sardinops sagax). Canadian Journal of Fisheries and Aquatic Sciences, 67(11), pp.1782-1790.

McGowan, J.A., and Miller, C.B., 1980. Larval fish and zooplankton community structure. CalCOFI Report, 21, pp.29-36.

McGowan, J.A., Cayan, D.R. and Dorman, L.M., 1998. Climate-ocean variability and ecosystem response in the Northeast Pacific. Science, 281(5374), pp.210-217. https://doi.org/0.1126/science.281.5374.210

Megrey, B.A., Rose, K.A., Klumb, R.A., Hay, D.E., Werner, F.E., Eslinger, D.L. and Smith, S.L., 2007. A bioenergetics-based population dynamics model of Pacific herring (Clupea harengus pallasi) coupled to a lower trophic level nutrient-phytoplankton-zooplankton model: description, calibration, and sensitivity analysis. Ecological modelling, 202(1-2), pp.144-164. https://doi.org/10.1016/j.ecolmodel.2006.08.020

Meinvielle, M. and Johnson, G.C., 2013. Decadal water?property trends in the California Undercurrent, with implications for ocean acidification. Journal of Geophysical Research: Oceans, 118(12), pp.6687-6703. https://doi.org/10.1002/2013JC009299

Messié, M., Sancho-Gallegos, D.A., Fiechter, J., Santora, J.A. and Chavez, F.P., 2022. Satellite-based Lagrangian model reveals how upwelling and oceanic circulation shape krill hotspots in the California Current System. Frontiers in Marine Science, 9, p.835813. https://doi.org/10.3389/fmars.2022.835813

Miller, T.J., 2007. Contribution of individual-based coupled physical-biological models to understanding recruitment in marine fish populations. Marine Ecology Progress Series, 347, pp.127-138. https://doi.org/10.3354/meps06973

Miller, T.J., Crowder, L.B., Rice, J.A. and Marschall, E.A., 1988. Larval size and recruitment mechanisms in fishes: toward a conceptual framework. Canadian Journal of Fisheries and Aquatic Sciences, 45(9), pp.1657-1670. https://doi.org/10.1139/f88-197

Miller, T.W., Brodeur, R.D., 2007. Diet of and trophic relationships among dominant marine nekton within the Northern California Current ecosystem. Fish Bull 105: 548?559

Miller, T.W., Brodeur, R.D., Rau, G. and Omori, K., 2010. Prey dominance shapes trophic structure of the northern California Current pelagic food web: evidence from stable isotopes and diet analysis. Marine Ecology Progress Series, 420, pp.15-26. DOI: https://doi.org/10.3354/meps08876

Moser, H.G. and Boehlert, G.W., 1991. Ecology of pelagic larvae and juveniles of the genus Sebastes. Environmental Biology of Fishes, 30, pp.203-224. https://doi.org/10.1007/BF0229689

Mulder, C., Hendriks, A.J., 2014. Half-saturation constants in functional responses. Global Ecology and Conservation, 2, pp.161-169. https://doi.org/10.1016/j.gecco.2014.09.006

Munday, P.L., Leis, J.M., Lough, J.M., Paris, C.B., Kingsford, M.J., Berumen, M.L. and Lambrechts, J., 2009. Climate change and coral reef connectivity. Coral reefs, 28, pp.379-395. https://doi.org/10.1007/s00338-008-0461-9

Myers, R.A., 1998. When do environment-recruitment correlations work?. Reviews in Fish Biology and Fisheries, 8, pp.285-305.

Nelson, J.S., Grande, T.C. and Wilson, M.V., 2016. Fishes of the World. John Wiley & Sons.

Neveu, E., Moore, A.M., Edwards, C.A., Fiechter, J., Drake, P., Crawford, W.J., Jacox, M.G. and Nuss, E., 2016. An historical analysis of the California Current circulation using ROMS 4D-Var: System configuration and diagnostics. Ocean Modelling, 99, pp.133-151. https://doi.org/10.1016/j.ocemod.2015.11.012

North, E.W., Gallego, A. and Petitgas, P., 2009. Manual of recommended practices for modelling physical-biological interactions during fish early life. ICES Cooperative Research Report, (295).

Norton, E.C., MacFarlane, R.B. and Mohr, M.S., 2001. Lipid class dynamics during development in early life stages of shortbelly rockfish and their application to condition assessment. Journal of Fish Biology, 58(4), pp.1010-1024. https://doi.org/10.1111/j.1095-8649.2001.tb00551.x

O'Connor, M.I., Bruno, J.F., Gaines, S.D., Halpern, B.S., Lester, S.E., Kinlan, B.P. and Weiss, J.M., 2007. Temperature control of larval dispersal and the implications for marine ecology, evolution, and conservation. Proceedings of the National Academy of Sciences, 104(4), pp.1266-1271. https://doi.org/10.1073/pnas.0603422104

Ohman, M.D., Barbeau, K., Franks, P.J., Goericke, R., Landry, M.R. and Miller, A.J.,
2013. Ecological transitions in a coastal upwelling ecosystem. Oceanography,
26(3), pp.210-219.

Ord, J.K. and Getis, A., 1995. Local spatial autocorrelation statistics: distributional
issues and an application. Geographical analysis, 27(4), pp.286-306.
https://doi.org/10.1111/j.1538-4632.1995.tb00912.x

Pacific Fishery Management Council (PFMC). 2022. Pacific Coast Fishery
Ecosystem Plan for the U.S. Portion of the California Current Large Marine
Ecosystem (Revised and Updated). Pacific Fishery Management Council,
7700 NE Ambassador Place, Suite 101, Portland, Oregon 97220-1384.
https://www.pcouncil.org/documents/2022/04/pacific-coast-fishery-
ecosystem-plan-march-2022.pdf/

Palacios, D.M., Bograd, S.J., Mendelssohn, R. and Schwing, F.B., 2004. Long?term
and seasonal trends in stratification in the California Current, 1950-1993.
Journal of Geophysical Research: Oceans, 109(C10).

Peck, M.A. and Hufnagl, M., 2012. Can IBMs tell us why most larvae die in the sea?
Model sensitivities and scenarios reveal research needs. Journal of Marine
Systems, 93, pp.77-93. https://doi.org/10.1016/j.jmarsys.2011.08.005

Peck, M.A. and Moyano, M., 2016. Measuring respiration rates in marine fish larvae:
challenges and advances. Journal of Fish Biology, 88(1), pp.173-205.
https://doi.org/10.1111/jfb.12810

Pepin, P., 1991. Effect of temperature and size on development, mortality, and

survival rates of the pelagic early life history stages of marine fish. Canadian

Journal of Fisheries and Aquatic Sciences, 48(3), pp.503-518. 10.1139/f91-06

Petersen, C.H., Drake, P.T., Edwards, C.A. and Ralston, S., 2010. A numerical study

of inferred rockfish (Sebastes spp.) larval dispersal along the central

California coast. Fisheries Oceanography, 19(1), pp.21-41.

https://doi.org/10.1111/j.1365-2419.2009.00526.x

Peterson, W.T., Fisher, J.L., Peterson, J.O., Morgan, C.A., Burke, B.J. and Fresh,

K.L., 2014. Applied fisheries oceanography: Ecosystem indicators of ocean

conditions inform fisheries management in the California Current.

Oceanography, 27(4), pp.80-89. https://doi.org/10.5670/oceanog.2014.88

Politikos, D.V., Curchitser, E.N., Rose, K.A., Checkley Jr, D.M. and Fiechter, J.,

2018. Climate variability and sardine recruitment in the California Current: a

mechanistic analysis of an ecosystem model. Fisheries Oceanography, 27(6),

pp.602-622.

Pörtner, H.O. and Knust, R., 2007. Climate change affects marine fishes through the

oxygen limitation of thermal tolerance. science, 315(5808), pp.95-97. DOI:

10.1126/science.1135471

Pörtner, H.O. and Farrell, A.P., 2008. Physiology and climate change. Science,

322(5902), pp.690-692. DOI: 10.1126/science.1163156

Pozo Buil, M., Jacox, M.G., Fiechter, J., Alexander, M.A., Bograd, S.J., Curchitser, E.N., Edwards, C.A., Rykaczewski, R.R. and Stock, C.A., 2021. A dynamically downscaled ensemble of future projections for the California current system. Frontiers in Marine Science, 8, p.612874.

Press, W.H., 2007. Numerical recipes 3rd edition: The art of scientific computing. Cambridge university press.

Purcell, J.E., 1981. Feeding ecology of Rhizophysa eysenhardti, a siphonophore predator of fish larvae 1. Limnology and Oceanography, 26(3), pp.424-432.

Ralston, S. 1995. The influence of oceanographic variables on time series of otolith growth in pelagic young of-the-year rockfish, Sebastes spp. pp. 97-118. In: Secor, D. H., Dean, J.M., and S. E. Campana [eds.]. Recent Developments in Fish Otolith Research. University of South Carolina Press, Columbia, SC.

Ralston, S. and Stewart, I.J., 2013. Anomalous distributions of pelagic juvenile rockfish on the US west coast in 2005 and 2006. California Cooperative Oceanic and Fisheries Investigations Reports, 54, pp.155-166.

Ralston, S., and Howard, D.F., 1995. On the development of year-class strength and cohort variability in two northern California rockfishes. Fish. Bull., 93, pp.710-720.

Ralston, S., Bence, J.R., Eldridge, M.B. and Lenarz, W.H., 2003. An approach to estimating rockfish biomass based on larval production, with application to Sebastes jordani. Fishery Bulletin, 101, 129- 146.

Ralston, S., Sakuma, K.M. and Field, J.C., 2013. Interannual variation in pelagic juvenile rockfish (Sebastes spp.) abundance-going with the flow. Fisheries Oceanography, 22(4), pp.288-308. https://doi.org/10.1111/fog.12022

Rebstock, G.A., 2001. Long-term stability of species composition in calanoid copepods off southern California. Marine Ecology Progress Series, 215, pp.213-224. doi:10.3354/meps215213

Reilly, C.A., Echeverria, T.W. and Ralston, S., 1992. Interannual variation and overlap in the diets of pelagic juvenile rockfish(genus: Sebastes) off Central California. Fishery Bulletin, 90(3), pp.505-515.

Ricker, W.E., 1954. Stock and recruitment. Journal of the Fisheries Board of Canada, 11(5), pp.559-623.

Ricker, W.E., 1979. Growth rates and models. Fish physiology, pp.677-744.

Robert, D., Takasuka, A., Nakatsuka, S., Kubota, H., Oozeki, Y., Nishida, H. and Fortier, L., 2010. Predation dynamics of mackerel on larval and juvenile anchovy: is capture success linked to prey condition? Fisheries Science, 76, pp.183-188. https://doi.org/10.1007/s12562-009-0205-y

Robert, D., Shoji, J., Sirois, P., Takasuka, A., Catalán, I.A., Folkvord, A., Ludsin, S.A., Peck, M.A., Sponaugle, S., Ayón, P.M. and Brodeur, R.D., 2023. Life in the fast lane: Revisiting the fast growth-High survival paradigm during the early life stages of fishes. Fish and Fisheries. 24(5), pp. 863-888. https://doi.org/10.1111/faf.12774

Rooper, C.N., Boldt, J.L., Batten, S. and Gburski, C., 2012. Growth and production of Pacific ocean perch (Sebastes alutus) in nursery habitats of the Gulf of Alaska. Fisheries Oceanography, 21(6), pp.415-429. https://doi.org/10.1111/j.1365-2419.2012.00635.x

Rose, K.A., Rutherford, E.S., McDermot, D.S., Forney, J.L. and Mills, E.L., 1999(a). Individual?based model of yellow perch and walleye populations in Oneida Lake. Ecological Monographs, 69(2), pp.127-154. https://doi.org/10.1890/0012-9615(1999)069[0127:IBMOYP]2.0.CO;2

Rose, K.A., Cowan Jr, J.H., Clark, M.E., Houde, E.D. and Wang, S.B., 1999(b). An individual-based model of bay anchovy population dynamics in the mesohaline region of Chesapeake Bay. Marine Ecology Progress Series, 185, pp.113-132. https://doi.org/10.3354/meps185113

Rose, K.A., Fiechter, J., Curchitser, E.N., Hedstrom, K., Bernal, M., Creekmore, S., Haynie, A., Ito, S.I., Lluch-Cota, S., Megrey, B.A. and Edwards, C.A., 2015. Demonstration of a fully-coupled end-to-end model for small pelagic fish using sardine and anchovy in the California Current. Progress in Oceanography, 138, pp.348-380. https://doi.org/10.1016/j.pocean.2015.01.012

Ross, J.R. and Larson, R.J., 2003. Influence of water column stratification on the depth distributions of pelagic juvenile rockfishes off central California. California Cooperative Oceanic Fisheries Investigations Reports, 44, pp.65-75.

Rothschild, B.J. and Osborn, T.R., 1988. Small-scale turbulence and plankton contact

rates. Journal of plankton Research, 10(3), pp.465-474.

https://doi.org/10.1093/plankt/10.3.465

Rykaczewski, R.R. and Checkley Jr, D.M., 2008. Influence of ocean winds on the

pelagic ecosystem in upwelling regions. Proceedings of the National Academy

of Sciences, 105(6), pp.1965-1970.

Sakuma, K.M., Field, J.C., Mantua, N.J., Ralston, S., Marinovic, B.B. and Carrion,

C.N., 2016. Anomalous epipelagic micronekton assemblage patterns in the

neritic waters of the California Current in spring 2015 during a period of

extreme ocean conditions. California Cooperative Oceanic Fisheries

Investigations Report, 57, pp.163-183.

Santora, J.A., Sydeman, W.J., Schroeder, I.D., Wells, B.K. and Field, J.C., 2011.

Mesoscale structure and oceanographic determinants of krill hotspots in the

California Current: Implications for trophic transfer and conservation.

Progress in Oceanography, 91(4), pp.397-409.

https://doi.org/10.1016/j.pocean.2011.04.002

Santora, J.A., Schroeder, I.D., Field, J.C., Wells, B.K. and Sydeman, W.J., 2014.

Spatio-temporal dynamics of ocean conditions and forage taxa reveal regional

structuring of seabird-prey relationships. Ecological Applications, 24(7),

pp.1730-1747.

Santora, J.A., Hazen, E.L., Schroeder, I.D., Bograd, S.J., Sakuma, K.M. and Field, J.C., 2017. Impacts of ocean climate variability on biodiversity of pelagic forage species in an upwelling ecosystem. Marine Ecology Progress Series, 580, pp.205-220. https://doi.org/10.3354/meps12278

Santora, J.A., Rogers, T.L., Cimino, M.A., Sakuma, K.M., Hanson, K.D., Dick, E.J., Jahncke, J., Warzybok, P. and Field, J.C., 2021b. Diverse integrated ecosystem approach overcomes pandemic-related fisheries monitoring challenges. Nature communications, 12(1), p.6492.

Santora, J.A., Schroeder, I.D., Bograd, S.J., Chavez, F.P., Cimino, M.A., Fiechter, J., Hazen, E.L., Kavanaugh, M.T., Messié, M., Miller, R.R. and Sakuma, K.M., 2021a. Pelagic biodiversity, ecosystem function, and services. Oceanography, 34(2), pp.16-37.

Schirripa, M.J. and Colbert, J.J., 2006. Interannual changes in sablefish (Anoplopoma fimbria) recruitment in relation to oceanographic conditions within the California Current System. Fisheries Oceanography, 15(1), pp.25-36. https://doi.org/10.1111/j.1365-2419.2005.00352.x

Schroeder, I.D., Sydeman, W.J., Sarkar, N., Thompson, S.A., Bograd, S.J. and Schwing, F.B., 2009. Winter pre-conditioning of seabird phenology in the California Current. Marine Ecology Progress Series, 393, pp.211-223. https://doi.org/10.3354/meps08103

Schroeder, I.D., Black, B.A., Sydeman, W.J., Bograd, S.J., Hazen, E.L., Santora, J.A. and Wells, B.K., 2013. The North Pacific High and wintertime pre?conditioning of California current productivity. Geophysical Research Letters, 40(3), pp.541-546. https://doi.org/10.1002/grl.50100

Schroeder, I.D., Santora, J.A., Moore, A.M., Edwards, C.A., Fiechter, J., Hazen, E.L., Bograd, S.J., Field, J.C. and Wells, B.K., 2014. Application of a data?assimilative regional ocean modeling system for assessing California Current System ocean conditions, krill, and juvenile rockfish interannual variability. Geophysical Research Letters, 41(16), pp.5942-5950. https://doi.org/10.1002/2014GL061045

Schroeder, I.D., Santora, J.A., Bograd, S.J., Hazen, E.L., Sakuma, K.M., Moore, A.M., Edwards, C.A., Wells, B.K. and Field, J.C., 2019. Source water variability as a driver of rockfish recruitment in the California Current Ecosystem: implications for climate change and fisheries management. Canadian Journal of Fisheries and Aquatic Sciences, 76(6), pp.950-960.

Schwing, F.B., Murphree, T., deWitt, L. and Green, P.M., 2002. The evolution of oceanic and atmospheric anomalies in the northeast Pacific during the El Niño and La Niña events of 1995-2001. Progress in Oceanography, 54(1-4), pp.459-491.

Schwing, F.B., Bond, N.A., Bograd, S.J., Mitchell, T., Alexander, M.A. and Mantua, N., 2006. Delayed coastal upwelling along the US West Coast in 2005: A

historical perspective. Geophysical Research Letters, 33(22).

https://doi.org/10.1029/2006GL026911

Secor, D.H., 2007. The year-class phenomenon and the storage effect in marine

fishes. Journal of Sea Research, 57(2-3), pp.91-103.

Shaffer, J.A., Doty, D.C., Buckley, R.M. and West, J.E., 1995. Crustacean community

composition and trophic use of the drift vegetation habitat by juvenile

splitnose rockfish Sebastes diploproa. Marine Ecology Progress Series, 123,

pp.13-21. doi:10.3354/meps123013

Shchepetkin, A.F. and McWilliams, J.C., 2005. The regional oceanic modeling system

(ROMS): a split-explicit, free-surface, topography-following-coordinate

oceanic model. Ocean modelling, 9(4), pp.347-404.

https://doi.org/10.1016/j.ocemod.2004.08.002

Shepherd, J.G., Pope, J.G., Cousens, R.D., 1984. Variations in fish stocks and

hypotheses concerning their links with climate. Rapp. P.-v. Réun. Cons. int.

Explor. Mer, 185, pp.255-267.

Sibly, R.M., Grimm, V., Martin, B.T., Johnston, A.S., Ku?akowska, K., Topping, C.J.,

Calow, P., Nabe?Nielsen, J., Thorbek, P. and DeAngelis, D.L., 2013.

Representing the acquisition and use of energy by individuals in agent?based

models of animal populations. Methods in Ecology and Evolution, 4(2),

pp.151-161. https://doi.org/10.1111/2041-210x.12002

Sinclair, M. and Iles, T.D., 1985. Atlantic herring (Clupea harengus) distributions in the Gulf of Maine-Scotian Shelf area in relation to oceanographic features. Canadian Journal of Fisheries and Aquatic Sciences, 42(5), pp.880-887.

Sinclair, M. and Iles, T.D., 1989. Population regulation and speciation in the oceans. ICES Journal of Marine Science, 45(2), pp.165-175. https://doi.org/10.1093/icesjms/45.2.165

Sinclair, M., 1988. The member/vagrant hypothesis. pp. 67-77. In: M. Sinclair (ed.), Marine Populations: An essay on Pop-ulation Regulation and Speciation, Washington Sea grant Program, University of Washington Press, Seattle, Washington.

Smith, J.A., Buil, M.P., Muhling, B., Tommasi, D., Brodie, S., Frawley, T.H., Fiechter, J., Koenigstein, S., Himes-Cornell, A., Alexander, M.A. and Bograd, S.J., 2023. Projecting climate change impacts from physics to fisheries: A view from three California Current fisheries. Progress in Oceanography, 211, p.102973.

Sogard, S.M., 1997. Size-selective mortality in the juvenile stage of teleost fishes: a review. Bulletin of marine science, 60(3), pp.1129-1157.

Sogard, S.M., Berkeley, S.A. and Fisher, R., 2008. Maternal effects in rockfishes Sebastes spp.: a comparison among species. Marine Ecology Progress Series, 360, pp.227-236.

Stachura, M.M., Essington, T.E., Mantua, N.J., Hollowed, A.B., Haltuch, M.A., Spencer, P.D., Branch, T.A. and Doyle, M.J., 2014. Linking N ortheast P acific recruitment synchrony to environmental variability. Fisheries Oceanography, 23(5), pp.389-408. https://doi.org/10.1111/fog.12066

Stefánsson, G., 1996. Analysis of groundfish survey abundance data: combining the GLM and delta approaches. ICES journal of Marine Science, 53(3), pp.577-588. https://doi.org/10.1006/jmsc.1996.0079

Stevenson, D. K., Campana, S. E. 1992. Otolith Microstructure Examination and Analysis. Department of Fisheries and Oceans. Ottawa, Canada.

Sumida, B.Y. and Moser, H.G., 1984. Food and feeding of bocaccio (Sebastes paucispinis) and comparison with Pacific hake (Merluccius productus) larvae in the California Current. Calif. Coop. Oceanic Fish. Invest. Rep, 25, pp.112-118.

Sundby, S. and Fossum, P., 1990. Feeding conditions of Arcto-Norwegian cod larvae compared with the Rothschild-Osborn theory on small-scale turbulence and plankton contact rates. Journal of Plankton Research, 12(6), pp.1153-1162. https://doi.org/10.1093/plankt/12.6.1153

Sydeman, W.J., Bradley, R.W., Warzybok, P., Abraham, C.L., Jahncke, J., Hyrenbach, K.D., Kousky, V., Hipfner, J.M. and Ohman, M.D., 2006. Planktivorous auklet Ptychoramphus aleuticus responses to ocean climate, 2005: Unusual

atmospheric blocking?. Geophysical Research Letters, 33(22).

https://doi.org/10.1029/2006GL026736

Szoboszlai, A.I., Thayer, J.A., Wood, S.A., Sydeman, W.J. and Koehn, L.E., 2015.

Forage species in predator diets: synthesis of data from the California Current.

Ecological Informatics, 29, pp.45-56.

https://doi.org/10.1016/j.ecoinf.2015.07.003

Takasuka, A., Aoki, I. and Mitani, I., 2003. Evidence of growth-selective predation on

larval Japanese anchovy Engraulis japonicus in Sagami Bay. Marine Ecology

Progress Series, 252, pp.223-238. https://doi.org/10.3354/meps252223

Talley, L.D., 2011. Descriptive physical oceanography: an introduction. Academic

press.

Thayer, J.A., Field, J.C. and Sydeman, W.J., 2014. Changes in California Chinook

salmon diet over the past 50 years: relevance to the recent population crash.

Marine Ecology Progress Series, 498, pp.249-261.

Thomas, A.C. and Brickley, P., 2006. Satellite measurements of chlorophyll

distribution during spring 2005 in the California Current. Geophysical

Research Letters, 33(22). https://doi.org/10.1029/2006GL026588

Thompson, A.R., Hyde, J.R., Watson, W., Chen, D.C. and Guo, L.W., 2016. Rockfish

assemblage structure and spawning locations in southern California identified

through larval sampling. Marine Ecology Progress Series, 547, pp.177-192.

DOI: https://doi.org/10.3354/meps11633

Thompson, A.R., Chen, D.C., Guo, L.W., Hyde, J.R. and Watson, W., 2017. Larval abundances of rockfishes that were historically targeted by fishing increased over 16 years in association with a large marine protected area. Royal Society open science, 4(9), p.170639. https://doi.org/10.1098/rsos.170639

Thompson, A.R., Bjorkstedt, E.P., Bograd, S.J., Fisher, J.L., Hazen, E.L., Leising, A., Santora, J.A., Satterthwaite, E.V., Sydeman, W.J., Alksne, M. and Auth, T.D., 2022. State of the California Current Ecosystem in 2021: Winter is coming? Frontiers in Marine Science, 9, p.958727. https://doi.org/10.3389/fmars.2022.958727

Thornton, K.W. and Lessem, A.S., 1978. A temperature algorithm for modifying biological rates. Transactions of the American Fisheries Society, 107(2), pp.284-287. https://doi.org/10.1577/1548-8659(1978)107<284:ATAFMB>2.0.CO;2

Tolimieri, N., Haltuch, M.A., Lee, Q., Jacox, M.G. and Bograd, S.J., 2018. Oceanographic drivers of sablefish recruitment in the California Current. Fisheries Oceanography, 27(5), pp.458-474. https://doi.org/10.1111/fog.12266

Trenberth, K.E., 1997. The definition of El Niño. Bulletin of the American Meteorological Society, 78(12), pp.2771-2777.

Vasbinder, K., Fiechter, J., Santora, J.A., Anderson, J.J., Mantua, N., Lindley, S.T., Huff, D.D. and Wells, B.K., 2023. Size?selective predation effects on juvenile

Chinook salmon cohort survival off Central California evaluated with an
individual?based model. Fisheries Oceanography.
https://doi.org/10.1111/fog.12654

Vestfals, C.D., Marshall, K.N., Tolimieri, N., Hunsicker, M.E., Berger, A.M., Taylor,
I.G., Jacox, M.G. and Turley, B.D., 2023. Stage?specific drivers of Pacific
hake (Merluccius productus) recruitment in the California Current Ecosystem.
Fisheries Oceanography. https://doi.org/10.1111/fog.12634

Warner, R.R. and Chesson, P.L., 1985. Coexistence mediated by recruitment
fluctuations: a field guide to the storage effect. The American Naturalist,
125(6), pp.769-787.

Warzybok, P., Santora, J.A., Ainley, D.G., Bradley, R.W., Field, J.C., Capitolo, P.J.,
Carle, R.D., Elliott, M., Beck, J.N., McChesney, G.J. and Hester, M.M., 2018.
Prey switching and consumption by seabirds in the central California Current
upwelling ecosystem: Implications for forage fish management. Journal of
Marine Systems, 185, pp.25-39.

Washburn, L. and McPhee-Shaw, E., 2013. Coastal transport processes affecting
inner-shelf ecosystems in the California Current System. Oceanography,
26(3), pp.34-43.

Wells, B.K. and Santora, J.A., 2023. Implementing an ecosystem oceanography
program to increase capacity and preparedness for dynamic ocean

management and fishery challenges. Frontiers in Marine Science. 10:1192052. https://doi.org/10.3389/fmars.2023.1192052

Wells, B.K., Santora, J.A., Henderson, M.J., Warzybok, P., Jahncke, J., Bradley, R.W., Huff, D.D., Schroeder, I.D., Nelson, P., Field, J.C. and Ainley, D.G., 2017. Environmental conditions and prey-switching by a seabird predator impact juvenile salmon survival. Journal of Marine Systems, 174, pp.54-63. https://doi.org/10.1016/j.jmarsys.2017.05.008

Wheeler, S.G., Anderson, T.W., Bell, T.W., Morgan, S.G. and Hobbs, J.A., 2017. Regional productivity predicts individual growth and recruitment of rockfishes in a northern California upwelling system. Limnology and Oceanography, 62(2), pp.754-767. https://doi.org/10.1002/lno.10458

Winberg, G.G., 1956. Rate of metabolism and food requirements of fishes. Fish. Res. Bd. Canada Trans. Ser., 433, pp.1-251. https://doi.org/10.2307/1440948

Wing, S.R., Botsford, L.W., Ralston, S.V. and Largier, J.L., 1998. Meroplanktonic distribution and circulation in a coastal retention zone of the northern California upwelling system. Limnology and Oceanography, 43(7), pp.1710-1721. https://doi.org/10.4319/lo.1998.43.7.1710

Wood, S.N., 2017. Generalized additive models: an introduction with R. CRC press.

Woodbury, D., and Ralston, S., 1991. Interannual variation in growth rates and back-calculated birthdate distributions of pelagic juvenile rockfishes (Sebastes spp.) off the central California coast. Fish. Bull., 89, pp.523-533.

Wyllie-Echeverria, T.W., 1987. Thirty-four species of California rockfishes: maturity and seasonality of reproduction. Fishery Bulletin, 85(2), pp.229-250.

Yang, T.H., 1992. The physiological and biochemical responses of fishes to different oxygen concentrations and feeding conditions, (Doctoral dissertation, University of California, San Diego).

Young, K.V., Dower, J.F. and Pepin, P., 2009. A hierarchical analysis of the spatial distribution of larval fish prey. Journal of Plankton Research, 31(6), pp.687-700. https://doi.org/10.1093/plankt/fbp017

Yurkowski, D.J., Auger Méthé, M., Mallory, M.L., Wong, S.N., Gilchrist, G., Derocher, A.E., Richardson, E., Lunn, N.J., Hussey, N.E., Marcoux, M. and Togunov, R.R., 2019. Abundance and species diversity hotspots of tracked marine predators across the North American Arctic. Diversity and Distributions, 25(3), pp.328-345. https://doi.org/10.1111/ddi.12860

Zwolinski, J.P. and Demer, D.A., 2019. Re-evaluation of the environmental dependence of Pacific sardine recruitment. Fisheries Research, 216, pp.120-125.